ISSN 1023-9855

Thoracic Medicine

Volume 40 • Number 1 • March 2025

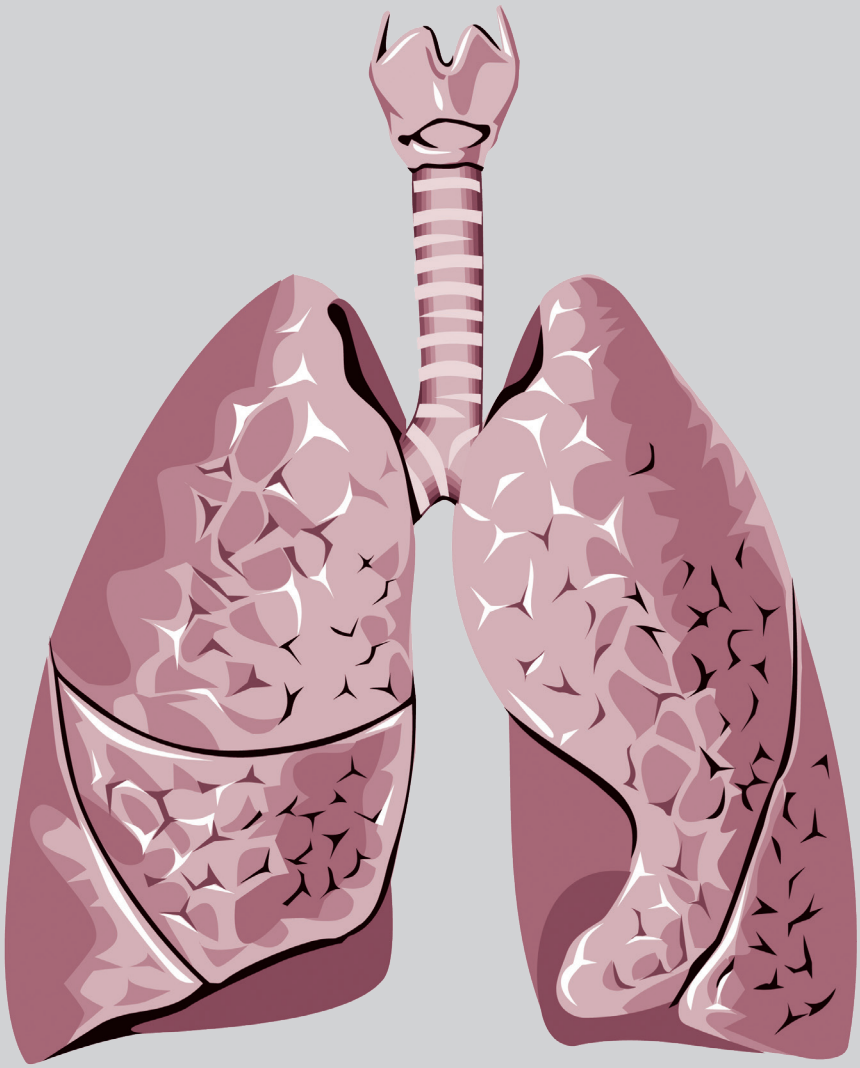

The Official Journal of

Taiwan Society of Pulmonary and Critical Care Medicine

Taiwan Society of Sleep Medicine

Taiwan Society for Respiratory Therapy

Taiwan Society of Tuberculosis and Lung Diseases

Thoracic Medicine

The Official Journal of
Taiwan Society of Pulmonary and Critical Care Medicine
Taiwan Society for Respiratory Therapy
Taiwan Society of Sleep Medicine
Taiwan Society of Tuberculosis and Lung Diseases

Thoracic Medicine

The Official Journal of
Taiwan Society of Pulmonary and Critical Care Medicine
Taiwan Society for Respiratory Therapy
Taiwan Society of Sleep Medicine
Taiwan Society of Tuberculosis and Lung Diseases

Volume 40
Number 1
March 2025

CONTENTS

Influence of a Pay-for-Performance Program on 3-Year Follow-Up of Patients with COPD: A Retrospective Study from Taiwan

You-Cyuan Liang[1*], Shu-Farn Tey[1,2*], Shyh-Ren Chiang[1], Kuo-Chen Cheng[1], Mei-I Sung[3], Jui-Lin Liang[4]

Background: Chronic obstructive pulmonary disease (COPD) is a heterogeneous lung condition that cause airway obstruction, and is a leading cause of morbidity and mortality worldwide, with an economic and social burden. In recent years, multidisciplinary management of COPD has been emphasized for the purpose of improving the quality of patient care and reducing acute exacerbations. Pay for performance (P4P) is a strategy that aligns healthcare provider incentives with improvements in care quality and cost control. This study was conducted to assess the effectiveness of a COPD P4P program in patients with COPD.

Methods: This study retrospectively included patients diagnosed with COPD under ICD-10 codes J41-J44, who registered for the P4P program in our hospital between September 2018 and August 2019 and had been diagnosed at the same hospital at least 1 year prior to participation. Patients who did not complete the COPD Assessment Test (CAT), the modified Medical Research Council (mMRC) symptom score assessment, and pulmonary function tests (FEV1 and FVC) were excluded from the study.

Results: From Sep 1, 2018 to Aug 31, 2019, 388 patients were enrolled. The number of hospitalized patients decreased from 55 during the year in which the study cases were included to 26 patients at the third year; the ratio of the number of hospitalized patients decreased from 14.2% to 9.6%, and the number of hospitalizations decreased from 83 to 45. However, the mean length of stay per hospitalization increased from 7.17 days to 10.73 days, with statistical significance (p = 0.011). The total cost of hospitalization of patients with diagnostic codes J41-J44 and/or J12-J18 did not reveal a decreasing trend from 1 year before, to the third year after study enrollment, with a similar trend regarding the cost of hospitalization per day per hospitalization. Regardless of whether the patients had diagnostic codes J41-J44 or J12-J18, both the number of hospitalized patients and the number of hospitalizations decreased from the time of study enrollment to the subsequent 3 years. The

[1]Division of Chest Medicine, Department of Internal Medicine, Chi Mei Medical Center, Tainan, Taiwan, [2]School of Medicine, College of Medicine, National Sun Yat-sen University, Kaohsiung, Taiwan, [3]Department of Medical Research, Chi Mei Medical Center, Tainan, Taiwan, [4]Department of Intensive Care, Chi-Mei Medical Center, Liuying, Tainan, Taiwan.

[*]These authors contributed equally to this work

Address reprint requests to: Dr. Jui-Lin Liang, No. 901, Zhonghua Rd., Yongkang Dist., Tainan City 71004, Taiwan (R.O.C.)

number and rate of intensive care unit admissions showed a decreasing trend between the year of enrollment and the third year, as did the number of in-hospital deaths and the mortality rate of those hospitalized revealed. In terms of emergency department (ED) visits only, the total cost, number of patients and number of visits generally revealed a downward trend, but the mean cost per ED visit did not show a consistent trend. Subgroup analysis demonstrated that patients with diabetes mellitus, a GOLD classification, lower mean pre- and post-bronchodilator FEV1 at baseline lung function, COPD, a higher CAT score, an mMRC score and episodes of COPD exacerbations in the prior year had a significantly higher tendency of visiting the ED or being hospitalized. The GOLD classification was a potential risk factor for an ED visit or hospitalization, with overall statistical significance ($p = 0.002$), and GOLD grade III seemed to have higher risk tendency than GOLD grade I. Likewise, COPD was a potential risk factor for an ED visit or hospitalization, with overall statistical significance ($p < 0.001$), and COPD groups C and D seemed to have a higher risk tendency than groups A and B.

Conclusion: This study revealed the benefits of P4P program enrollment for patients with COPD. Our results suggest a different kind of medical care concept using an integrated multidisciplinary approach. Further studies with a longer follow-up period are warranted to distinguish the effectiveness of P4P and other factors or comorbidities that may have an impact on ED visits or hospitalization of patients with COPD. ***(Thorac Med 2025; 40: 1-12)***

Key words: chronic obstructive pulmonary disease, pay-for-performance, multidisciplinary management, medical costs

Introduction

Chronic obstructive pulmonary disease (COPD) is a heterogeneous lung condition characterized by chronic respiratory symptoms due to abnormalities of the airways and/or alveoli that cause airflow obstruction [1]. COPD is a leading cause of morbidity and mortality worldwide with an economic and social burden that is both substantial and increasing [1]. Patients with COPD may experience symptoms such as dyspnea, wheezing, chest tightness, fatigue, activity limitations, and coughing with or without sputum production. They may also have acute exacerbations, characterized by increased respiratory symptoms, which affect their health status and prognosis. Risk factors for COPD include cigarette smoking, air pollution, genetic factors, asthma, and infections such as tuberculosis. [1].

COPD exacerbations contribute to disease progression, and patients with COPD are also at increased risk of other acute events, particularly decompensated heart failure, pneumonia, and pulmonary embolism that may also mimic or aggravate an exacerbation of COPD [1]. Exacerbations of COPD not only negatively impact health status, rates of hospitalization and readmission, and disease progression [1], but increase medical costs. A systematic review

from 2020 disclosed that in the USA, annual per patient direct medical costs and hospitalization costs were reported as US$10,367 and US$6852, respectively. Direct medical costs depend upon the frequency of exacerbation [2]. A study based on the Taiwan National Health Insurance Research Database revealed that the average outpatient department cost per patient increased 29.3%, from US$1,070 in 2004 to US$1,383 in 2010 [3].

In addition to pharmacotherapy, there are several non-pharmacological treatment methods with proven benefits for patients with COPD, including smoking cessation, vaccinations, and pulmonary rehabilitation [1]. For example, smoking cessation improves daily symptoms [4], decreases the frequency of exacerbations [5], has lower declines in forced expiratory volume in 1 second (FEV1) [6], and reduces the mortality rate [7]. Pulmonary rehabilitation also provides benefits for COPD, including an improved readmission rate [8-10] and reduced mortality [9]. The benefit of mortality reduction is also supported by real-world evidence [11]. Patients with COPD could benefit from these aforementioned multidisciplinary interventions in terms of clinical care and prognosis.

Pay-for-performance (P4P) is a strategy designed to promote behavior change in healthcare providers by aligning financial incentives with improvement in health care quality and cost control [12]. In Taiwan, the COPD P4P program was initiated in 2017. It aims to improve the quality of COPD treatment and reduce exacerbations by introducing financial incentives and enhancing healthcare providers' adherence to guidelines [12]. Previous studies in Taiwan showed the positive effect of the COPD P4P program [12-13]. Similar integrative medical care programs can be seen in other countries. Implementation of the Hospital Readmissions Reduction Program (HRRP) in the U.S. has led to a reduction in 30-day readmissions [13-14]. Another study also disclosed the association between the initial phase of the HRRP and a decrease in both all-cause and COPD-related readmissions, even before COPD became a target diagnosis [15]. The COPD Quality Assessment Program (CQAP) launched by the Korean Health Insurance Review and Assessment Service (HIRA) in South Korea significantly reduced the risk of admission and the all-cause mortality rate in the assessed subject groups [13, 16]. In England and Wales, completion of the combined COPD BPT criteria did not appear to be associated with a reduction in 30-day mortality or readmission. However, a specialist review was associated with reduced inpatient mortality [17]. Hence, we conducted this study of Taiwan's COPD P4P program with the aim of assessing patients with COPD, and to evaluate its impact on an improvement in healthcare quality.

Methods

Study Design

Taiwan's COPD P4P program was initiated on April 1, 2017, and our hospital was approved as a healthcare provider within the program in September 2018. The P4P team includes thoracic specialists, pharmacists, respiratory therapists, and medical managers, all of whom had received professional COPD training certified by the Taiwan Society of Pulmonary and Critical Care Medicine (TSPCCM). According to the guidelines of the COPD P4P program, patients with International Classification of Diseases, Tenth Revision (ICD-10) diagnostic codes J41-J44, who were diagnosed through

pulmonary function tests (post-bronchodilator FEV1/forced vital capacity (FVC) < 70%) within a 90-day outpatient period at a medical institution, were eligible for enrollment in the program. Once enrolled, patients maintained regular treatment every 3 months with the same pulmonologist at the same hospital. Participants in the P4P program were given COPD patient-specific pulmonary rehabilitation exercises, smoking cessation, family and patient disease education, self-care information, and help in preventing exacerbations. Pulmonologists assessed and adjusted patients' medication and treatment management, while respiratory therapists guided patients through personalized training plans or short-term outpatient pulmonary rehabilitation courses. This study defines severe exacerbations requiring hospital admission or emergency department visits as an exacerbation of COPD.

Study Participants

This study included patients diagnosed with COPD under ICD-10 codes J41-J44, who had registered for the P4P program at Chi Mei Hospital between September 2018 and August 2019, and who had been diagnosed at the same hospital at least 1 year prior to participation. Patients who did not complete the COPD Assessment Test (CAT), the modified Medical Research Council (mMRC) symptom score, and pulmonary function tests (FEV1 and FVC) were excluded from the study. After approval from the Chi Mei Hospital ethics committee, retrospective clinical data collection was conducted, including demographic characteristics, symptoms, initial pulmonary function test results, frequency of exacerbations, and medical costs.

Statistical Analysis

Continuous variables were calculated as means and standard deviations, while categorical variables were presented as frequencies and percentages. Additionally, differences in baseline characteristics were assessed using the Mann-Whitney U test for continuous variables and the Pearson chi-square test or Fisher's exact test for categorical variables. All statistical analyses were performed using SPSS for Windows (version 26.0, IBM Corp, Armonk, NY, USA); a p value < 0.05 was considered statistically significant.

Results

From Sep 1, 2018 to Aug 31, 2019, 388 patients were enrolled in the study; 302 (77.84%) of the enrollees were males. The mean age of the patients was 72.63 years (standard deviation, SD 9.28), and the mean body mass index (BMI) was 24.67 kg/m2 (SD 4.20). Of the enrolled patients, 273 (70.36%) had a history of smoking, and of them, 197 (50.77%) had quit smoking; 206 (53.09%) had hypertension, 89 (22.94%) had diabetes mellitus (DM), 179 (46.13%) had cardiovascular disease and 37 (9.54%) had old pulmonary tuberculosis infection. In terms of GOLD classification, 85 (21.91%) of the 388 patients were categorized as GOLD I, 202 (52.06%) as GOLD II, 86 (22.16%) as GOLD III and 15 (3.87%) as GOLD IV. The mean pre- and post-BD FEV1 was 1.30 liters (SD 0.51), 60.11% (SD 19.64), and 1.37 liters (SD 0.53), 63.20% (SD 20.25), respectively. The mean pre- and post-BD FEV1/FVC was 53.24% (SD 11.64) and 53.69% (SD 12.15), respectively. In all, 191 (49.23%) were classified as COPD group A, 69 (17.78%) as group B, 63 (16.24%) as group C and 65 (16.75%) as group D. The

mean COPD Assessment Test (CAT) score was 8.57 (SD 5.67), and the modified Medical Research Council (mMRC) score was 1.36 (SD 0.90). The mean episode of COPD exacerbation in the prior year was 1.12 (SD 1.80) (Table 1).

Of the 388 patients, the hospitalized patient

Table 1. Baseline Characteristics of the Patients

Variables	Overall n=388
Gender, n (%)	
Female	86 (22.16)
Male	302 (77.84)
Age (y), mean (SD)	72.63 (9.28)
BMI (kg/m2), mean (SD)	24.67 (4.20)
Smoking status (%)	
History of smoking	273 (70.36)
Quit smoking	197 (50.77)
Underlying disease, n (%)	
Hypertension	206 (53.09)
Diabetes mellitus	89 (22.94)
Cardiovascular disease	179 (46.13)
Old pulmonary TB	37 (9.54)
Gold classification, n (%)	
GOLD I	85 (21.91)
GOLD II	202 (52.06)
GOLD III	86 (22.16)
GOLD IV	15 (3.87)
Baseline lung function	
Pre-BD-FEV1 (L), mean (SD)	1.30 (0.51)
Pre-BD-FEV1(%), mean (SD)	60.11 (19.64)
Pre-BD-FEV1/FVC(%), mean (SD)	53.24 (11.64)
Post-BD-FEV1(L), mean (SD)	1.37 (0.53)
Post-BD-FEV1(%), mean (SD)	63.20 (20.25)
Post-BD-FEV1/FVC(%), mean (SD)	53.69 (12.15)
COPD Group, n (%)	
A	191 (49.23)
B	69 (17.78)
C	63 (16.24)
D	65 (16.75)
CAT score, mean (SD)	8.57 (5.67)
mMRC score, mean (SD)	1.36 (0.90)
Episode of COPD exacerbation in the prior year, mean (SD)	1.12 (1.80)

Acronyms: SD, standard deviation; BMI, body mass index; TB, tuberculosis; BD, bronchodilator; FEV1, forced expiratory volume in 1 second; FVC, forced vital capacity; COPD, chronic obstructive pulmonary disease; CAT, COPD Assessment Test; mMRC, modified Medical Research Council.

numbers decreased from 55 during the year in which the study cases were included to 26 at the third year, as did the ratio of the number of hospitalized patients, from 14.2% to 9.6%, and the number of hospitalizations, from 83 to 45 (Table 2, Fig. 1). However, the mean length of stay (LOS) per hospitalization significantly increased, from 7.17 days to 10.73 days (p = 0.011). The total cost of hospitalization with diagnostic codes J41-J44 and/or J12-J18 did not reveal a decreasing trend between the year before and the third year after study enrollment, with an upward trend in the cost of hospitalization per day per hospitalization. The number and rate of intensive care unit (ICU) admissions showed a decreasing trend between the year of enrollment and the third year. The number of hospitalization deaths and the mortality rate of hospitalized patients revealed a decreasing trend as well.

In terms of emergency department (ED) visits only, the total cost, number of patients and number of visits generally revealed a downward trend, but the mean cost per ED visit did not show a consistent trend. The total number of ED visits and hospitalizations decreased year by year since study enrollment. The total costs for ED visits and hospitalizations were decreasing, except in the third year after study enrollment. The mean cost per hospitalization and per ED visit was insignificantly inconsistent (p=0.170 and 0.879, respectively) (Table 2). The mean medical costs for ED visits and hospitalizations with codes J41-J44 and J12-J18 disclosed an upward trend (p=0.039), but the number of hospitalizations or ED visits only revealed a significant downward trend (p=0.035) (Table 3).

Table 4 lists the statistical data on hospitalizations only, including the number of patients, number of hospitalizations, costs, and mean LOS categorized by ICD-10 codes. Regardless of whether the diagnostic codes were J41-J44 or J12-J18, the number of hospitalized patients and the number of hospitalizations for both codes showed a decreasing trend between study enrollment and the 3-year follow-up. Nevertheless, the mean LOS and cost of hospitalizations for both the J41-J44 and J12-J18 groups did not reveal a consistent decreasing trend.

Subgroup analysis revealed that patients with DM, a GOLD classification, lower mean pre- and post-BD FEV1 at baseline lung function, COPD, a higher mean CAT and mMRC score, and an episode of COPD exacerbation within the prior year had a significantly higher tendency to visit the ED or become hospitalized (Table 5). The GOLD classification was a

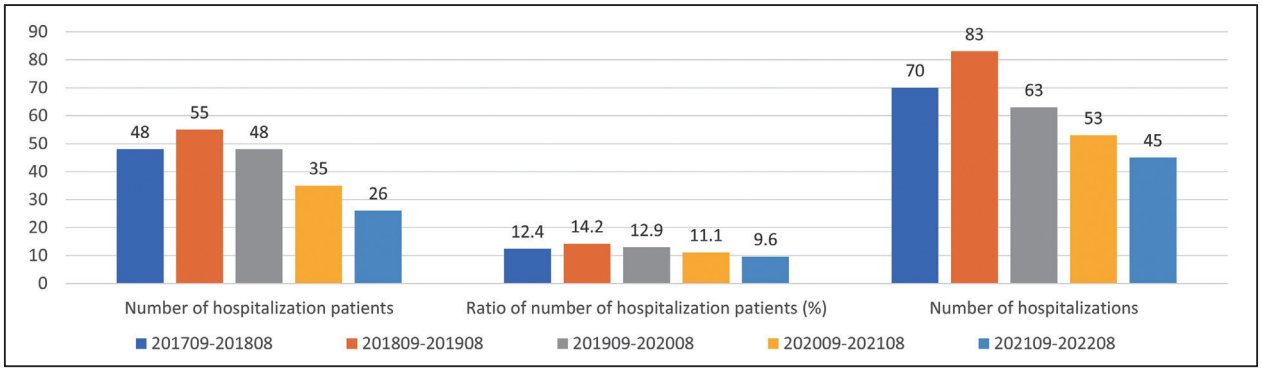

Fig. 1. Statistical data on the number of hospitalized patients, ratio of number of hospitalized patients and number of hospitalizations

Table 2. Statistical Data on emergency or Hospital Admissions with Primary Diagnosis Codes of J41-J44 and J12-J18

	Time interval for J41-J44 and J12-J18					*p* value
	2017/09-2018/08	2018/09-2019/08	2019/09-2020/08	2020/09-2021/08	2021/09-2022/08	
Number of hospitalized patients	48	55	48	35	26	
Ratio of number of hospitalized patients (%)	12.4 (48/388)	14.2 (55/388)	12.9 (48/373)	11.1 (35/316)	9.6 (26/271)	
Number of hospitalizations	70	83	63	53	45	
Total LOS	472	595	441	420	483	
Total cost of hospitalization	2,789,055	3,611,625	2,574,709	2,613,270	2,938,738	
Cost of hospitalization per day per hospitalization	84.4	73.1	92.7	117.4	135.2	
LOS per hospitalization, mean (SD)	6.74 (5.86)	7.17 (4.79)	7.00 (5.15)	7.92 (7.18)	10.73 (9.32)	0.011
Medical costs per hospitalization, mean (SD)	39,843.64 (53,786.45)	43,513.55 (44,564.62)	40,868.40 (40,826.21)	49,306.98 (81,391.66)	65,305.29 (75,150.96)	0.170
Number of ICU admissions	1	4	0	1	2	
Rate of ICU admission	1.43% (1/70)	4.82% (4/83)	0.00% (0/63)	1.89% (1/53)	4.44% (2/45)	
Number of hospitalization deaths	-	5	4	1	1	
Mortality rate of hospitalization	-	6.02% (5/83)	6.35% (4/63)	1.89% (1/53)	2.22% (1/45)	
Number of patients with an ED visit only	20	29	25	10	9	
Number of ED visits only	23	45	26	10	11	
Total costs for patients with ED visits only	98 934	2 150 19	130 105	50 731	46 485	
Costs per ED visit, mean (SD)	4,301.5 (2,127.60)	4,778.2 (3,341.53)	5,004.0 (3,059.04)	5,073.1 (2,629.61)	4,225.9 (2,323.34)	0.879
Number of ED visits and hospitalizations	93	128	89	63	56	
Total costs for ED visit and hospitalization	2,887,989	3,826,644	2,704,814	2,664,001	2,985,223	

Acronyms: LOS, length of stay; SD, standard deviation; ED, emergency department; ICU, intensive care unit.

* The cost unit is the New Taiwan dollar.

** If the primary diagnosis in the ER is J41-J44 or J12-J18, but the primary diagnosis during hospitalization is not J41-J44 or J12-J18, then it is not included in the above statistics.

*** There are 46 records where the primary diagnostic code in the ER is J41-J44, but the primary diagnostic code during hospitalization is J12-J18.

**** There are 14 records where the primary diagnostic code in the ER is J12-J18, but the primary diagnostic code during hospitalization is J41-J44.

Table 3. Medical Costs for Emergency Department Visits and Hospitalizations

	Time interval for J41-J44 and J12-J18					*p* value
	2017/09-2018/08 (n=93)	2018/09-2019/08 (n=128)	2019/09-2020/08 (n=89)	2020/09-2021/08 (n=63)	2021/09-2022/08 (n=56)	
Mean medical cost (SD)	31,053.65 (49,076.74)	29,895.66 (40,384.54)	30,391.17 (38,026.17)	42,285.73 (76,306.06)	53,307.55 (71,545.02)	0.039
Number of hospitalizations or ED visits only, n (%)						0.035
Number of hospitalizations	70 (75.27)	83 (64.84)	63 (70.79)	53 (84.13)	45 (80.36)	
Number of ED visits only	23 (24.73)	45 (35.16)	26 (29.21)	10 (15.87)	11 (19.64)	

Acronyms: ED, emergency department; SD, standard deviation.

* The cost unit is the New Taiwan dollar.

Table 4. Statistical Data on Hospitalization Only with Primary Diagnostic Codes of J41-J44 and J12-J18, Separately

	Time interval					*p* value
	2017/09-2018/08	2018/09-2019/08	2019/09-2020/08	2020/09-2021/08	2021/09-2022/08	
Number of patients hospitalized for J41-J44	35	33	22	21	12	
Number of hospitalizations for J41-J44	45	47	31	28	21	
LOS per hospitalization for J41-J44, mean (SD)	5.64 (3.59)	5.74 (3.18)	5.90 (2.49)	8.32 (9.31)	7.81 (5.18)	0.094
Mean medical cost per hospitalization for J41-J44 (SD)	29819.93 (25,245.96)	30280.53 (14,770.01)	28970.39 (13,157.76)	55844.14 (110,855.83)	43519.48 (29,715.44)	0.130
Total medical cost of hospitalization for J41-J44	1,341,897	1,423,185	898,082	1,563,636	913,909	
Number of hospitalization patients for J12-J18	22	28	28	17	16	
Number of hospitalizations for J12-J18	25	36	32	25	24	
LOS per hospitalization for J12-J18, mean (SD)	8.72	9.03	8.06	7.48	13.29	
Total medical costs of hospitalization for J12-J18	1,447,158	2,188,440	1,676,627	1,049,634	2,024,829	

Acronyms: LOS, length of stay; SD, standard deviation.

* The cost unit is the New Taiwan dollar.

Table 5. Subgroup Analysis of Patients who Have or Have not had an ED visit or Hospitalization (Data on Variables is from the Time of Enrollment in the P4P Program)

Variables	No ED visit or hospitalization n=231	Have had an ED visit or hospitalization n=157	*p* value
Gender, n (%)			0.095
Female	44 (19.05)	42 (26.75)	
Male	187 (80.95)	115 (73.25)	
Age (y), mean (SD)	72.18 (8.91)	73.30 (9.80)	0.254
BMI (kg/m2), mean (SD)	24.91 (4.13)	24.32 (4.28)	0.177
Smoking status (%)			
History of smoking	161 (69.70)	112 (71.34)	0.815
Quit smoking	112 (48.48)	85 (54.14)	0.322
Underlying disease, n (%)			
Hypertension	116 (50.22)	90 (57.32)	0.203
Diabetes mellitus	40 (17.32)	49 (31.21)	0.002
Cardiovascular disease	102 (44.16)	77 (49.04)	0.398
Old pulmonary TB	22 (9.52)	15 (9.55)	0.868
Gold classification, n (%)			0.002
GOLD I	64 (27.71)	21 (13.38)	
GOLD II	119 (51.52)	83 (52.87)	
GOLD III	41 (17.75)	45 (28.66)	
GOLD IV	7 (3.03)	8 (5.10)	
Baseline lung function			
Pre-BD-FEV1 (L), mean (SD)	1.41 (0.54)	1.14 (0.42)	<0.001
Pre-BD-FEV1(%), mean (SD)	63.88 (19.73)	54.55 (18.20)	<0.001
Pre-BD-FEV1/FVC(%), mean (SD)	54.17 (10.85)	51.88 (12.62)	0.065
Post-BD-FEV1(L), mean (SD)	1.47 (0.56)	1.21 (0.44)	<0.001
Post-BD-FEV1(%), mean (SD)	66.90 (20.46)	57.75 (18.71)	<0.001
Post-BD-FEV1/FVC(%), mean (SD)	54.54 (11.63)	52.43 (12.82)	0.101
COPD Group, n (%)			<0.001
A	152 (65.80)	39 (24.84)	
B	44 (19.05)	25 (15.92)	
C	22 (9.52)	41 (26.11)	
D	13 (5.63)	52 (33.12)	
CAT score, mean (SD)	7.22 (5.04)	10.57 (5.96)	<0.001
mMRC score, mean (SD)	1.16 (0.80)	1.64 (0.96)	<0.001
Episode of COPD exacerbation in the prior year mean (SD)	0.58 (1.29)	1.91 (2.12)	<0.001

Acronyms: SD, standard deviation; BMI, body mass index; TB, tuberculosis; BD, bronchodilator; FEV1, forced expiratory volume in 1 second; FVC, forced vital capacity; COPD, chronic obstructive pulmonary disease; CAT, COPD Assessment Test; mMRC, modified Medical Research Council.

potential risk factor for an ED visit or hospitalization, with overall statistical significance ($p = 0.002$), and GOLD grade III seemed to have a higher risk tendency than GOLD grade I. Likewise, COPD was a potential risk factor for an ED visit or hospitalization, with overall statistical significance ($p < 0.001$), and COPD groups C and D seemed to have a higher risk tendency than groups A and B (Table 5).

Discussion

Our study results suggested that the number and ratio of hospitalized patients, the number of hospitalizations and the number of ED visits tended to decrease within 3 years after the patients enrolled in the P4P program. However, for patients with diagnostic codes J41-J44 and/or J12-J18, there was no obvious decreasing trend in the mean medical costs for ED visits and hospitalizations, ED visits only or hospitalization. Similar findings were observed for cases coded J41-J44, in that the mean costs per hospitalization did not reveal a downward trend. Regardless of ICD-10 codes, the mean LOS also revealed an inconsistent trend. During the study period, COVID-19 was prevalent globally, including in Taiwan. Possible factors affecting medical costs included pneumonia caused by COVID-19 infection, the severity of the disease, and additional out-of-pocket expenses requested by family members, such as private rooms or other items which were not included in Taiwan's National Health Insurance (NHI) system.

In addition, a study published in 2024 found that during the COVID-19 pandemic, there was a substantial decrease in hospital admissions for AECOPD and an increase in in-hospital deaths [18]. Another report using data from the National Inpatient Sample (NIS) and Nationwide Emergency Department Sample (NEDS), Healthcare Cost and Utilization Project (HCUP) and Agency for Healthcare Research and Quality found that compared to the previous year, the number of hospitalizations for AECOPD, the aggregate hospitalization cost, and the total number of visits to the ED decreased in 2020, while the cost per hospital stay increased [19]. Decreased availability of hospital beds and staff for non-COVID-19 diseases and greater reluctance to visit hospitals during a respiratory pandemic were also proposed in this article [19], and it may be an explanation of why the number of ED visits and hospitalizations decreased during our study period. In addition, a decreasing trend in the number of hospitalizations or hospitalized patients, with an increasing trend in medical costs and LOS may imply an increasing severity of diseases, including COPD, pneumonia and other comorbidities.

Previous studies demonstrated the benefits of the P4P program in Taiwan [12-13]. Cheng SL, *et al*. published a retrospective study on the nationwide COPD P4P program with regard to COPD exacerbations using Taiwan's NHI database in 2021 that revealed a significantly decreased prevalence of COPD-related ED visits and hospitalizations in patients with COPD in the COPD P4P program at 1 year after enrollment [12]. Cheng KC, *et al*. also published a real-world, retrospective study of 1081 patients who participated in the national COPD P4P program in Taiwan [13], and reported that the intervention of the P4P program could help improve the clinical outcome of COPD patients after 1 year of follow-up. However, neither of the aforementioned studies presented the economic effect of the P4P program. In addition, the follow-up period for the study cases was

only 1 year. To our knowledge, this is the first Taiwanese COPD P4P study that introduced data including medical costs up to the 3-year follow-up.

Subgroup analysis in our study revealed DM as a significant factor, in that patients with COPD and DM had a higher tendency to visit the ED or to be hospitalized, even if the patients were included in the P4P program. A review in 2023 found that elevated blood glucose levels, with or without DM, are strongly associated with an increased risk of subsequent severe AECOPD [20]. Comorbid diseases, including DM, are associated with a higher risk of hospitalization [21]. Another study also reported that patients hospitalized for COPD and with coexisting DM have worse clinical outcomes and higher 30-day readmissions rates than patients hospitalized for COPD without DM [22]. Hyperglycemia increases susceptibility to infection, and infections are a major cause of exacerbations [23], which are mainly triggered by respiratory viral and/or bacterial infections [1, 24]. This may explain why patients with COPD and DM in our study had higher percentages of ED visits or hospitalization.

There are several limitations in this study. First, our database did not include information such as residences, work, types and doses of BD treatment, eosinophil counts or other factors that might have a possible influence on study results. Second, no control group was included in this study, hence there should be careful interpretation of the results. Third, we did not list COVID-19 infection case numbers in the study. Whether these results may be influenced by P4P program enrollment is unknown.

Conclusion

This study revealed the benefits of enrollment in the P4P program for patients with COPD. The P4P program provides a different kind of medical care concept in an integrated multidisciplinary manner. The program is expected to improve patients' outcomes, reduce medical costs, based on Taiwan's NHI system, and facilitate the provision of quality healthcare by physicians. Further studies with longer follow-up periods are warranted to distinguish the effectiveness of the P4P program and other factors or comorbidities that may have an impact on emergency visits or hospitalization of patients with COPD.

References

1. Global Initiative for Chronic Obstructive Lung Disease (GOLD). Global Strategy for the Diagnosis, Management and Prevention of Chronic Obstructive Pulmonary Disease: 2024 Report. Available from: https://goldcopd.org/wp-content/uploads/2024/02/GOLD-2024_v1.2-11Jan24_WMV.pdf
2. Rehman AU, Ahmad Hassali MA, Muhammad SA, *et al*. The economic burden of chronic obstructive pulmonary disease (COPD) in the USA, Europe, and Asia: results from a systematic review of the literature. Expert Rev Pharmacoecon Outcomes Res 2020; 20(6): 661-672.
3. Tsai YH, Yang TM, Lin CM, *et al*. Trends in health care resource utilization and pharmacological management of COPD in Taiwan from 2004 to 2010. Int J Chron Obstruct Pulmon Dis 2017; 12: 2787-2793.
4. Willemse BW, Postma DS, Timens W, *et al*. The impact of smoking cessation on respiratory symptoms, lung function, airway hyperresponsiveness and inflammation. Eur Respir J 2004; 23(3): 464-476.
5. Bauer CMT, Morissette MC, Stämpfli MR. The influence of cigarette smoking on viral infections: translating bench science to impact COPD pathogenesis and acute exacerbations of COPD clinically. Chest 2013; 143(1): 196-206.
6. Anthonisen NR, Connett JE, Murray RP. Smoking and lung function of Lung Health Study participants after 11

years. Am J Respir Crit Care Med 2002; 166(5): 675-679.
7. Anthonisen NR, Skeans MA, Wise RA, *et al*. The effects of a smoking cessation intervention on 14.5-year mortality: a randomized clinical trial. Ann Intern Med 2005; 142(4): 233-239.
8. Lu HY, Chen CF, Lee DL, *et al*. Effects of early pulmonary rehabilitation on hospitalized patients with acute exacerbation of chronic obstructive pulmonary disease: a systematic review and meta-analysis. Int J Chron Obstruct Pulmon Dis 2023 May 15; 18: 881-893.
9. Ryrsø CK, Godtfredsen NS, Kofod LM, *et al*. Lower mortality after early supervised pulmonary rehabilitation following COPD-exacerbations: a systematic review and meta-analysis. BMC Pulm Med 2018 Sep 15; 18(1): 154.
10. Puhan MA, Gimeno-Santos E, Cates CJ, *et al*. Pulmonary rehabilitation following exacerbations of chronic obstructive pulmonary disease. Cochrane Database Syst Rev 2016 Dec 8; 12(12): CD005305.
11. Lindenauer PK, Stefan MS, Pekow PS, *et al*. Association between initiation of pulmonary rehabilitation after hospitalization for COPD and 1-year survival among Medicare beneficiaries. JAMA 2020 May 12; 323(18): 1813-1823.
12. Cheng SL, Li YR, Huang N, *et al*. Effectiveness of nationwide COPD pay-for-performance program on COPD exacerbations in Taiwan. Int J Chron Obstruct Pulmon Dis 2021; 16: 2869-2881.
13. Cheng KC, Lai CC, Wang CY, *et al*. The impact of the pay-for-performance program on the outcome of COPD patients in Taiwan after one year. Int J Chron Obstruct Pulmon Dis 2022; 17: 883-891.
14. Puebla Neira DA, Hsu ES, Kuo YF, *et al*. Readmissions reduction program: mortality and readmissions for chronic obstructive pulmonary disease. Am J Respir Crit Care Med 2021; 203(4): 437-446.
15. Myers LC, Faridi MK, Hasegawa K, *et al*. The Hospital Readmissions Reduction Program and readmissions for chronic obstructive pulmonary disease, 2006-2015. Ann Am Thorac Soc 2020; 17(4): 450-456.
16. Park HJ, Kim SR, Kim S, *et al*. Influence of government-driven quality assessment program on patients with chronic obstructive pulmonary disease. Respir Res 2021; 22(1): 87.
17. Stone PW, Adamson A, Hurst JR, *et al*. Does pay-for-performance improve patient outcomes in acute exacerbation of COPD admissions? Thorax 2022; 77(3): 239-246.
18. Ahn C, Park Y. Chronic obstructive pulmonary disease mortality and hospitalization during the COVID-19 pandemic compared with before the pandemic: a systematic review and meta-analysis. J Pers Med 2024; 14(3): 296.
19. Balavenkataraman A, Saunders H, Helgeson SA. Trends in outcomes of hospitalizations from acute exacerbations of chronic obstructive pulmonary disease during the COVID-19 pandemic. Lung India 2024; 41(1): 77-79.
20. Cazzola M, Rogliani P, Ora J, *et al*. Hyperglycaemia and chronic obstructive pulmonary disease. Diagnostics (Basel) 2023; 13(21): 3362.
21. Mannino DM, Thorn D, Swensen A, *et al*. Prevalence and outcomes of diabetes, hypertension and cardiovascular disease in COPD. Eur Respir J 2008; 32(4): 962-969.
22. Belligund P, Attaway A, Lopez R, *et al*. Diabetes associated with higher health care utilization and poor outcomes after COPD-related hospitalizations. Am J Manag Care 2022; 28(9): e325-e332.
23. Crisafulli E, Torres A, Huerta A, *et al*. C-reactive protein at discharge, diabetes mellitus and ≥ 1 hospitalization during previous year predict early readmission in patients with acute exacerbation of chronic obstructive pulmonary disease. COPD 2015; 12(3): 306-314.
24. Sapey E, Bafadhel M, Bolton CE, *et al*. Building toolkits for COPD exacerbations: lessons from the past and present. Thorax 2019; 74(9): 898-905.

Characteristics and Outcome Analysis of Pneumonia with Bloodstream Infection Caused by Carbapenem-Resistant *Klebsiella Pneumoniae* in Critically Ill Patients with Respiratory Failure: A 5-Year Retrospective Study

Mei-Yuan Teo[1], Bing-Chen Wu[1], Shaw-Woei Leu[1], Kuo-Chin Kao[1,2], Han-Chung Hu[1,2]

Background: Infections caused by carbapenem-resistant *Klebsiella pneumoniae* (CRKP) have emerged as a serious threat to the lives of patients in intensive care units (ICUs). In this study, we aimed to analyze the outcome of critically ill patients with pneumonia with bloodstream infections (BSIs) caused by CRKP to enhance treatment and prognosis.

Methods and materials: We conducted a retrospective study involving data from ICU-treated patients with CRKP-induced pneumonia with BSIs at Chang Gung Memorial Hospital, Linkou branch, from January 2017 to December 2021. Clinical characteristics, laboratory data, and treatment and outcome information were collected. Predictive factors were analyzed using statistical methods to determine their association with outcomes.

Results: A total of 161 patients were included in the study. The all-cause ICU mortality rate was 72%, and the 30-day mortality rate was 65%. Most CRKP clinical isolates were carbapenemase producers (132/161; 81.9%), of which *K. pneumoniae* carbapenemase-producing isolates were most prevalent (112/132; 84.8%). Cox regression analysis revealed that the use of appropriate antibiotics within 48 hours (HR 0.47, CI 95% 0.26–0.85, $p = 0.013$) was associated with a favorable outcome, while a high sequential organ failure assessment score (HR 1.24, CI 95% 1.15–1.35, $p < 0.001$) was associated with death.

Conclusion: Administering appropriate antibiotics within 48 hours after onset of CRKP pneumonia with BSI has been identified as vital for reducing 30-day mortality in critically ill patients with respiratory failure. ***(Thorac Med 2025; 40: 13-21)***

Key words: Bloodstream infections, carbapenem-resistant *Klebsiella pneumoniae*, mortality rate, appropriate antibiotic treatments, critically ill patients

[1]Department of Thoracic Medicine, Chang Gung Memorial Hospital, Taoyuan 33305, Taiwan, [2]Department of Respiratory Therapy, Chang Gung University College of Medicine, Taoyuan 33302, Taiwan.
Address reprint requests to: Dr. Han-Chung Hu, No.5, Fuxing St., Guishan Dist., Taoyuan City 333, Taiwan.

Introduction

Treatment for carbapenem-resistant Klebsiella pneumoniae (CRKP) infections is gradually becoming a challenge for clinicians worldwide because of the limited choice of antimicrobial agents [1]. Due to the widespread use of broad-spectrum antibiotics in critically ill and immunocompromised patients, the incidence of carbapenem-resistant strains is continuously increasing in intensive care units (ICU) [2]. Compared to carbapenemase-susceptible *K. pneumoniae* infections, CRKP infections carry a higher risk of fatal outcomes in critically ill patients [3].

According to the Taiwan Centers for Disease Control, *K. pneumoniae* has been the leading cause of infections in the ICUs of medical centers in Taiwan since 2018. The prevalence of CRKP infections in Taiwan's ICUs increased from 14.4% in 2014 to 45.5% in 2023 [4].

In critically ill patients, pneumonia with bloodstream infection (BSI) is common, particularly in patients with mechanical ventilation (MV) [5]. A study has indicated that patients with pneumonia and BSI have a higher likelihood of developing septic shock and have increased hospital mortality rates compared to those without BSI; the most prevalent pathogen in blood culture from these patients was *K. pneumoniae*, a Gram-negative pathogen [6]. A Taiwanese study indicates that the 28-day mortality rate for patients with *K. pneumoniae*-induced nosocomial pneumonia with BSI is 60.2%, and the prevalence of CRKP is as high as 58.2% [7]. Therefore, it is evident that pneumonia with BSI is highly lethal in critically ill patients, and that it is crucial for clinicians to prioritize this condition and to determine the most effective treatment approach. However, most previous studies on CRKP infections have primarily focused on BSI. Only a few investigations have focused on CRKP pneumonia, and even fewer on critically ill patients.

In this study, we aimed to identify outcomes of critically ill patients with pneumonia with BSIs caused by CRKP, so as to enhance treatment and prognosis.

Materials and Methods

Study Design

This retrospective study was conducted from January 2017 to December 2021 in Chang Gung Memorial Hospital (CGMH), Linkou branch, a major medical center in Taiwan. We included adult patients aged ≥18 years, with respiratory failure necessitating MV, admitted to the ICU, and diagnosed with hospital-acquired pneumonia with BSI caused by CRKP. The protocol was approved by the institutional review board of CGMH, with the approval number 201801433B0, indicating that this research involving human subjects followed the necessary ethical guidelines.

Data Collection

The medical records of each patient were reviewed and the following data were collected from the day of diagnosis of pneumonia with BSI: age; sex; Charlson comorbidity index (CCI); carbapenemase genes; previous 30-day antibiotics used; days of MV; duration of appropriate antibiotic use, which is defined as the time required to use a sensitive antibiotic; antibiotic regimen used; and laboratory examinations. Disease severity was evaluated within 24 hours of diagnosis using the Sequential Organ Failure Assessment (SOFA) score and Pitt bacteremia score [8].

Definitions and Outcomes

We established the following definitions before conducting our data collection and analysis processes. The diagnosis of pneumonia was in accordance with the guidelines of the American Thoracic Society (ATS) and Infectious Diseases Society of America (IDSA) [9]. The guidelines require identification of new or progressive pulmonary infiltrates on chest radiography and collected cultures that exhibit evidence of the same pathogen found in the blood cultures. A CRKP-induced BSI was defined as the occurrence of a positive blood culture result for a CRKP strain and the presence of clinical signs of systemic inflammatory response syndrome [10]. Furthermore, appropriate antibiotic treatment within 24 or 48 hours after pneumonia with BSI onset was defined as the administration of 1 or more antibiotics to which the CRKP strain exhibited in vitro susceptibility within 24 or 48 hours after pneumonia with BSI onset. Finally, antibiotic treatment within the previous 30 days was defined as the intravenous administration of antibiotics for at least 5 days within the 30 days preceding pneumonia with BSI onset. The clinical outcome of the study was the identification of predictive factors for ICU all-cause mortality and 30-day mortality.

Microbiology Analysis

Microbiological studies, carbapenemase genes detection and capsular typing identification of *K. pneumoniae* was performed using a matrix-assisted laser desorption-time of flight mass spectrometry (MALDI-TOF-MS). Minimum inhibitory concentration (MIC) of tested antibiotics was determined by a BD PhoenixTM M50 automatic detection machine. CRKP was defined as MICs of $\geq 4\,\mu g/ml$ for either imipenem or meropenem, or MICs of $\geq 2\,\mu g/ml$ for ertapenem. MIC was classified according to breakpoints established by the Clinical and Laboratory Standards Institute (CLSI). The carbapenemase genes blaKPC, blaOXA-48, blaNDM, blaGES, blaVIM, blaIMP, blaSPM, blaGIM, and blaSIM were screened by multiplex polymerase chain reaction (PCR) using the DreamTaq system (Thermo Fisher Scientific, Vilnius, Lithuania). Two PCR reactions were conducted with a group of primers for detecting blaKPC, blaOXA-48, blaNDM, and blaGES, and a group of primers for detecting blaVIM, blaIMP, blaSPM, blaGIM, and blaSIM.

Statistical Analyses

Unless otherwise indicated, all data are expressed as mean ± standard deviation or percentages. Student's t test was used to compare the means of normally distributed continuous data between the 2 groups; otherwise, the Mann–Whitney test was used. The modified Wald method was used to calculate 95% confidence intervals (CI) for proportions. Fisher's exact test, and Pearson testing were used for categorical variables where appropriate. Kaplan-Meier curves were used to compare time-to-hospital-mortality in the various cohorts. Cox proportional hazards models on time-to-hospital-mortality were used to calculate adjusted hazard ratios (aHR). For time-to-mortality analyses, patients were censored at the time of hospital discharge, or if they were still admitted and alive at 30 days after the first positive culture, their data were censored at 30 days after the date of the first positive culture. Forward selection was used for inclusion of variables in multivariable Cox proportional hazards models; any variable that was associated with time-to-hospital-mortality at $p < 0.1$ was included. Statistical analyses were performed using SPSS

software, version 26 122 (IBM Corporation, Armonk, New York, United States). The statistical significance level was set at a p value of <0.05.

Results

A total of 560 patients who had CRKP isolated from blood cultures during the period from January 2017 to December 2021 were identified. We ruled out patients aged < 18 years, those without ICU admissions, and those with other infection sites. Thus, 161 patients were included for analysis (Fig. 1). All patients experienced respiratory failure and were on MV. The 161 enrolled patients had a median age of 69.2 years, and 114 (71%) were male. At diagnosis, the median CCI, Pitt bacteremia score, and SOFA score were 6.6 ± 3.3, 6.2 ± 2.9, and 10.6 ± 4.5, respectively. A total of 111 patients (69%) suffered from acute kidney injury after pneumonia with BSI onset, and 36 of these patients (22%) required continuous renal replacement therapy. Intravenous antibiotics for at least 5 days within 30 days before CRKP-induced pneumonia with BSI onset had been received by 132 (82%) patients. The 132 patients had carbapenemase, and the majority was KPC (70%), followed by OXA-48 (12%) and NDM (7%). Table 1 shows the baseline characteristics of the patients who did and did not survive in the ICU after pneumonia with BSI onset.

The all-cause ICU mortality rate was 72% and the 30-day mortality rate was 65%. Compared with surviving patients, those who died had a higher CCI (7.7 ± 4.0 vs 6.1 ± 2.9, $p < 0.015$), Pitt bacteremia score (6.9 ± 2.7 vs 4.1 ± 2.6, $p < 0.001$), and SOFA score (11.9±4.0 vs 7.1 ± 3.7, $p < 0.001$), more patients who had underlying disease with leukemia (9% vs 0%, $p < 0.032$), and a greater need for continuous renal replacement therapy in the ICU (28% vs 7%, $p < 0.001$). In addition, lower hemoglobin levels (8.9 ± 1.5 vs 9.4 ± 1.3, $p < 0.029$), lower platelet counts (87.5 ± 78.3 vs 156.7 ± 99.0, $p < 0.001$) and higher CRP levels (135.3 ± 97.4 vs 88.3 ± 73.0, $p < 0.001$) were found in non-

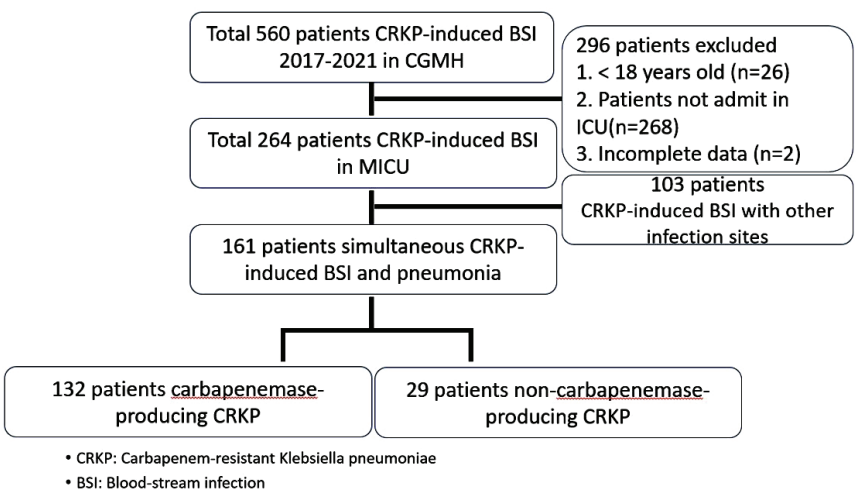

Fig. 1. Study flow chart Use "(number) patients with…." Below On the right side, use "Patients not admitted to the ICU (n=268) Also, use "bloodstream"

Table 1. Baseline Characteristics and Comorbidities of Critically ill Patients with Simultaneous Carbapenem-Resistant *K. pneumoniae*-Induced Bloodstream Infections and Pneumonia

	Total (N=161)	Surviving (N=45)	Non-surviving (N=116)	*p*-value
Age, years, mean (SD)	69.2±14.4	71.9±13.0	68.1±14.8	0.142
Male, n (%)	114 (71%)	29 (64%)	85 (73%)	0.292
Charlson comorbidity index	6.6±3.3	6.1±2.9	7.7±4.0	0.015
Pitt bacteremia score	6.2±2.9	4.1±2.6	6.9±2.7	<0.001
SOFA score	10.6±4.5	7.1±3.7	11.9±4.0	<0.001
Carbapenemase, n (%)	132 (82%)	38 (84%)	94 (81%)	0.616
KPC, n (%)	112 (70%)	31 (69%)	81 (70%)	0.908
NDM, n (%)	12 (7%)	10 (11%)	7 (6%)	0.336
OXA-48, n (%)	20 (12%)	7 (16%)	13 (11%)	0.456
IMP, n (%)	1 (1%)	0 (0%)	1 (1%)	0.535
DM	72 (45%)	17 (38%)	55 (47%)	0.270
Hypertension	94 (58%)	25 (56%)	69 (59%)	0.650
Liver cirrhosis	27 (17%)	5 (11%)	22 (19%)	0.231
Cardiovascular disease	31 (19%)	6 (13%)	25 (22%)	0.235
Congestive heart failure	29 (18%)	9 (20%)	20 (17%)	0.683
CKD	66 (41%)	19 (42%)	47 (41%)	0.844
COPD	21 (13%)	3 (7%)	18 (16%)	0.135
Autoimmune disease	13 (8%)	2 (5%)	11 (9%)	0.307
Leukemia	11 (7%)	0 (0%)	11 (9%)	0.032
Lymphoma	8 (5%)	1 (2%)	7 (6%)	0.308
Solid organ malignancy	30 (19%)	10 (23%)	20 (17%)	0.427
WBC (K)	13.7±9.8	12.1±7.2	14.3±10.7	0.152
Hb	9.0±1.4	9.4±1.3	8.9±1.5	0.029
Platelet (K)	106.6±89.7	156.7±99.0	87.5±78.3	<0.001
CRP	121.8±93.3	88.3±73.0	135.3±97.4	0.001
AKI, n (%)	111 (69%)	27 (60%)	84 (72%)	0.147
CRRT, n (%)	36 (22%)	3 (7%)	33 (28%)	<0.001
Previous 30-day antibiotic use, n (%)	132 (82%)	41 (91%)	91 (78%)	0.061
48-hour appropriate antibiotic, n (%)	97 (60%)	26 (58%)	71 (61%)	0.692

Table 2. Cox Regression Analysis for Identifying Factors Associated with 30-day Mortality in Critically Ill Patients with Simultaneous Carbapenem-Resistant *K. pneumoniae*-Induced Bloodstream Infections and Pneumonia

Variables	Univariate		Multivariate	
	HR (95%CI)	*P* value	HR (95%CI)	*P* value
C	0.62 (0.21-0.93)	0.022		
Pitt bacteremia score	1.12 (1.05-1.20)	0.001		
SOFA score	1.16 (1.09-1.22)	<0.001	1.24 (1.15-1.35)	<0.001
48-hour appropriate antibiotic	1.57 (1.07-2.31)	0.023	0.47 (0.26-0.85)	0.013

surviving patients.

The most common treatment regimens for CRKP-induced pneumonia with BSI were colistin-based (96 patients, 60%) and ceftazidime-avibactam-based (16 patients, 16%). A total of 97 patients (60%) received appropriate antibiotic treatments within 48 hours after BSI onset.

Cox regression analysis of factors associated with 30-day mortality is presented in Table 2. The presence of blaKPC genes, the Pitt bacteremia score, the SOFA score, and the administration of an appropriate antibiotic within 48 hours were found to have significant differences in univariate analysis. A higher SOFA score was associated with a higher HR (HR=1.24, 95% CI=1.15-1.35) for 30-day mortality, while the use of an appropriate antibiotic within 48 hours (HR=0.47, 95% CI=0.26-0.85) was associated with lower HRs for 30-day mortality (Fig 2).

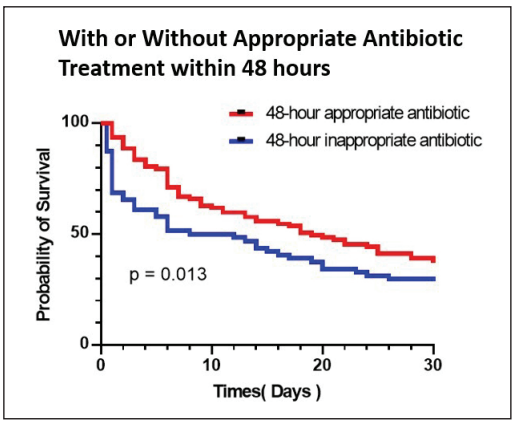

Fig. 2. Kaplan-Meier survival curves comparing survival outcomes in critically ill patients with simultaneous carbapenemase-resistant *K. pneumoniae*-induced bloodstream infections and pneumonia: Patients with or without appropriate antibiotic treatment within 48 hours after bloodstream infections onset.

Discussion

The results of our study revealed that the non-survival group had higher CCI scores, higher Pitt bacteremia scores, and higher SOFA scores. Comorbidity with leukemia was higher in the non-survival group. Additionally, in the multivariate Cox regression analysis, we found that the use of appropriate antibiotic treatments within 48 hours after BSI onset could improve 30-day mortality in critically ill patients with MV.

The ICU mortality rate in our study was notably high at 72%, and the 30-day mortality rate stood at 65%. These figures were higher than those from other studies [11-13], primarily due to the elevated comorbidity and severity observed in our patient population. Our study population consisted of critically ill patients who had respiratory failure that was treated in the ICU, multiple comorbidities, and high disease severity at the onset of simultaneous CRKP-

induced BSIs and pneumonia, as indicated by our CCI, Pitt bacteremia scores, and SOFA scores. Therefore, the higher mortality rates observed in our study underscore the unique challenges and risks associated with managing CRKP infections in critically ill individuals. Further research is needed to better understand and address these specific patient populations' healthcare needs and outcomes.

Comorbidity with leukemia was more prevalent in the non-survival group, although the total number of such cases was limited to just 11 patients. A retrospective study revealed a significant association between CRKP-induced BSIs and hematologic malignancies, with a notably high 28-day mortality rate of 77.3% [14]. In addition, several studies have consistently indicated that acute myeloid leukemia patients face a heightened risk of developing CRKP BSIs, emphasizing the effectiveness of timely diagnosis and treatment in improving survival outcomes [15-16].

In our study, carbapenemase-producing isolates accounted for 132 cases, constituting 82% of the total isolates. Among these, KPC-producing isolates were the most prevalent, representing 84.8%, followed by OXA-48 at 15.1%. This pattern is consistent with findings reported in other studies [3, 17-19]. An Italian study indicated that the use of 2 or more in vitro active antibiotics as definitive therapy led to a better outcome in cases of KPC-producing CRKP infections [20]. however, our study did not reveal a significant difference. This discrepancy may be attributed to the high severity of the cases in our study population. Furthermore, our research found that the use of an appropriate antibiotic within 48 hours was associated with improved 30-day mortality outcomes, which aligns with data from other studies [21-23]. The rapid diagnosis of CRKP infections might be considered a factor contributing to better outcomes, emphasizing the importance of early and accurate identification of the pathogen in clinical practice [24].

Our study has several limitations, with the primary ones being its single-center and retrospective study design. Furthermore, patients were enrolled before the introduction of newer antibiotics such as ceftazidime-avibactam; only 16 patients (10%) in our study received antibiotics containing ceftazidime-avibactam. Recent studies have indicated that ceftazidime-avibactam may offer potential advantages over colistin and other conventional antibiotics, which aligns with the findings in our study. Despite these limitations, the comprehensive data on critically ill patients can provide clinicians with valuable therapeutic insights and clinical guidance for managing CRKP-induced pneumonia with BSI.

Conclusion

Administering appropriate antibiotics within 48 hours after onset of CRKP-induced pneumonia with BSI has been identified as vital for reducing 30-day mortality in critically ill patients with respiratory failure. Employing advanced rapid molecular tests in patients at high risk of hospital-acquired CRKP infections is necessary and would enable timely and effective antibiotic treatment for these critically ill patients.

List of acronyms

BSIs: blood-stream infections; CCI: Charlson comorbidity index; CI: confidence interval; CRKP: carbapenem-resistant Klebsiella pneumoniae; CRP: C-reactive protein; HR: hazard

ratio; ICU: intensive care unit; KPC: Klebsiella pneumoniae carbapenemase; MIC: minimum inhibitory concentration; MV: mechanical ventilation; OR: odds ratios; PCR: polymerase chain reaction; SOFA: sequential organ failure assessment.

Declarations

Ethics approval and consent to participate:

This study was reviewed and approved by the Institutional Review Board of Chang Gung Memorial Hospital (Approval number: 201801433B0). Written informed consent for participation was not required for this study, in accordance with national legislation and institutional requirements.

Consent for publication: Not applicable.

Availability of data and materials:

The datasets used and/or analyzed during the current study are available from the corresponding author on reasonable request.

Competing interests:

The authors declare that they have no competing interests.

Authors' contributions:

MYT, BCW, and HCH planned and designed the study. MYT and BCW collected data. MYT and BCW performed microbiological analysis. MYT and BCW performed the statistical analysis. MYT, BCW, and HCH drafted the manuscript and designed tables and figures. SWL, KCK, and HCH reviewed the final version of the manuscript for intellectual content. All authors read and approved the final manuscript.

References

1. Kohler PP, Volling C, Green K, *et al*. Carbapenem resistance, initial antibiotic therapy, and mortality in Klebsiella pneumoniae bacteremia: a systematic review and meta-analysis. Infect Control Hosp Epidemiol 2017; 38(11): 1319-28.
2. Potter RF, D'Souza AW, Dantas G. The rapid spread of carbapenem-resistant Enterobacteriaceae. Drug Resist Updat 2016; 29: 30-46.
3. Chang YY, Chuang YC, Siu LK, *et al*. Clinical features of patients with carbapenem nonsusceptible Klebsiella pneumoniae and Escherichia coli in intensive care units: a nationwide multicenter study in Taiwan. J Microbiol Immunol Infect 2015; 48(2): 219-25.
4. Taiwan Healthcare-associated Infection and Antimicrobial Resistance Surveillance Report 2023. 2023.
5. Timsit JF, Ruppé E, Barbier F, *et al*. Bloodstream infections in critically ill patients: an expert statement. Intensive Care Med 2020; 46(2): 266-84.
6. Kim TW, Lee SU, Park B, *et al*. Clinical effects of bacteremia in sepsis patients with community-acquired pneumonia. BMC Infect Dis 2023; 23(1): 887.
7. Chen IR, Lin SN, Wu XN, *et al*. Clinical and microbiological characteristics of bacteremic pneumonia caused by Klebsiella pneumoniae. Front Cell Infect Microbiol 2022; 12: 903682.
8. Moreno R, Vincent JL, Matos R, *et al*. The use of maximum SOFA score to quantify organ dysfunction/failure in intensive care. Results of a prospective, multicentre study. Working Group on Sepsis related Problems of the ESICM. Intensive Care Med 1999; 25(7): 686-96.
9. Metlay JP, Waterer GW, Long AC, *et al*. Diagnosis and treatment of adults with community-acquired pneumonia. An official clinical practice guideline of the American Thoracic Society and Infectious Diseases Society of America. Am J Respir Crit Care Med 2019; 200(7): e45-e67.
10. Jeffrey M, Denny KJ, Lipman J, *et al*. Differentiating infection, colonisation, and sterile inflammation in critical illness: the emerging role of host-response profiling. Intensive Care Med 2023; 49(7): 760-71.
11. Chen IR, Huang PH, Wu PF, *et al*. Clinical characteristics

and outcomes of 56 patients with pneumonia caused by carbapenem-resistant Klebsiella pneumoniae. J Glob Antimicrob Resist 2021; 25: 326-30.

12. Hauck C, Cober E, Richter SS, *et al*. Spectrum of excess mortality due to carbapenem-resistant Klebsiella pneumoniae infections. Clin Microbiol Infect 2016; 22(6): 513-9.
13. Zhou C, Sun L, Li H, *et al*. Risk factors and mortality of elderly patients with hospital-acquired pneumonia of carbapenem-resistant Klebsiella pneumoniae infection. Infect Drug Resist 2023; 16: 6767-79.
14. Zhang P, Wang J, Hu H, *et al*. Clinical characteristics and risk factors for bloodstream infection due to carbapenem-resistant Klebsiella pneumoniae in patients with hematologic malignancies. Infect Drug Resist 2020; 13: 3233-42.
15. de Souza ILA, Cappellano P, Ferreira DB, *et al*. Carbapenem-resistant Klebsiella pneumoniae bloodstream infections in haematological malignances and hematopoietic stem cell transplantation: clinical impact of combination therapy in a 10-year Brazilian cohort. PLoS One 2024; 19(1): e0297161.
16. Trecarichi EM, Pagano L, Martino B, *et al*. Bloodstream infections caused by Klebsiella pneumoniae in onco-hematological patients: clinical impact of carbapenem resistance in a multicentre prospective survey. Am J Hematol 2016; 91(11): 1076-81.
17. Hsu JY, Chuang YC, Wang JT, *et al*. Healthcare-associated carbapenem-resistant Klebsiella pneumoniae bloodstream infections: risk factors, mortality, and antimicrobial susceptibility, 2017-2019. J Formos Med Assoc 2021; 120(11): 1994-2002.
18. Han R, Shi Q, Wu S, *et al*. Dissemination of carbapenemases (KPC, NDM, OXA-48, IMP, and VIM) among carbapenem-resistant enterobacteriaceae isolated from adult and children patients in China. Front Cell Infect Microbiol 2020; 10: 314.
19. Wu AY, Chang H, Wang NY, *et al*. Clinical and molecular characteristics and risk factors for patients acquiring carbapenemase-producing and non-carbapenemase-producing carbapenem-nonsusceptible-Enterobacterales bacteremia. J Microbiol Immunol Infect 2022; 55(6 Pt 2): 1229-38.
20. Falcone M, Russo A, Iacovelli A, *et al*. Predictors of outcome in ICU patients with septic shock caused by Klebsiella pneumoniae carbapenemase-producing *K. pneumoniae*. Clin Microbiol Infect 2016; 22(5): 444-50.
21. Falcone M, Bassetti M, Tiseo G, *et al*. Time to appropriate antibiotic therapy is a predictor of outcome in patients with bloodstream infection caused by KPC-producing Klebsiella pneumoniae. Crit Care 2020; 24(1): 29.
22. Zarkotou O, Pournaras S, Tselioti P, *et al*. Predictors of mortality in patients with bloodstream infections caused by KPC-producing Klebsiella pneumoniae and impact of appropriate antimicrobial treatment. Clin Microbiol Infect 2011; 17(12): 1798-803.
23. Satlin MJ, Chen L, Patel G, *et al*. Multicenter clinical and molecular epidemiological analysis of bacteremia due to carbapenem-resistant Enterobacteriaceae (CRE) in the CRE epicenter of the United States. Antimicrob Agents Chemother 2017; 61(4).
24. Satlin MJ, Chen L, Gomez-Simmonds A, *et al*. Impact of a rapid molecular test for Klebsiella pneumoniae carbapenemase and ceftazidime-avibactam use on outcomes after bacteremia caused by carbapenem-resistant Enterobacterales. Clin Infect Dis 2022; 75(12): 2066-75.

Multiple Myeloma with Mediastinal Lymphadenopathy and Lung Consolidation Leading to Pulmonary Amyloidosis Diagnosis

Wei-Syun Hung[1], Chun-Yu Lin[1], Chih-Wei Wang[2], Yueh-Fu Fang[1]

Multiple myeloma is a rare hematologic malignancy. It is rarely involved in the lung, but may be associated with systemic amyloidosis and result in pulmonary amyloidosis. Pulmonary parenchymal involvement and mediastinal lymphadenopathy are rare manifestations of pulmonary amyloidosis, and have a poor outcome. Recently, amyloidosis showed a good response to a novel targeted therapy regimen. We reported a 66-year-old woman who was diagnosed with multiple myeloma and presented with mediastinal lymphadenopathy and lung consolidation. Pulmonary amyloidosis was confirmed by transbronchial lung biopsy and endobronchial ultrasound-guided transbronchial needle aspiration. Clinical physicians should be aware of pulmonary amyloidosis in multiple myeloma patients, and administer prompt, risk-adapted therapy. ***(Thorac Med 2025; 40: 22-27)***

Key words: multiple myeloma, pulmonary amyloidosis

Introduction

Multiple myeloma (MM) is a rare hematologic malignancy and is rarely involved in the lung [1]. However, MM has been associated with amyloid light chain (AL) amyloidosis, and both cases presented with a light chain protein deposit of 10-15% [2-3]. Amyloidosis involving the lung is relatively common, but rarely symptomatic [4]. Mediastinal adenopathy is common in systemic amyloidosis [5]. We report a woman with MM, who presented with mediastinal lymphadenopathy and lung consolidation that was further diagnosed as pulmonary amyloidosis.

Case Presentation

This was a 66-year-old female who had the underlying diseases of chronic hepatitis B and thalassemia without regular follow-up. She was found to have subnephrotic proteinuria and paraproteinemia in 2016 with an elevated IgA level (1030 mg/dl), and immunofixation electrophoresis revealed paraprotein of an IgA-lambda light chain. She refused the nephrologist's sug-

[1]Department of Thoracic Medicine, Chang Gung Memorial Hospital at Linkou, Taoyuan, Taiwan, [2]Department of Anatomic Pathology, Chang Gung Memorial Hospital, Tao-Yuan, Taiwan.
Address reprint requests to: Dr. Yueh-Fu Fang, Department of Thoracic Medicine, Chang Gung Memorial Hospital, No.5, Fuxing St., Guishan Dist., Taoyuan City 333, Taiwan.

gestion of a renal biopsy, but came back to the nephrology department for a proteinuria follow-up in 2022. Bone marrow exam was performed and MM was diagnosed. She was treated with a VTD (bortezomib, thalidomide and dexamethasone) regimen for the MM.

The patient was also referred to the chest department because her chest computed tomography (CT) revealed bilateral lung consolidation, interstitial thickening, enlarged mediastinal lymph node and right-side pleural effusion (Fig. 1). She presented with mild exertional dyspnea and night sweating, but no fever, cough, chest pain or weight loss was noted. Thoracentesis revealed yellowish, cloudy lymphocyte-predominant transudate, using Light criteria (leukocyte count: 1668, lymphocytes: 87%, pleural effusion total protein: 2.4 g/dL, LDH: 133 U/L, serum total protein: 7.5 d/dL, LDH: 365 U/L), but cytology of pleural effusion showed no malignancy.

Endobronchial ultrasound-guided transbronchial needle aspiration (EBUS-TBNA) and transbronchial lung biopsy (TBLB) were performed (Fig. 2), and pathology showed an amyloid deposit using Congo red stain (Fig.

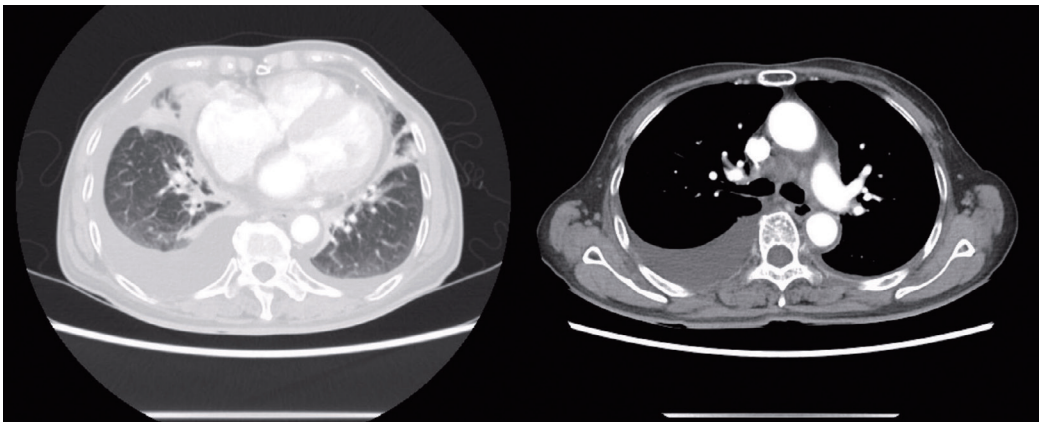

Fig. 1. Chest CT revealed bilateral lung consolidation, interlobular and septal thickening, an enlarged mediastinal lymph node and bilateral pleural effusion.

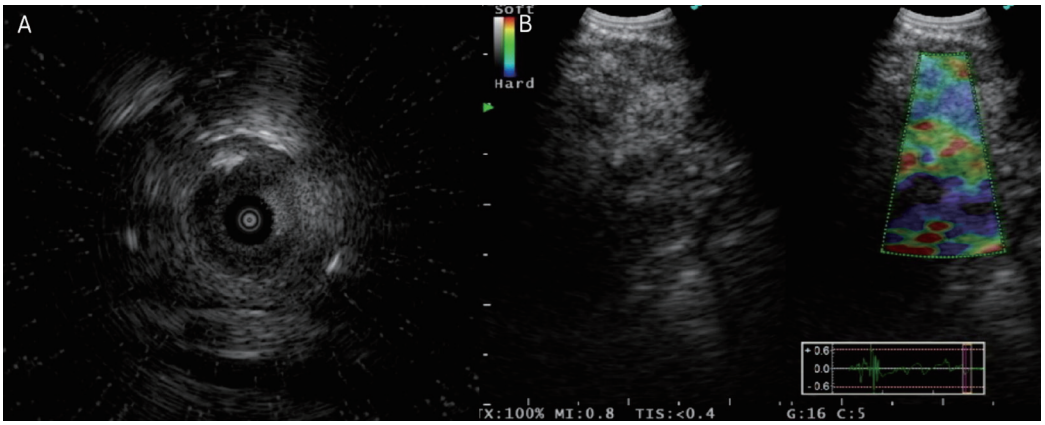

Fig. 2. A. Endobronchial ultrasound (EBUS) revealed an ill-defined margin with heterogeneous echogenicity and airbronchogram. B. Real-time EBUS showed a mediastinal lymph node with homogenous echogenicity, irregular shape and predominantly blue under elastography.

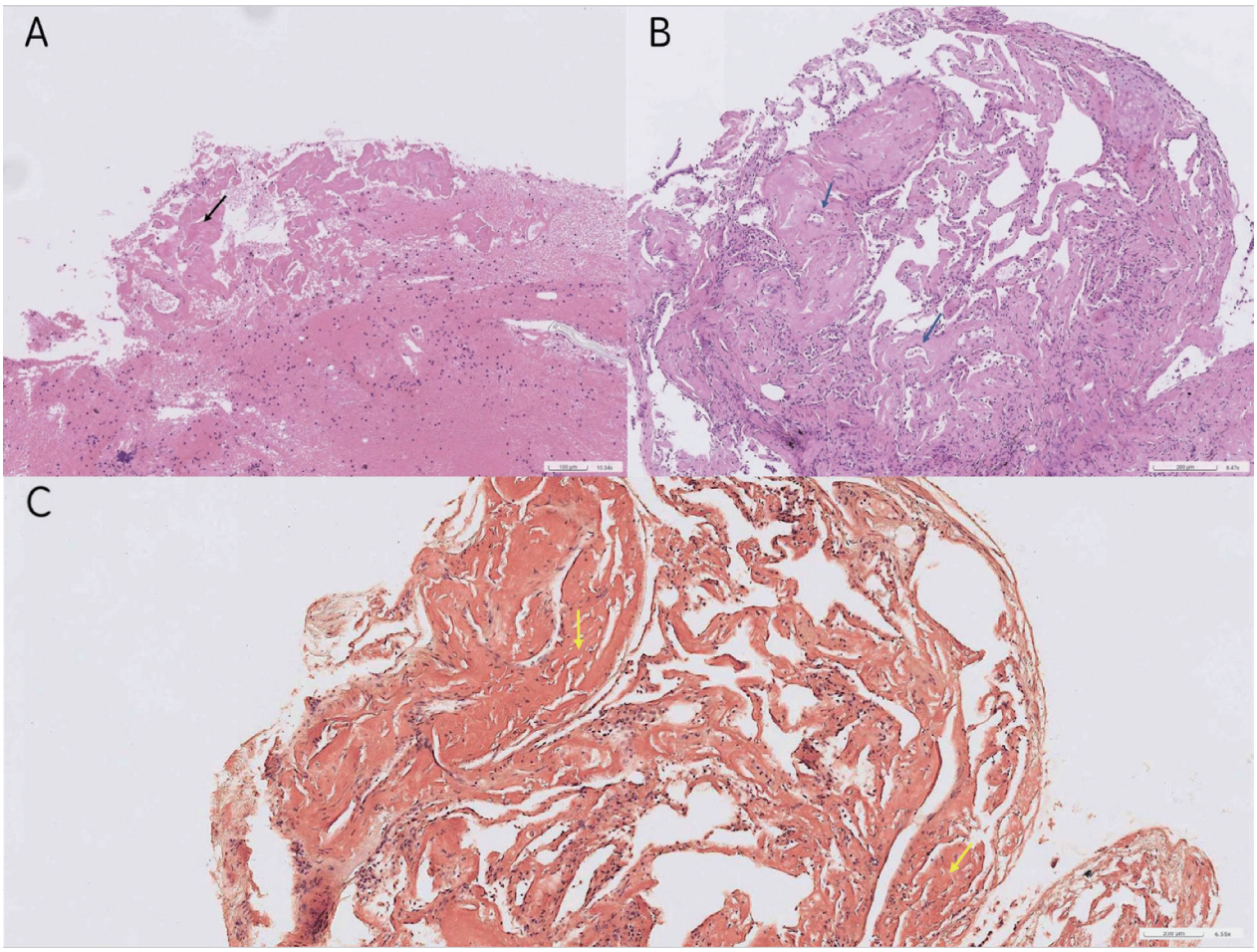

Fig. 3. A. Lymph node aspiration showed deposition of eosinophilic amyloid (hematoxylin and eosin stain, 200X, black arrow). B. The lung biopsy showed interstitial and perivascular deposition of amyloid (hematoxylin & eosin stain, 200X, blue arrow). C. The amyloid was positive for Congo red (200X, Congo red stain, yellow arrow).

3). Thus, pulmonary amyloidosis, with a more favored diffuse parenchymal pattern with an amyloid interstitial and perivascular deposit, was confirmed. Combined with her MM history with light chain monoclonal gammopathy, AL amyloidosis was favored. She refused cardiac or renal biopsy for further survey, but echocardiography revealed pulmonary hypertension. The patient now has regular follow-up at the chest department for persistent right pleural effusion and regular thoracentesis for symptom relief.

Discussion

Multiple myeloma (MM) accounts for 1% of all cancers, and approximately 10% of all hematologic malignancies [6]. The pulmonary area is an uncommon site of extramedullary involvement of MM. A review of 958 patients with MM disclosed that pulmonary infiltration is common (10%), and is mostly caused by infection; only 1 patient had lung myeloma. In addition, extramedullary intrathoracic plasmacytoma is rare, and is mostly presented in the

lung with a single lesion [1]. AL amyloidosis occurs in 10% to 15% of MM cases, but MM-associated pulmonary amyloidosis is uncommon (3.4%), as noted in amyloidosis autopsy reviews [2, 7-8].

Pulmonary amyloidosis is more common in systemic amyloidosis, compared to localized amyloidosis [4]. In addition, pulmonary parenchymal involvement is common in myeloma-associated amyloidosis [4, 7]. Pleural effusion, mediastinal lymphadenopathy and pulmonary hypertension are considered to be extraparenchymal pulmonary amyloidosis [9]. Our patient presented pulmonary parenchymal infiltration, mediastinal lymphadenopathy, pleural effusion, and pulmonary hypertension. Mediastinal lymphadenopathy is commonly related to systemic amyloidosis and is presented in punctuated, diffuse or eggshell calcification, but is often associated with parenchymal lung disease or pleural effusions [5, 10-11].

We compared some case reports on MM patients with pulmonary amyloidosis (Table 1) [12, 13]. Most cases presented with diffuse ground glass opacities or consolidation. Mediastinal lymphadenopathy was also noted, but none of these cases had approached mediastinal lymphadenopathy. Pulmonary hypertension is noted in most cases, and may be associated not only with left-side restrictive cardiomyopathy from amyloid deposition (group II pulmonary hypertension), but also with diffuse lung disease, as previous studies discussed [14-15].

Lung tissue biopsy is still the gold standard to diagnose myeloma in lung or pulmonary amyloidosis. Surgical lung biopsy (SLB) used to be the standard diagnostic method, due to its high yield (over 90%) in diagnosing interstitial lung disease [16]. However, it also carries a high inpatient mortality rate (6.4%), and other

Table 1. Case Reports of Multiple Myeloma with Pulmonary Amyloidosis

Case	Age	Sex	Lung lesion presentation	Mediastinal lymphadenopathy	Diagnostic method	Other finding
Our case	66	female	Bilateral consolidation and interstitial thickening	yes	TBLB and EBUS-TBNA	Pulmonary hypertension, pleural effusion
Chim, C.S., *et al*. (2008)[12]	69	female	Consolidation at bilateral lower lobes	no	SLB	Pulmonary hypertension
Liu, Y., *et al*. (2018)[10]	58	female	Bilateral diffuse ground-glass opacifications with interlobular septal thickening	no	SLB	Soft tissue infiltration of the subcutaneous fat layer at the chest and abdominal wall
Kronen, R., *et al*. (2022)[13]	58	male	Diffuse ground glass opacities with peripheral nodularity, mosaic attenuation	yes	SLB	Pulmonary hypertension

complications like pneumothorax and respiratory failure [17]. Transbronchial lung cryotherapy (TBLC) is an emerging approach with a low mortality rate and better yield, compared to TBLB. There are some reports on primary amyloidosis involving the mediastinal lymph node that was mostly was diagnosed by TBNA [18-20]. However, the radiographic features of nodal amyloidosis are not specific and cannot be differentiated from malignancy [21]. Even though mediastinal nodal calcifications are proposed as a sign of indolent localized amyloidosis [22], they can still be seen in healed infectious granulomatous disease, sarcoidosis, treated lymphoma, or metastatic carcinoma [23], and not all patients with mediastinal amyloidosis had lymph node calcification [21].

In patients with pulmonary amyloidosis combined with MM, which is often considered systemic AL amyloidosis, the treatment protocol targets plasma cells in the bone marrow, aiming to halt the production of the toxic light chain [6, 24]. Bortezomib-based regimens were the most commonly used after 2010, and the variations had efficacy similar to the treatment of amyloidosis [25]. Recent clinical trials and evidence revealed that adding anti-CD38 agents led to higher frequencies of hematologic complete responses [24-25].

Patients with pulmonary diffuse parenchymal amyloidosis usually have a poor prognosis, based on the underlying systemic amyloidosis, with median survival of 13 months for untreated patients [26]. In addition, patients with systemic AL amyloidosis have a poorer prognosis than localized amyloidosis patients with multi-organ involvement [27]. Organ failure, sudden unexpected death and infection are major causes of death in systemic AL amyloidosis, especially in the first 6 months after diagnosis [28]. Therefore, treatment for AL amyloidosis should be risk-adapted when the diagnosis is confirmed.

Conclusion

MM may rarely contribute to pulmonary amyloidosis, but when it occurs, it has a poor prognosis. TBLC and TBNA provide a safer approach to diagnosis than SLB. Clinical physicians should be aware of the possibility of pulmonary amyloidosis in MM patients.

References

1. Kintzer JS Jr, Rosenow EC, 3rd, Kyle RA. Thoracic and pulmonary abnormalities in multiple myeloma. A review of 958 cases. Arch Intern Med 1978 May; 138(5): 727-30.
2. Röllig C, Knop S, Bornhäuser M. Multiple myeloma. Lancet 2015; 385(9983): 2197-2208.
3. Wechalekar AD, Gillmore JD, Hawkins PN. Systemic amyloidosis. Lancet 2016; 387(10038): 2641-2654.
4. Milani P, Basset M, Russo F, *et al*. The lung in amyloidosis. Eur Respir Rev 2017; 26(145): 170046.
5. Pickford HA, Swensen SJ, Utz JP. Thoracic cross-sectional imaging of amyloidosis. AJR Am J Roentgenol 1997; 168(2): 351-355.
6. Rajkumar SV. Multiple myeloma: 2022 update on diagnosis, risk stratification, and management. Am J Hematol 2022; 97(8): 1086-1107.
7. Smith RR, Hutchins GM, Moore GW, *et al*. Type and distribution of pulmonary parenchymal and vascular amyloid. Correlation with cardiac amyloid. Am J Med 1979; 66(1): 96-104.
8. Bahlis NJ, Lazarus HM. Multiple myeloma-associated AL amyloidosis: is a distinctive therapeutic approach warranted?. Bone Marrow Transplant 2006; 38(1): 7-15.
9. Riehani A, Soubani AO. The spectrum of pulmonary amyloidosis. Respir Med 2023; 218: 107407.
10. Liu Y, Jin Z, Zhang H, *et al*. Diffuse parenchymal pulmonary amyloidosis associated with multiple myeloma: a case report and systematic review of the literature. BMC Cancer Aug 8 2018; 18(1): 802.

11. Aylwin AC, Gishen P, Copley SJ. Imaging appearance of thoracic amyloidosis. J Thorac Imaging 2005; 20(1): 41-46.
12. Chim CS, Wong M, Fan Y. Pulmonary interstitial amyloidosis complicating multiple myeloma. J Clin Oncol 2008; 26(3): 504-506.
13. Kronen R, Ziehr DR, Kane AED, *et al*. Pulmonary amyloidosis as the presenting finding in a patient with multiple myeloma. Respir Med Case Rep 2022; 37: 101626.
14. Dingli D, Utz JP, Gertz MA. Pulmonary hypertension in patients with amyloidosis. Chest 2001; 120(5): 1735-1738.
15. Eder L, Zisman D, Wolf R, *et al*. Pulmonary hypertension and amyloidosis--an uncommon association: a case report and review of the literature. J Gen Intern Med 2007; 22(3): 416-419.
16. Thomson CC, Duggal A, Bice T, *et al*. 2018 c…linical practice guideline summary for clinicians: diagnosis of idiopathic pulmonary fibrosis. Ann Am Thorac Soc 2019; 16(3): 285-290.
17. Hutchinson JP, Fogarty AW, McKeever TM, *et al*. In-hospital mortality after surgical lung biopsy for interstitial lung disease in the United States. 2000 to 2011. Am J Respir Crit Care Med 2016; 193(10): 1161-1167.
18. Fujiwara T, Yasufuku K, Nakajima T, *et al*. Primary amyloidosis involving mediastinal lymph nodes diagnosed by EBUS-TBNA. Respir Med CME 2009/01/01/ 2009; 2(1): 51-53.
19. Kumar A, Sivasailam B, Marciniak E, *et al*. EBUS-TBNA diagnosis of localised amyloidosis presenting as mediastinal lymphadenopathy. BMJ Case Rep 2018; 11(1): e226619.
20. Leiro V, Fernández-Villar A, Bandrés R, *et al*. Primary amyloidosis involving mediastinal lymph nodes: diagnosis by transbronchial needle aspiration. Respiration 2008; 76(2): 218-220.
21. Naqvi A, Bonert M, Finley C, *et al*. Role of EBUS-TBNA/EUS-FNA and mass spectrometry for diagnosis and typing of lymph node amyloidosis: 10-year experience in two tertiary care academic centers. Cancer Cytopathol 2023; 131(11): 724-734.
22. Matsuguma H, Suzuki H, Ishikawa Y, *et al*. Localized mediastinal lymph node amyloidosis showing an unusual unsynchronized pattern of enlargement and calcification on serial CT. Br J Radiol 2008; 81(969): e228-e230.
23. Glazer HS, Molina PL, Siegel MJ, *et al*. High-attenuation mediastinal masses on unenhanced CT. AJR Am J Roentgenol 1991; 156(1): 45-50.
24. Dima D, Mazzoni S, Anwer F, *et al*. Diagnostic and treatment strategies for AL amyloidosis in an era of therapeutic innovation. JCO Oncol Pract 2023; 19(5): 265-275.
25. Palladini G, Schönland S, Merlini G, *et al*. The management of light chain (AL) amyloidosis in Europe: clinical characteristics, treatment patterns, and efficacy outcomes between 2004 and 2018. Blood Cancer J 2023; 13(1): 19.
26. Poletti V, Costabel U, Casoni GL, *et al*. Rare infiltrative lung diseases: a challenge for clinicians. Respiration 2004; 71(5): 431-443.
27. Baumgart JV, Stuhlmann-Laeisz C, Hegenbart U, *et al*. Local vs. systemic pulmonary amyloidosis-impact on diagnostics and clinical management. Virchows Arch 2018; 473(5): 627-637.
28. Staron A, Zheng L, Doros G, *et al*. Marked progress in AL amyloidosis survival: a 40-year longitudinal natural history study. Blood Cancer J 2021; 11(8): 139.

Iatrogenic Tracheal Laceration Treated with Silicone Y-stents

Hao-Ming Wu[1], Horng-Chyuan Lin[1,2,3], How-Wen Ko[1,2], Po-Jui Chang[1,2], Li-Pang Chuang[1,2,3,4]

We reported the case of an 86-year-old female who was brought to the emergency department due to sepsis. She had emergency intubation due to a decreased level of consciousness and paradoxical breathing. Subcutaneous emphysema developed rapidly after intubation. Fiberoptic bronchoscopy found a 4-cm tracheal laceration in the posterior wall. Since traditional surgical repair was not feasible, a silicone Y-stent implantation procedure was employed. Follow-up chest X-ray showed resolution of the subcutaneous emphysema on the 10th day, and the patient was weaned from the ventilator successfully. ***(Thorac Med 2025; 40: 28-32)***

Key words: tracheal laceration, silicone stents, Y-stents

Introduction

Tracheal laceration is a serious complication that occurs during intubation. It has been reported to have a high mortality rate, especially in those intubated in an emergency situation [1]. Surgical repair is considered the preferred treatment for cases where the laceration exceeds 4 cm in length, where it is concomitant with esophageal injury, or where there is a rapid progression of emphysema during mechanical ventilation (MV) [2]. However, comorbidities may preclude patients from undergoing surgical intervention, presenting a dilemma for decision-makers.

Case Description

An 86-year-old female (145 cm in height, 40 kg in weight) presented to the emergency room (ER) due to altered consciousness. Prior to admission, the patient was independent in her activities of daily living, and had a history of hypertension and stage III chronic kidney disease since 2021, which was regularly monitored at our hospital. Initially, the patient complained

[1]Department of Thoracic Medicine, Chang Gung Memorial Hospital at Linkou, Taoyuan, Taiwan, [2]School of Medicine, Chang-Gung University, Taoyuan, Taiwan. [3]Department of Respiratory Therapy, Chang Gung Memorial Hospital at Linkou, Taoyuan, Taiwan, [4]Sleep Center, Chang Gung Memorial Hospital, Taoyuan, Taiwan.
Address reprint requests to: Dr. Li-Pang Chuang, Department of Thoracic Medicine, Chang Gung Memorial Hospital No. 5, Fu-Hsing Street, Kweishan, Taoyuan 33305, Taiwan.

of shortness of breath, accompanied with progressive fatigue, loss of appetite, and skin itching over the past 10 days.

On the morning of admission, her family found her unresponsive to calls and brought her promptly to the emergency department. Upon triage, she exhibited a decreased level of consciousness (E2V1M1) with paradoxical breathing. Her body temperature was 34.7°C, systemic arterial pressure was 89/51 mmHg, and heart rate was 49 beats per minute. The respiratory rate was 30 breaths per minute with 91% oxygen saturation. The patient was intubated using a video-assisted laryngoscope with an endotracheal tube, 7.5 mm in diameter, and at a fixed depth of 21 cm. The initial ventilator settings for this patient were a respiratory rate 20 breaths per minute, PEEP of 8 mmHg, and peak inspiratory pressure of 24 mmHg. An arterial blood gas sample while under 100% FiO_2 ventilation showed pH 7.12, PaO_2 400 mmHg, $PaCO_2$ 34 mmHg, bicarbonate 10 mEq/L, and oxygen saturation 100%. A further abdominal computed tomography (CT) revealed left kidney atrophy with hydronephrosis. Besides, E. coli was reported in the blood and urine culture, so urosepsis was impressed.

A chest X-ray (CXR) revealed normal lung fields, but the tip of the endotracheal tube was too close to the carina, and there was inappropriate distension of the endotracheal cuff (3.5 cm) (Fig. 1). The endotracheal tube then was withdrawn 2 cm from its previous position and fixed at a depth of 19 cm in the ER. The patient regained consciousness (E4VeM6) and was synchronized with MV following initial treatment.

However, 12 hours after intubation, subcutaneous emphysema developed on the scalp, upper extremities, and chest wall. A repeated CXR confirmed subcutaneous emphysema and pneumomediastinum. CT identified a defect in the tracheal membrane just behind the endotracheal tube (Fig. 2). Fiberoptic bronchoscopy revealed a 4 cm laceration in the posterior wall of the trachea, 2 cm above the carina, and 3 cm below the vocal cords, which demonstrated dynamic changes during the respiratory cycle (Fig. 3 and Video 1).

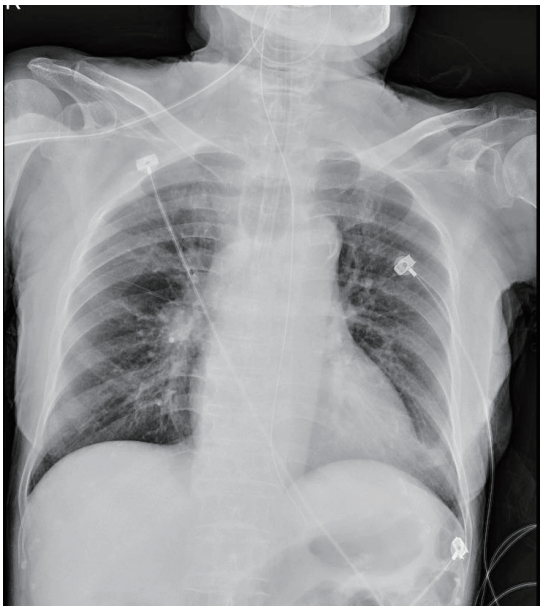

Fig. 1. Chest plain film shows the tip of the endotracheal tube too close to the carina, with the cuff overinflated.

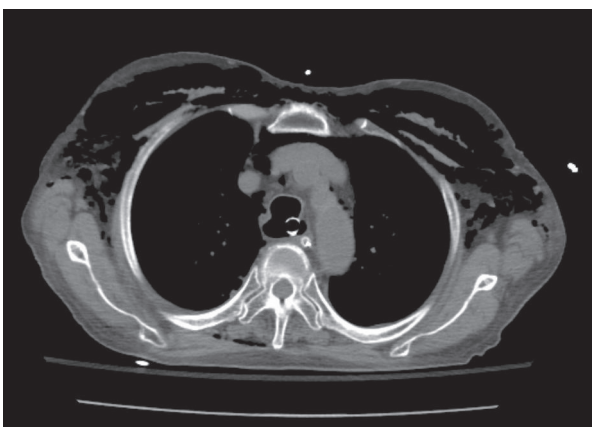

Fig. 2. Chest computed tomography reveals a defect in the posterior trachea.

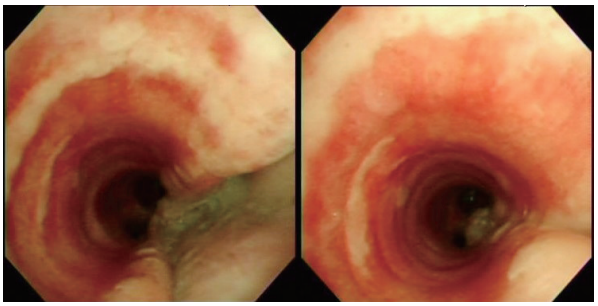

Fig. 3. Bronchoscopic view shows a large posterior defect in the membranous trachea.

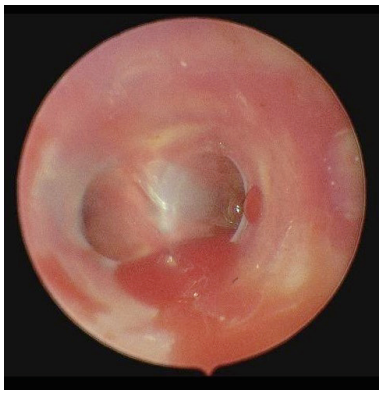

Fig. 4. Bronchoscopic view shows stability of the laceration wound after the Dumon Y stent is inserted.

Video 1: Dynamic changes in the laceration wound during the respiratory cycle.

A chest surgeon was consulted, and an operation was performed through rigid bronchoscopy to insert a Dumon Y-stent (TFDA license number: 17452) at 2.5 cm below the vocal cords, providing a safety margin of 0.5 cm (Fig. 3). On the 10th day, a follow-up chest X-ray showed resolution of the subcutaneous emphysema and pneumomediastinum (Fig. 4), and fiberoptic bronchoscopy indicated stability of the tracheal laceration. The patient was later weaned from the ventilator, but passed away during a prolonged hospital stay.

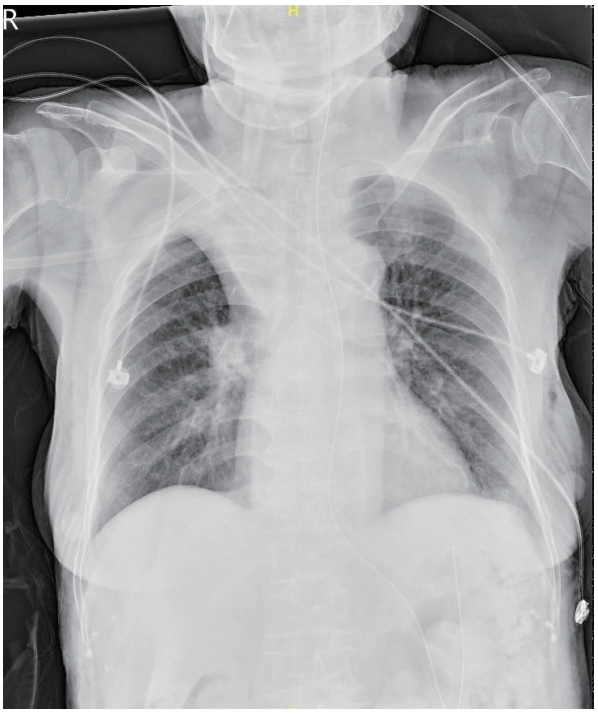

Fig. 5. Follow-up chest plain film showed resolution of the subcutaneous emphysema and pneumomediastinum.

Discussion

Postintubation tracheal laceration is a rare complication with an estimated incidence of approximately 1 in 20,000, and is associated with increased mortality and morbidity [3]. Female patients are presumed to be more susceptible to tracheal laceration [1]. According to a systematic review of 50 articles, females were predominant (85.7%), with a mean age of 61 years [1] Among females with tracheal lacerations, a previous study reported that 50% were less than 160 cm in height [4]. Some speculated that a shorter average height may correspond to a smaller tracheal diameter, making the endotracheal tube inappropriately large for women [4]. In addition to body size and sex, several mechanical and anatomical factors have been proposed, including multiple vigorous attempts

at intubation, inexperienced anesthesiologists, overinflation, rapid inflation, and rupture of the cuff or large mediastinal collections, lymph nodes, or neoplasms causing tracheal distortion [5].

The exact cause of tracheal laceration is difficult to clearly define. Though a few cases have occurred in patients who have already been extubated after general anesthesia [6], no cases have been reported under non-invasive ventilation. According to the study by Marty-Ane, *et al*. [5], mechanical factors from the intubation process, tracheal laceration due to a weakened trachealis muscle under MV, or over-inflation of the endotracheal cuff are possible risk factors. Since intubation and positive pressure ventilation are administered consecutively, we cannot accurately distinguish the exact cause.

Repeated attempts to insert an endotracheal tube is also a risk factor for tracheal trauma [5]. To reduce the number of attempts, the patient should be optimally positioned, pre-oxygenated, anesthetized, and neuromuscularly relaxed [7]. Multiple guidelines recommend the use of neuromuscular blocking agents (NMBAs), since they can decrease intubation complications in critically ill patients [8-9]. NMBAs enhance intubating conditions, eliminate muscle tone in the upper airway, reduce the number of intubation attempts, and subsequently decrease complications. In addition, operators should be well-trained and proficient in all the techniques they plan to use. A recent systematic review of videolaryngoscopy found that it improves laryngeal views, reduces airway trauma, and lowers failure rates [10]. One study, in its guidelines, has suggested that videolaryngoscopy should be the preferred method for all intubations in critically ill patients [7].

Some studies indicate that conservative treatment has a similar mortality rate to surgical treatment under specific conditions, such as tears smaller than 2 cm without associated esophageal injuries, rapidly progressive subcutaneous or mediastinal emphysema, or mediastinitis [3, 11]. However, the mortality rate remains high even after surgical repair, particularly in patients who require emergency intubation due to critical illness and high surgical risk [1].

Yopp's algorithm, supported by case reports, suggests that tracheal stenting is an option for poor candidates for surgery [2]. Bronchoscopic placement of a silicone stent is used in benign airway disease, since there is less granulation formation [12]. Considering tracheal laceration as a treatable condition, silicone stents offer advantages due to their removability. Compared to straight silicone stents, Dumon Y-shaped stents have a lower risk of migration and potentially better efficacy in wound healing [13]. Self-expandable metallic stents may be an alternative option, although they have been reported in only a few cases [14-15]. Covered metallic stents are commonly used for malignancy-related airway obstruction, but are associated with significant complications after long-term use, including granulation formation, stent fracture, and difficulty with stent removal [16].

Both covered metallic stents and silicone stents are transparent, allowing observation of tracheal laceration healing under bronchoscopy. However, there is no convincing evidence regarding the optimal timing for stent removal. In previous case reports, tracheal lacerations in patients receiving conservative treatment have mostly healed within 28 days [17, 18]. However, in cases where stents are used for treatment, they tend to be placed for a longer duration [2, 14, 15], with Bozzo C, *et al*. reporting stent

placement for more than 6 months [15]. In summary, tracheal lacerations typically heal within 1 month without surgical suturing, and the presence of a stent may expedite the recovery process. In the absence of complications or discomfort, such as granulation [14], stent removal may not be necessary.

Summary

In an aging society, critically ill patients in the ICU face higher surgical risks due to age and severity of illness, leading decision-makers to lean towards avoiding surgical treatment. We reported our experience with placing a Dumon Y-shaped stent in an extremely elderly patient following tracheal laceration. Although the benefits of stent placement have not been definitively established, it provides an alternative option for patients who are not suitable candidates for surgery.

References

1. Minambres E, Buron J, Ballesteros MA, *et al*. Tracheal rupture after endotracheal intubation: a literature systematic review. Eur J Cardiothorac Surg 2009; 35(6): 1056-62.
2. Yopp AC, Eckstein JG, Savel RH, *et al*. Tracheal stenting of iatrogenic tracheal injury: a novel management approach. Ann Thorac Surg 2007; 83(5): 1897-9.
3. Gomez-Caro Andres A, Moradiellos Díez FJ, Herrero PA, *et al*. Successful conservative management in iatrogenic tracheobronchial injury. Ann Thorac Surg 2005; 79(6): 1872-8.
4. Hofmann HS, Rettig G, Radke J, *et al*. Iatrogenic ruptures of the tracheobronchial tree. Eur J Cardiothorac Surg 2002; 21(4): 649-52.
5. Marty-Ané CH, Picard E, Jonquet O, *et al*. Membranous tracheal rupture after endotracheal intubation. Ann Thorac Surg 1995; 60(5): 1367-71.
6. Kim SW, Oh GJ, Roh SG, *et al*. Tracheal laceration related to endotracheal intubation. Arch Plast Surg 2014; 41(2): 182-3.
7. Higgs A, McGrath BA, Goddard C, *et al*. Guidelines for the management of tracheal intubation in critically ill adults. Br J Anaesth 2018; 120(2): 323-352.
8. Apfelbaum JL, Hagberg CA, Connis RT, *et al*. 2022 American Society of Anesthesiologists Practice Guidelines for Management of the Difficult Airway. Anesthesiology 2022; 136(1): 31-81.
9. Acquisto NM, Mosier JM, Bittner EA, *et al*. Society of Critical Care Medicine Clinical Practice Guidelines for Rapid Sequence Intubation in the Critically Ill Adult Patient. Crit Care Med 2023; 51(10).
10. De Jong A, Clavieras N, Conseil M, *et al*. Implementation of a combo videolaryngoscope for intubation in critically ill patients: a before-after comparative study. Intensive Care Med 2013; 39(12): 2144-52.
11. Carbognani P, Bobbio A, Cattelani L, *et al*. Management of postintubation membranous tracheal rupture. Ann Thorac Surg 2004; 77(2): 406-9.
12. Mughal MM, Gildea TR, Murthy S, *et al*. Short-term deployment of self-expanding metallic stents facilitates healing of bronchial dehiscence. Am J Respir Crit Care Med 2005; 172(6): 768-71.
13. Oki M, Saka H. Double Y-stenting for tracheobronchial stenosis. Eur Respir J 2012; 40(6): 1483-8.
14. Lee BE, Korst RJ. Successful treatment of an iatrogenic tracheal laceration with a temporary polyurethane-coated nitinol stent. Ann Thorac Surg 2016; 102(1): e11-2.
15. Bozzo C, Profili S, Masala S. Successful use of self-expandable metal stents in a case of iatrogenic tracheal rupture. Radiol Case Rep 2019; 14(3): 377-380.
16. Madden BP, Loke T-K, Sheth AC. Do expandable metallic airway stents have a role in the management of patients with benign tracheobronchial disease? Ann Thorac Surg 2006; 82(1): 274-278.
17. Hung MS, Kao KC, Tsai YH. Successful conservative treatment for a large tracheal laceration caused by endotracheal cuff overinflation. Thorac Med 2004; 19: 484-490.
18. Cardillo G, Carbone L, Carleo F, *et al*. Tracheal lacerations after endotracheal intubation: a proposed morphological classification to guide non-surgical treatment. Eur J Cardiothorac Surg 2010; 37(3): 581-7.

Chest Wall Reconstruction in a Young Male Patient with Left Chest Wall Ewing's Sarcoma Involving the Left Lower Lobe of the Lung and Adjacent Ribs

Sung-Yang Liao[1], Chia-Ying Li[2]

Ewing's sarcoma is a malignant tumor found mostly in adolescents, and accounts for 5% of soft tissue malignancies. Ewing's sarcoma of the chest wall has a 5-year survival ranging from 35% to 55%, as reported in recent studies. The common invasion site is the bone, with about 25% originating from soft tissues; about 25% of cases have metastases at the time Ewing's sarcoma is diagnosed. The clinical symptoms and signs of primary chest wall sarcomas usually originate from the mass effect on adjacent thoracic structures such as the lung, mediastinum, vertebra, diaphragm, and chest wall. Consequently, aggressive chest wall sarcomas often induce pain, shortness of breath, and in some cases, systemic symptoms. We report the case of a young male who presented to the emergency department complaining of shortness of breath and cough. ***(Thorac Med 2025; 40: 33-37)***

Key words: soft tissue sarcoma, Ewing's sarcoma, chest wall sarcoma with lung and ribs involvement, chest wall reconstruction

Introduction

Chest wall tumors comprise 1% to 2% of all thoracic neoplasms. They are classified according to their tissue of origin (bone, cartilage, soft tissue, or other origin) and their malignant potential (benign vs. malignant). Approximately 60% of primary chest wall tumors are malignant sarcomas; of these, about 60% arise from bone or cartilage, about 25% originate from soft tissue elements, and 15% from other origins [5]. Ewing's sarcomas represent 14-16% of chest wall tumors and have a reported 5-year survival ranging from 35% to 55% in recent studies [2, 6]. The clinical symptoms and signs of primary chest wall sarcomas are usually a result of the mass effect on adjacent thoracic structures such as the lung, mediastinum, vertebra, diaphragm, and chest wall. Consequently, aggressive chest wall sarcomas often induce pain, shortness of breath, and in some cases, systemic symptoms [5, 8].

The foundation of treatment for chest wall sarcomas is complete surgical resection to achieve clear surgical margins. In advanced cases, chemotherapy and radiation are utilized

[1]Thoracic Surgery, Department of Surgery, Show Chwan Memorial Hospital. [2]Show Chwan Memorial Hospital, Superintendent Office.
Address reprint requests to: Dr. Sung-Yang Liao, No. 28, Ln. 270, Neilikeng St., Xinpu Township, Hsinchu County, Taiwan (R.O.C.)

either as neoadjuvant treatments to downstage the tumor and permit resection or as adjuvant treatments to prevent local and systemic recurrence [7]. Given the uncommon nature of primary chest wall sarcomas, only a limited number of reports on this clinical scenario have been published. We herein report our experience with a 19-year-old male who underwent chest wall resection and reconstruction for pulmonary Ewing's sarcoma.

Case Presentation

A 19-year-old male presented to the Thoracic Unit of the Surgery Department at Show Chwan Memorial Hospital with gradually progressive shortness of breath for 6 months, associated with left-side chest pain (axillary region). A chest X-ray revealed a well-defined opacity involving the left middle zone (Fig. 1). There was no history of fever, cough, hemoptysis, loss of appetite, or trauma. On auscultation, there was decreased breathing sounds on the left side. The patient was then advised to undergo a computed tomography (CT) scan of the chest with contrast (Fig. 2), which showed a well-defined mass on the left posterior chest wall. For confirmatory diagnosis, a fine needle aspiration cytology from the left thoracic region was performed, and the findings were positive for Ewing's sarcoma (CD99 and NKX2.2 markers). The patient was then advised to undergo neoadjuvant chemotherapy (a combination of vincristine, cyclophosphamide, and doxorubicin) for 4 cycles. After that, the tumor size decreased from 13 × 7 cm to 9 × 4 cm, as shown in the chest CT (Fig. 3).

Further management involved planning for left VATS chest wall tumor resection with chest wall reconstruction. Intraoperative find-

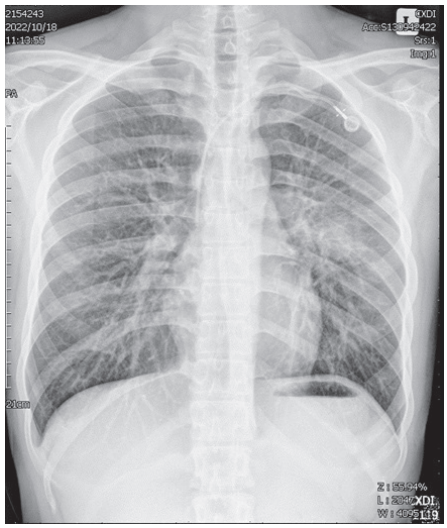

Fig. 1. A well-defined opacity involving the left middle zone of the lung.

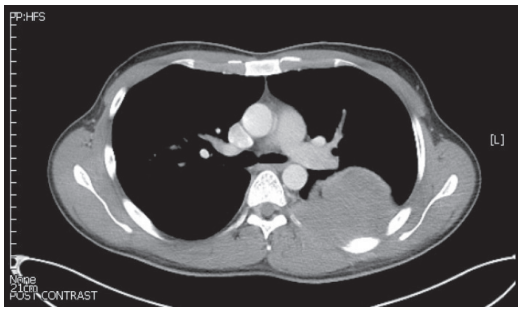

Fig. 2. Computed tomography scan of the chest before the 4 courses of neoadjuvant concurrent chemoradiotherapy, showing the location of the chest.

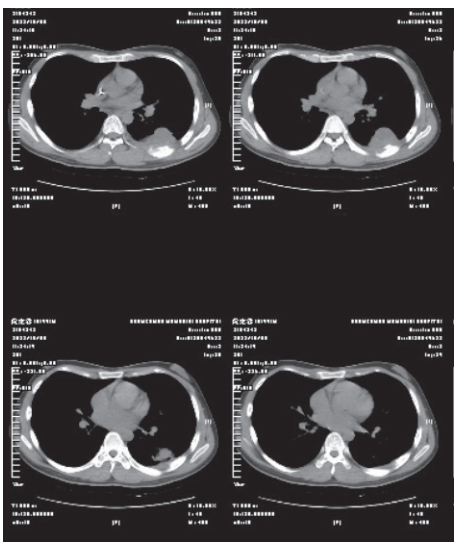

Fig. 3. The tumor size decreased from 13×7 cm to 9×4 cm, as shown in the chest .

ings suggested the presence of an intrathoracic tumor, sized 9 × 4 cm, originating from the left latissimus dorsi and sixth and seventh ribs, extending up to the left upper lobe and left lower lobe of the lung. Feeders from the subclavian vessels supplying the anterior and superior part of the tumor were found. The resected tissue, along with the sixth and seventh ribs and partial latissimus dorsi muscle, were sent for histopathological examination (Fig. 4). Following resection, the defect was traced on sterile paper. Using that measurement, 2 titanium plates were placed in the resected area of the sixth and seventh ribs (Fig. 5). Bone cement was shaped to the defect and adhered to the plates on both sides. This was placed in the defect and secured by suturing, using sternal wire with the adjacent ribs and nylon with the soft tissue. Histopathological findings confirmed Ewing's sarcoma, consistent with the previous fine needle aspiration cytology report.

The patient stayed in the SICU for 1 day after the operation, was successfully weaned off the endotracheal tube on the third day of admission, and was transferred to the ordinary ward on the same day. He spent 1 week in the ordinary ward and was discharged on the 10th day of admission. The patient was followed up at our outpatient department, and the sutures were removed 1 week later. He had no significant complaints and was advised to undergo a follow-up chest X-ray, as shown in Fig. 6. As of this writing, he has had no new symptoms and is recovering well.

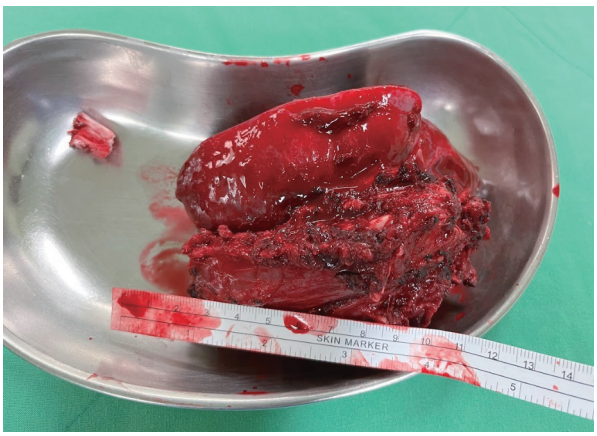

Fig. 4. Resected tumor along with the sixth and seventh ribs.

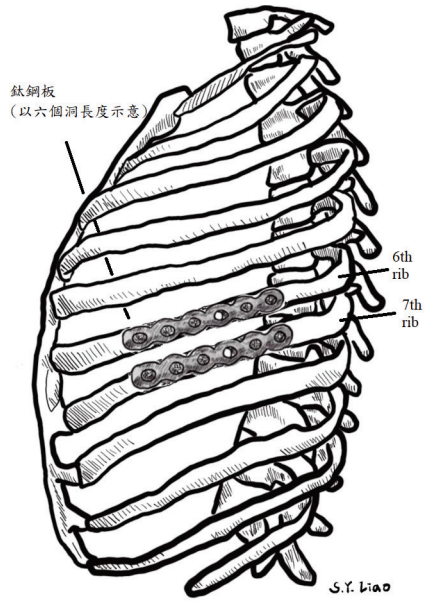

Fig. 5. Illustration of the titanium bars placed at the resected sixth and seventh ribs.

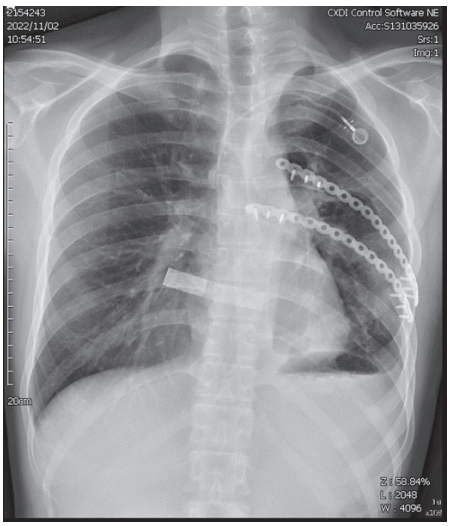

Fig. 6. Chest X-ray during follow-up at the OPD.

Discussion

Ewing's sarcoma is a rare tumor that frequently affects young male patients. The most common clinical course involves an initial biopsy, followed by chemotherapy and partial or complete chest wall resection. Neoadjuvant chemotherapy reduces tumor dimensions, as shown in our case, facilitating a complete removal with negative resection margins, reducing the risk of local recurrence, and improving survival. In addition to treatment of the tumor, chest wall reconstruction is also important. As Lardinois *et al*. [9] asserted, reconstruction of the chest wall plays a crucial role in determining postoperative morbidity and mortality. The core principle of the reconstruction technique is to restore maximum thoracic volume, thus avoiding the bi-dimensional thoracic deformity responsible for acute thoracic insufficiency syndrome. There are no consensus guidelines worldwide for reconstruction methods, and each surgeon chooses their own method, depending on the tumor site, size of the chest wall defect, their own preference, and even the cost of the material. For our patient, we performed partial resection of his left upper and lower lobes and removed the involved soft tissues, muscles, and ribs. We reconstructed the chest wall with titanium prostheses for 2 ribs.

After extensive chest wall resection in young patients, we suggest using 3D-printed rib titanium prostheses in the reconstruction to provide adequate stability and a similar thoracic shape for pulmonary functional and cosmetic results, due to their flexibility and fit. The flexibility of titanium allows the rib nails to easily adapt to the contour of the ribs, avoiding the risk of loosening. The fit minimizes movement between the ribs and the prostheses, promoting bone and soft tissue healing and reducing postoperative pain and neurologic signs. Titanium is also a low-chemical-activity element, remaining corrosion-free. The rarity of the disease and the lack of multicenter-randomized studies prevent the establishment of an optimal and uniform method for chest wall reconstruction.

The advantages of titanium bars in the reconstruction have been previously reported after subtotal sternectomy for primary tumors [10]. Gonfiotti *et al*. reported the feasibility of these new rib prostheses and the good results obtained in the reconstruction of wide anterolateral chest wall resections, also in young patients [11]. Our singular experience with this 19-year-old adolescent with a relatively short follow-up did not permit us to establish an optimal reconstructive strategy and evaluate the long-term cosmetic and functional results. However, titanium prostheses have shown excellent short-term results and represent an additional device that is useful in chest wall reconstruction.

Conclusions

In this case report, we described the management and chest wall reconstruction for a rare case of Ewing's sarcoma in a 19-year-old adolescent. The patient underwent surgery without significant complications, and the 3D-printed titanium prostheses showed excellent short-term results. Since we have only 1 case involving this new material at our hospital, further studies and longer follow-ups are needed.

References

1. Ludwig JA. Ewing sarcoma: historical perspectives, current state-of-the-art, and opportunities for targeted therapy in the future. Cur Opin Oncol 2008; 20: 412-8.

2. Basharkhah A, Lackner H, Karastaneva A, *et al*. Interdisciplinary radical “en-bloc” resection of Ewing sarcoma of the chest wall and simultaneous chest wall repair achieves excellent long-term survival in children and adolescents. Front Pediatr 2021; 9: 661025.
3. Riggi N, Stamenkovic I. The biology of Ewing sarcoma. Cancer Lett 2007; 254: 1-10.
4. Cotterill SJ, Ahrens S, Paulussen M, *et al*. Prognostic factors in Ewing’s tumor of bone: analysis of 975 patients from the European Intergroup Cooperative Ewing’s Sarcoma Study Group. J Clin Oncol 2000; 18: 3108-14.
5. Cipriano A, Burfeind W Jr. Management of primary soft tissue tumors of the chest wall. Thorac Surg Clin 2017; 27: 139-147. doi: 10.1016/j.thorsurg.2017.01.007
6. Goldman L, Cecil RL, Schafer AI. Goldman's Cecil Medicine (24th ed.). Philadelphia: Elsevier Saunders, 2012: 1326. ISBN 978-1-4377-2788-3. OCLC 909785616
7. Athanassiadi K, Kalavrouziotis G, Rondogianni D, *et al*. Primary chest wall tumors: early and long-term results of surgical treatment. Eur J Cardiothorac Surg 2001; 19: 589-593. doi: 10.1016/S1010-7940(01)00655-8.
8. Thomas M, Shen KR. Primary tumors of the osseous chest wall and their management. Thorac Surg Clin 2017; 27:181-193. doi: 10.1016/j.thorsurg.2017.01.012.
9. Lardinois D, Müller M, Furrer M, *et al*. Functional assessment of chest wall integrity after methylmethacrylate reconstruction. Ann Thorac Surg 2000; 69: 919-23.
10. Yasmin R, Stærk DR, Kalhauge A, et al. Role of CT angiography in bilateral pulmonary sequestration: a case report. Acta Radiologica Open 2018; 7(3): 1-5.
11. Kang M, Khandelwal N, Ojili V, et al. Multidetector CT angiography in pulmonary sequestration. J Comput Assist Tomogr 2006 Nov-Dec; 30(6): 926-32.

A Case Report of *Mycobacterium gordonae* Pulmonary Disease with a Favorable Treatment Response

Chih-Jung Chang[1], Sheng-Wei Pan[2,3]

Mycobacterium gordonae is one of the most commonly isolated nontuberculous mycobacteria (NTM) in respiratory samples. Although it seldom causes pulmonary disease and is often considered contamination or "non-pathogenic", there have been reports of true infections involving pulmonary disease, soft tissue, or disseminated disease. Currently, there are no evidence-based management guidelines for *M. gordonae* pulmonary disease. Treatment typically includes a combination of macrolides, fluoroquinolones, linezolid, and amikacin, based on limited data regarding susceptibility to *M. gordonae*. Here, we reported an 81-year-old woman presenting with significant body weight loss with an abnormal chest X-ray and high-resolution computed tomography (HRCT) showing lung clustered nodules. Further microbiological criteria for NTM pulmonary disease were met. Treatment with macrolide-based combination therapy was initiated. Clinical symptoms improved, an image showed resolution, and sputum conversion was achieved during treatment. The diagnosis of *M. gordonae* pulmonary disease was confirmed. The patient had nearly complete remission of lung lesions and completed treatment smoothly over 9-month period. ***(Thorac Med 2025; 40: 38-43)***

Key words: *Mycobacterium gordonae*-pulmonary disease; nontuberculous mycobacterial-pulmonary disease; immunocompetent; treatment

Introduction

The incidence of nontuberculous mycobacterial pulmonary disease (NTM-PD) has been increasing over the past three decades [1]. The diagnosis of NTM-PD should meet the clinical and microbiological criteria outlined in the 2020 official ATS/IDSA statement [1-2]. There are more than 190 NTM species, with Mycobacterium avium complex (MAC), *M. abscessus* and *M. kansassi* being the leading three species in most countries and in Taiwan [3]. Recommendations for the initiation of treatment for these common species have been stated in

[1]Department of Chest Medicine, Taipei Veterans General Hospital, Taipei, Taiwan, [2]School of Medicine, College of Medicine, National Yang Ming Chiao Tung University, Taipei, Taiwan. [3]Division of Pulmonary Immunology & Infectious Diseases, Department of Chest Medicine, Taipei Veterans General Hospital, Taipei, Taiwan.
Address reprint requests to: Dr. Sheng-Wei Pan, Division of Pulmonary Immunology & Infectious Diseases, Department of Chest Medicine, Taipei Veterans General Hospital, No. 201, Section 2, Shi-Pai Road, Taipei 112, Taiwan.

the practical guideline [1]. However, the initiation of treatment and the regimen for less common and low-virulence NTM-PD are largely controversial, with recommendations based on expert consensus, and focusing on comorbidities, radiography, the pathogenicity of NTM species, and the risk of disease progression [1, 4]. *Mycobacterium gordonae*, found in water and soil, has lower pathogenicity and seldom requires treatment, though cases causing infection have been reported [5-6]. Disseminated diseases occur in both immunocompromised and immunocompetent patients, as well as extrapulmonary diseases and empyema can occur in immunocompetent patients [5-6]. Here, we report a case of *M. gordonae* pulmonary disease in an immunocompetent patient who responded well to antimicrobial treatment with macrolide-based combination therapy.

Case Presentation

An 81-year-old woman was evaluated for body weight loss over the past six months and for abnormal findings on a high-resolution computed tomography (HRCT) scan (Figure 1A) at the chest outpatient department (OPD). An abnormal chest X-ray (CXR) was initially seen at a local medical department. Despite having no respiratory symptoms such as cough, hemoptysis, or chest pain, she reported significant body weight loss of 7-8 kg during the last 6 months. She experienced no fever, night sweats or palpable masses. Reviewing her medical history, we found she had type 2 diabetes mellitus, which was being managed with oral hypoglycemic agents, with an HbA1c level of 7 in a recent follow-up. Five years ago, she underwent right knee joint replacement due to osteoarthritis and had lumbar spine internal fixation between 2020 and 2022. She had no known allergies and no history of smoking. Subsequent diagnostic tests, including a CXR and an HRCT, confirmed the presence of persistent clustered lung nodules in the right upper lobe, along with scattered lung nodules predominantly in the right lung, compared to the CXR from one month earlier. Consequently, she was referred to this medical center for further evaluation.

On examination, she was breathing ambient air and appeared well. The lung was clear on auscultation. Her laboratory tests showed elevated creatinine levels, at 1.02 mg/dL. The rest of the results, including tumor markers were normal. Considering the lesions noted on HRCT, microbiological and cytological testing of sputum specimens were performed. Biopsy for the lung nodule was also suggested, but the patient refused. Acid-fast stain tests were positive in three consecutive sputum samples, with undetectable negative results of nucleic acid amplification tests for tuberculosis. Two weeks later, the sputum was culture-positive for NTM and identification tests confirmed the growth of *M. gordonae* in all three samples. The drug sensitivity test was not available. Cytology showed no malignant cells. To exclude malignancy, an abdominal CT scan was arranged, and the results were unremarkable. Tumor markers, including CEA, CA-125, CA-199 and SCC, were within normal limits. Since no growth was seen in the other microbiologic results, and no further evidence of malignancy was detected, a diagnosis of NTM-PD caused by *M. gordonae* was made.

Treatment for *M. gordonae* pulmonary disease was suggested, starting with azithromycin (250 mg/day, started after confirming there was no risk of QT prolongation on EKG) and levofloxacin (500 mg/day). Since the patient suf-

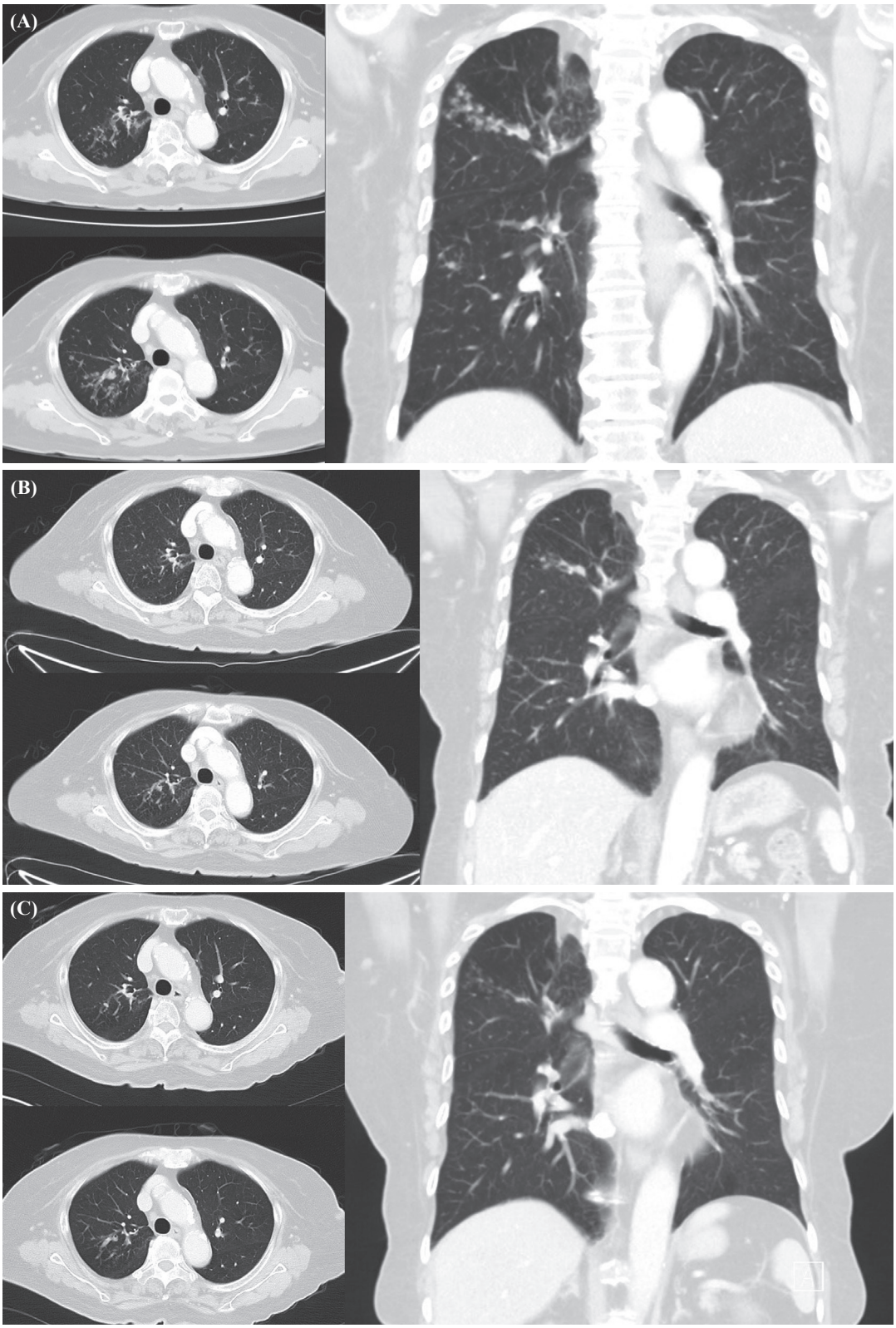

Fig. 1. Serial high-resolution computed tomography (HRCT) A. Clustered lung nodules with scattered lung nodules predominantly at the right upper lobe B. Three months after macrolide-based combination therapy for *M. gordonae* pulmonary disease, the lesion showed significant improvement. C. Nine months after treatment, the lesion was in nearly complete remission.

fered from subjective vision disturbance, ethambutol was not given due to concerns about optic nerve toxicity. The patient developed gastrointestinal upset in the second month of treatment, but it resolved after adjusting the dosage of azithromycin and levofloxacin from 250 mg and 750 mg once-daily to 250 mg and 750 mg thrice-weekly respectively, and adding famotidine and mosapride. She had sputum collection monthly at the OPD and achieved sputum conversion after 3 months of treatment. A follow-up chest CT showed great improvement in the lung lesions (Figure 1B). The patient continues to be followed in the OPD every 2 months, with stable tolerance of the medications and no further weight loss reported. Nine months after antibiotic treatment, an HRCT showed significant remission of the lung lesions (Figure 1C). The patient hesitated to continue the antibiotics at that moment. Considering the significant improvement of her lung lesions and symptoms, as well as sputum conversion after a 3-month antibiotic treatment regimen, the combination therapy was ended, with a total duration of 9 months.

Discussion

M. gordonae is one of the most commonly isolated NTMs, often considered to be "non-pathogenic", and rarely causes disease in humans. It is abundant in the environment, especially in water. A case of hot tub lung was found to be related to *M. gordonae* [7]. It is often seen as colonization or contamination in respiratory samples [8-9], and treatment is seldom necessary [10].

In cases of true infection, *M. gordonae* predominantly impacts the lungs and soft tissues, and can lead to disseminated diseases [11]. The peritoneum and genitourinary system have also been described as infected areas [11-12]. In a study that collected 209 cases with growth of *M. gordonae* in respiratory samples, only 5 (2.4%) met the criteria for a diagnosis of pulmonary disease, presenting nodular bronchiectasis and fibrocavitary lesions in chest radiographs [13]. In a retrospective study in Washington state, 16.5% of all NTM species identified were isolated as *M. gordonae*; 97.5% of isolated sites were pulmonary and 1.7% involved skin and soft tissue [14]. In our case presentation, the patient met the microbiological criteria for NTM infection. Furthermore, her clinical symptoms and the clustered lung nodules on the HRCT were consistent with the diagnosis. After a 9-month course of macrolide-based combination therapy, the lung nodules and weight loss resolved. To this end, the diagnosis of NTM-PD caused by *M. gordonae*, rather than mere NTM colonization, could be made.

Cases of *M. gordonae* pulmonary disease requiring treatment have been reported, and mostly responded well. However, there is no evidence-based regimen currently established through clinical trials, and there is no standard treatment that has been recommended for those with invasive disease. Limited data indicate that *M. gordonae* shows variable in vitro susceptibility to several antibiotics, including clarithromycin, ciprofloxacin, linezolid, and amikacin [15]. Susceptibility to levofloxacin has also been reported [16]. In a study on 121 individuals with *M. gordonae* isolates, only 2 (1.7%) had invasive disease and received ethambutol, flouroquinolone, macrolide and rifampicin combination therapy [14]. In a case series, a patient with active acute myeloid leukemia and *M. gordonae* pulmonary disease received treatment with levofloxacin, azithromycin and doxycy-

cline for 8 months, but ultimately died of leukemia. A patient without underlying diseases, who had empyema caused by *M. gordonae*, received drainage and moxifloxacin for 1 month and was cured after the treatment. A patient with lymphoma and disseminated *M. gordonae* infection involving the lung and bone marrow received ethambutol, azithromycin and doxycycline for 12 months, and was also cured [6]. In another case series, only 4 out of 209 cases needed antibiotic treatment with antimicrobial agents consisting of rifampicin, ethambutol, and clarithromycin [13]. In our patient with *M. gordonae* pulmonary disease, being relatively immunocompetent, without extrapulmonary infection or superimposed active malignancy, the successful treatment involved a 9-month course of azithromycin and levofloxacin, although the drug sensitivity test was unknown.

Our patient was given daily treatment initially. However, adverse drug reactions with gastrointestinal disturbance, defined as grade 2 using Common Terminology Criteria for Adverse Events criteria, developed in our patient. It was managed by transitioning to thrice-weekly treatment alongside supportive medications. Although intermittent treatment versus daily treatment has not been evaluated as treatment for *M. gordonae* pulmonary disease, the adjustment in our case seemed successful, without intolerance, which could be associated with failure of sputum conversion and clinical outcomes in NTMLD [17].

Currently, treatment for NTM-PD is recommended for 12 months after sputum conversion, based on expert consensus [1, 4]. For Mycobacterium avium complex-pulmonary disease (MAC-PD), a retrospective study in Taiwan found that a treatment duration of more than 12 months had better microbiological or clinical outcomes [18]. For patients with MAC-PD with a nodular-bronchiectasis radiographic pattern without cavitary lesions, a thrice-weekly macrolide-based therapy was considered acceptable [4]. For M. kansasii pulmonary disease, a fixed 12-month therapy was associated with high success rates [1]. For our patient, who had clustered nodular lung lesions only, achieved sputum conversion after 3 months of treatment, and had regression of the lung lesion and symptoms, a treatment duration of 9 months for *M. gordonae* may be acceptable, considering that the patient was immunocompetent and refused further treatment. Due to the lack of evidence for an optimal treatment duration for patients with *M. gordonae* pulmonary disease, individualized NTM-PD therapy should take into account the patient's immune status, and microbiologic and clinical response, in order to achieve treatment success.

Conclusion

We reported an immunocompetent patient with NTM-PD due to *M. gordonae* infection. She had an excellent response to antimicrobial agents, presenting both improved clinical symptoms and radiographic images after initiating azithromycin and levofloxacin treatment. Some gastrointestinal upset developed during the treatment course, but was controlled by dose adjustment and symptomatic agents. The treatment duration was completed smoothly after 9 months. Thus, *M. gordonae*, commonly seen as a contamination or colonization, could also cause pulmonary disease. Further investigation is needed to provide more evidence regarding the optimal treatment regimen and duration for NTM-PD due to *M. gordonae* infection. Combination antibiotic therapy should be individu-

alized, taking into account the patient's immune status, and microbiologic, radiographic and clinical response.

References

1. Daley CL, Iaccarino JM, Lange C, *et al*. Treatment of nontuberculous mycobacterial pulmonary disease: an official ATS/ERS/ESCMID/IDSA clinical practice guideline. Eur Respir J 2020; 56(1).
2. Griffith DE, Aksamit T, Brown-Elliott BA, *et al*. An official ATS/IDSA statement: diagnosis, treatment, and prevention of nontuberculous mycobacterial diseases. Am J Respir Crit Care Med 2007; 175(4): 367-416.
3. Huang HL, Cheng MH, Lu PL, *et al*. Epidemiology and predictors of NTM pulmonary infection in Taiwan - a retrospective, five-year multicenter study. Sci Rep 2017; 7(1): 16300.
4. Haworth CS, Banks J, Capstick T, *et al*. British Thoracic Society guidelines for the management of non-tuberculous mycobacterial pulmonary disease (NTM-PD). Thorax 2017; 72(Suppl 2): ii1.
5. Asija A, Prasad A, Eskridge E. Disseminated *Mycobacterium gordonae* infection in an immunocompetent host. Am J Ther 2011; 18(3): e75-7.
6. Chang HY, Tsai WC, Lee TF, *et al*. *Mycobacterium gordonae* infection in immunocompromised and immunocompetent hosts: a series of seven cases and literature review. J Formos Med Assoc 2021; 120(1 Pt 2): 524-32.
7. Utsugi H, Usui Y, Nishihara F, *et al*. *Mycobacterium gordonae*-induced humidifier lung. BMC Pulm Med 2015;15(1): 108.
8. Scorzolini L, Mengoni F, Mastroianni CM, *et al*. Pseudo-outbreak of *Mycobacterium gordonae* in a teaching hospital: importance of strictly following decontamination procedures and emerging issues concerning sterilization. New Microbiol 2016; 39(1): 25-34.
9. Tokars JI, McNeil MM, Tablan OC, *et al*. *Mycobacterium gordonae* pseudoinfection associated with a contaminated antimicrobial solution. J Clin Microbiol 1990; 28(12): 2765-9.
10. Lange C, Böttger EC, Cambau E, *et al*. Consensus management recommendations for less common non-tuberculous mycobacterial pulmonary diseases. Lancet Infect Dis 2022; 22(7): e178-e90.
11. Weinberger M, Berg SL, Feuerstein IM, *et al*. Disseminated infection with *Mycobacterium gordonae*: report of a case and critical review of the literature. Clin Infect Dis 1992; 14(6): 1229-39.
12. Jarikre LN. *Mycobacterium gordonae* genitourinary disease. Genitourin Med 1992; 68(1): 45-6.
13. Morimoto K, Kazumi Y, Shiraishi Y, *et al*. Clinical and microbiological features of definite *Mycobacterium gordonae* pulmonary disease: the establishment of diagnostic criteria for low-virulence mycobacteria. Trans R Soc Trop Med Hyg 2015; 109(9): 589-93.
14. Ford ES, Horne DJ, Shah JA, *et al*. Species-specific risk factors, treatment decisions, and clinical outcomes for laboratory isolates of less common nontuberculous mycobacteria in Washington state. Ann Am Thorac Soc 2017; 14(7): 1129-38.
15. Goswami B, Narang P, Mishra PS, *et al*. Drug susceptibility of rapid and slow growing non-tuberculous mycobacteria isolated from symptomatics for pulmonary tuberculosis, Central India. Indian J Med Microbiol 2016; 34(4): 442-7.
16. Rastogi N, Goh KS, Bryskier A, *et al*. Spectrum of activity of levofloxacin against nontuberculous mycobacteria and its activity against the Mycobacterium avium complex in combination with ethambutol, rifampin, roxithromycin, amikacin, and clofazimine. Antimicrob Agents Chemother 1996; 40 (11): 2483-7.
17. Marmor M, Sharifi H, Jacobs S, *et al*. Variables associated with antibiotic treatment tolerance in patients with Mycobacterium avium complex pulmonary disease. Respir Res 2024; 25(1): 123.
18. Wang P-H, Shu C-C, Chen C-Y, *et al*. The role of treatment regimen and duration in treating patients with Mycobacterium avium complex lung disease: a real-world experience and case–control study. J Microbiol Immunol Infect 2024; 57(1): 164-74.

IgA Vasculitis as a Rare Presentation of Tuberculosis: A Case Report

Shu-Fa He[1], Meng-Rui Lee[1], Jin-Yuan Shih[1]

Immunoglobulin A (IgA) vasculitis, formerly known as Henoch–Schönlein purpura, is a relatively uncommon form of vasculitis primarily affecting the skin, joints, gastrointestinal tract, and kidneys. We reported the case of an 81-year-old man who initially presented with purpura on both lower legs. He was admitted to the intensive care unit and was later intubated due to pneumonia. He also presented with microscopic hematuria, nephrotic range proteinuria, and renal failure. A skin biopsy showed diffuse neutrophilic infiltration around the capillaries, small venules, and small-to-medium-sized veins in the superficial to deep dermis. Combining the clinical presentations, IgA vasculitis was diagnosed. Miliary lung lesions were noted on the chest radiogram. Sputum acid-fast stain showed acid-fast Gram positive bacilli. *Mycobacterium tuberculosis* was confirmed by polymerase chain reaction, and later by sputum culture. Miliary tuberculosis (TB) and IgA vasculitis were identified and managed accordingly. Following treatment for IgA vasculitis and TB, the patient was successfully liberated from mechanical ventilation, with resolution of skin lesions and improvement in renal function, allowing for the gradual discontinuation of renal replacement therapy. This case highlights the importance of considering TB in the differential diagnosis of IgA vasculitis, as IgA vasculitis could also be a manifestation of active TB. ***(Thorac Med 2025; 40: 44-51)***

Key words: Henoch-Schönlein purpura, immunoglobulin A vasculitis (IgA vasculitis), *Mycobacterium tuberculosis*

Introduction

Immunoglobulin A (IgA) vasculitis, formerly known as Henoch–Schönlein purpura (HSP), is a relatively uncommon form of vasculitis primarily affecting the skin, joints, gastrointestinal tract, and kidneys [1-2]. While the precise etiopathogenesis of IgA vasculitis remains unclear, infections and medications are widely recognized as precipitating factors [3]. Several cases have documented the manifestation of HSP, either preceding or occurring concurrently with the diagnosis of *Mycobacterium tuberculosis* (*M. tuberculosis*) [4-5]. In this study, we present a case of HSP as the initial clinical presentation of pulmonary tuberculosis (TB).

[1]Division of Pulmonary and Critical Care Medicine, Department of Internal Medicine, National Taiwan University Hospital, Taipei, Taiwan.
Address reprint requests to: Dr. Meng-Rui Lee, Department of Internal Medicine, National Taiwan University Hospital, No. 7, Chung Shan S. Rd., Zhongzheng District, Taipei City 100225, Taiwan.

Case Presentation

An 81-year-old man presented to our outpatient department with a 3-day history of progressive purpura affecting both lower legs (Fig. 1). Approximately 1 month prior to his hospital visit, he experienced decreased appetite, progressive malaise, and weight loss. Additionally, he suffered from head contusion to the right occipital area after an accidental fall in the parking lot. Brain computed tomography (CT) revealed hemorrhagic contusions in the left temporal lobe and bilateral frontal lobes, along with spontaneous intracranial hemorrhage in the left parietal region. A neurosurgical consultation was sought, and close monitoring was recommended. Subsequently, he was admitted to our surgical intensive care unit (ICU) for observation. The initial vital signs were: body temperature 37°, blood pressure 128/59 mmHg, heart rate 102 beats per minute, and respiratory rate 20 breaths per minute; pulse oximetry on ambient air was 100%. Neurological examination revealed drowsiness and right-side hemiplegia. Over the ensuing days, vital signs remained stable, and consciousness gradually improved.

However, during the second week in the ICU, the patient developed fever accompanied by a productive cough. Yellowish purulent sputum and worsening purpura on the bilateral lower extremities were observed. Laboratory tests revealed elevated levels of C-reactive protein and serum creatinine, azotemia, and impaired oxygenation (see Table 1). Due to type 1 respiratory failure, the patient required intubation. Empirical treatment with piperacillin/tazobactam was initiated for suspected hospital-acquired pneumonia. Chest radiography and CT revealed diffuse consolidations in bilateral upper lung fields and miliary lung lesions (Fig. 2, Fig. 3). Sputum acid-fast stain showed acid-fast Gram positive bacilli, and *M. tuberculosis* was confirmed by polymerase chain reaction. Subsequent sputum culture identified *M. tuberculosis*.

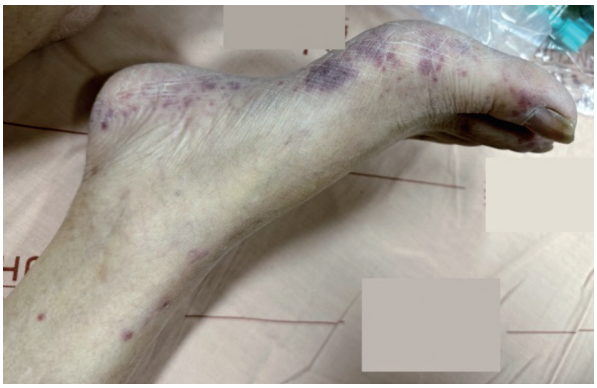

Fig. 1. Skin lesions.
* Purpura on his lower extremities, mainly located on the lower legs and feet.

Table 1. Lab Data

	Lab data	Normal range
Hb (g/dL)	9.1	13.1~17.2
PLT (K/μL)	117	150~378
WBC (K/μL)	7.91	3.25~9.16
AST (U/L)	46	8~31
ALT (U/L)	34	0~41
BUN (mg/dL)	118.0	7~25
CRE (mg/dL)	5.0	0.6~1.3
CRP (mg/dL)	14.34	<1
pH	7.439	7.35~7.45
$PaCO_2$ (mmHg)	26.0	35~45
PaO_2 (mmHg)	85.7	80~100
PaO2/FiO_2 ratio	142	
HCO_3 (mmol/L)	17.2	22~26

*Hb: hemoglobin, PLT: platelet count, WBC: white blood cell count, AST: aspartate transaminase, ALT: alanine aminotransferase, BUN: blood urea nitrogen, CRE: creatine, CRP: C-reactive protein

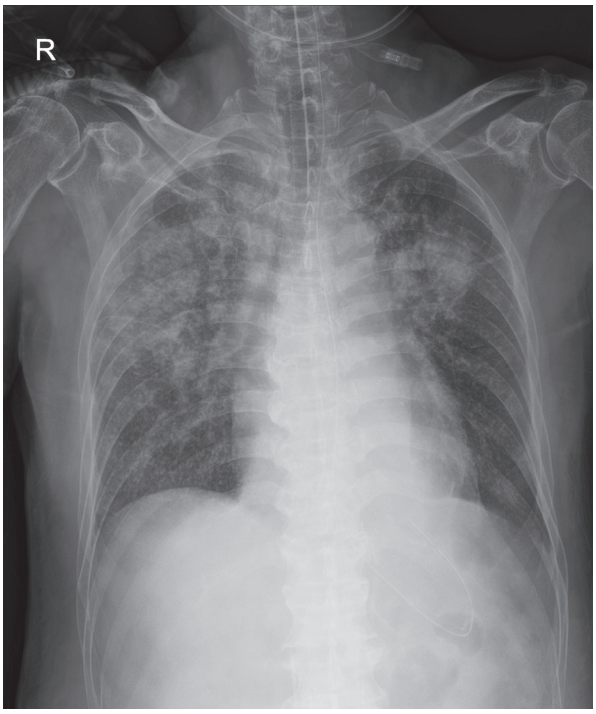

Fig. 2. Chest radiography.
* Chest radiography revealed diffuse consolidations in the bilateral upper lung fields and miliary lung lesions.

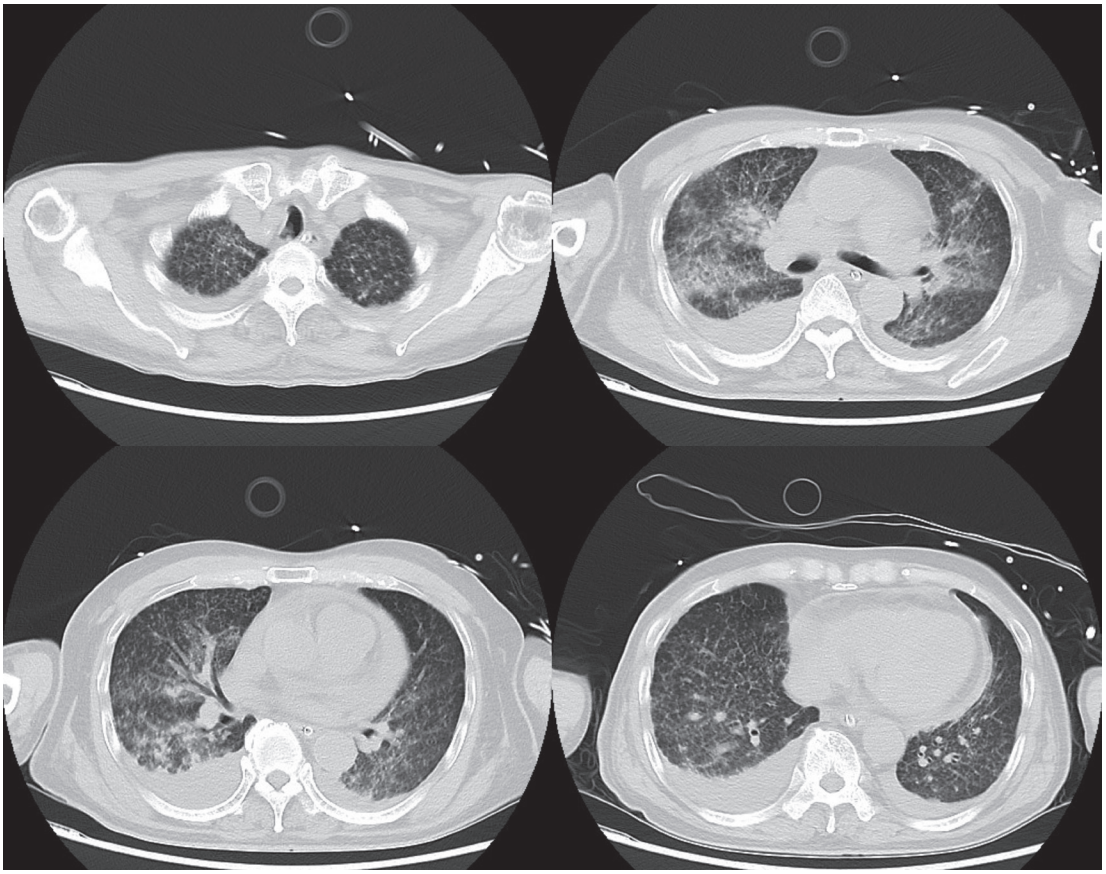

Fig. 3. Chest computed tomography.
* Chest computed tomography (CT) demonstrated diffuse consolidations in bilateral upper lung fields and miliary lung lesions.

The patient was diagnosed with miliary TB.

In addition to azotemia and elevated serum creatinine levels, the patient exhibited oliguria and pericardial effusion. Renal replacement therapy was initiated for supportive care. Urinalysis revealed microscopic hematuria and nephrotic-range proteinuria (Table 2). Serum testing showed negativity for HBV, HCV, cryoglobulin, HIV, syphilis, antistreptolysin O antibodies, c-ANCA, p-ANCA, and anti-GBM antibodies. Serum protein electrophoresis revealed polyclonal gammopathy.

At the same time, a skin biopsy was performed, which revealed diffuse neutrophilic infiltration around the capillaries, small venules, and small-to-medium-sized veins in the superficial to deep dermis. The findings included marked leukocytoclasia and fibrinoid necrosis of the vessel walls (Fig. 4, Fig. 5). Direct immunofluorescence revealed perivascular IgA deposition.

Table 2. Urine Analysis

pH	6.0
Protein	(++++) 300 mg/dl
Glucose	Negative
Ketone	Negative
Blood	(++++)
Bilirubin	Negative
Urobilinogen	Normal
RBC(morphology)	Negative
RBC/HPF	Numerous
WBC/HPF	6-8
Epi Cell/HPF	3-5
Cast	(+)-Granular
Crystals	0
Bacteria	Negative

Based on the aforementioned clinical presentation and results of laboratory tests, a diagnosis of IgA vasculitis was established. Treatment commenced with corticosteroids, specifically dexamethasone at a dose of 20 mg/day (equivalent to methylprednisolone 2 mg/kg/day). Methotrexate was administered for severe nephritis, nephrotic-range proteinuria, and renal failure, while hydroxychloroquine was prescribed for immunomodulation. Standard anti-TB therapy was also initiated.

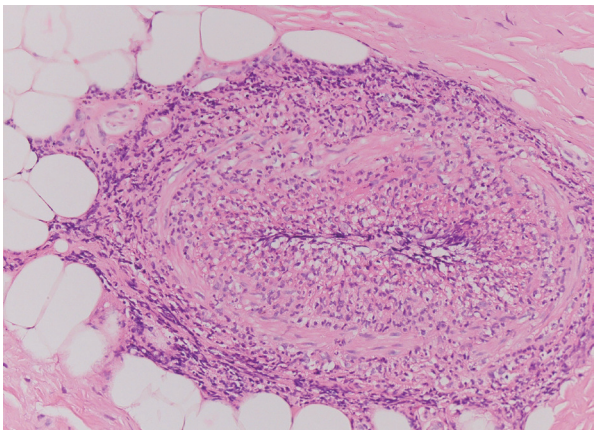

Fig. 4. Skin biopsy.
* Skin biopsy revealed diffuse neutrophilic infiltration around the capillaries, small venules, and small to medium-sized veins in the superficial to deep dermis.

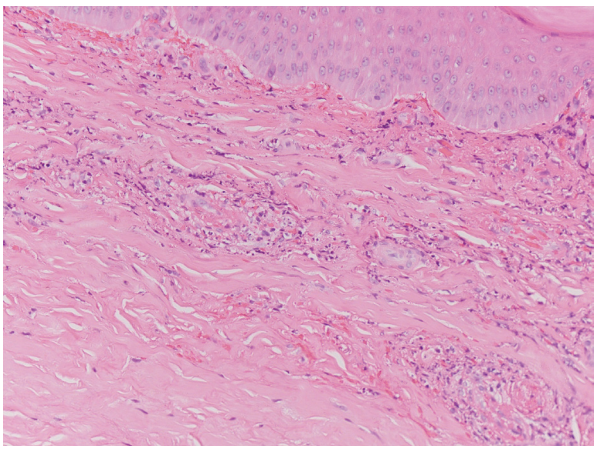

Fig. 5. Skin biopsy.
* Skin biopsy revealed diffuse neutrophilic infiltration around the capillaries, small venules, and small to medium-sized veins in the superficial to deep dermis.

Following a successful 1-month treatment period, the patient was successfully liberated from the ventilator. The chest radiograph revealed improvement in the miliary lesions (Fig. 6). The skin lesions resolved, and renal function improved, allowing the tapering off of renal replacement therapy at the same time. After a total of 37 days in the ICU, the patient was transferred to the general ward.

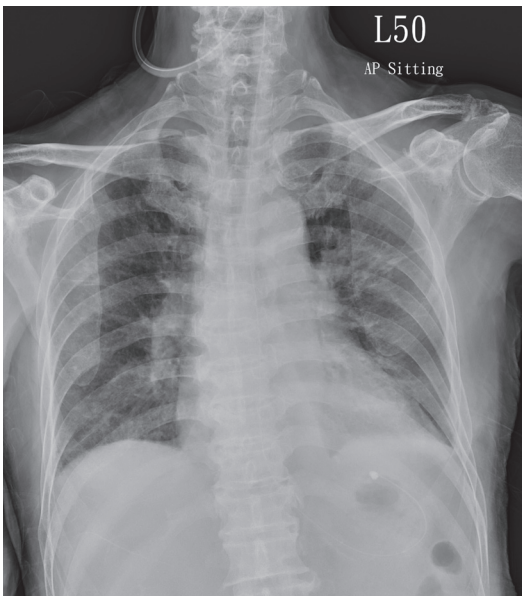

Fig. 6. Chest radiography.
* Chest radiograph revealed improvement in the miliary lesions after a 1-month-long anti-TB treatment.

Discussion

IgA vasculitis is a subset of vasculitis mediated by IgA immune complex deposition, and is clinically characterized by palpable purpura, abdominal pain, arthritis, and renal involvement. IgA vasculitis is more common in children and is rare in adults. The incidence of IgA vasculitis in adults is 0.8-5.1 per 100,000 people [3].

According to the European consensus-based recommendations for the diagnosis and treatment of IgA vasculitis [6-7], a patient is classified as having IgA vasculitis in the presence of purpura or petechiae with lower limb predominance (mandatory) plus 1 of 4 criteria: (1) abdominal pain; (2) histopathology (IgA); (3) arthritis or arthralgia; (4) renal involvement (Table 3).

Table 3. EULAR/PRINTO/PRES Criteria for Henoch-Schönlein Purpura, Childhood Polyarteritis nodosa, Childhood Wegener Granulomatosis and Childhood Takayasu Arteritis: Ankara 2008. Part II: Final Classification Criteria

Criteria	Definition
Purpura (mandatory criteria)	Purpura (commonly palpable and in crops) or petechiae, with lower limb predominance, not related to thrombocytopenia
1. Abdominal pain	Diffuse abdominal colicky pain with acute onset assessed by history and physical examination. May include intussusception and gastrointestinal bleeding
2. Histopathology	Typically leukocytoclastic vasculitis with predominant IgA deposit or proliferative glomerulonephritis with predominant IgA deposit
3. Arthritis or arthralgia	Arthritis of acute onset defined as joint swelling or joint pain with limitation on motion
	Arthralgia of acute onset defined as joint pain without joint swelling or limitation on motion
4. Renal involvement	Proteinuria >0.3 g/24 h or >30 mmol/mg of urine albumin/creatinine ratio on a spot morning sample
	Hematuria or red blood cell casts: >5 red blood cells/high power fields or red blood cells casts in urinary sediment or ≥2+ on a dipstick

*The presence of purpura with lower limb predominance and at least 1 of the other 4 criteria yields a sensitivity of 100% and a specificity of 87%.

Different from IgA vasculitis in children, adult-onset IgA vasculitis has a worse prognosis and higher relapse rate. Mortality rates range from 2.4% to 51.3% [3]. In 1 study, the estimated survival of patients with IgA vasculitis at 5 (72.7 vs 89.7%), 10 (61.6% vs 81.6%) and 20 years (45.2% vs 65.6%) after treatment were significantly lower than those of comparators free of rheumatic disease [8]. The relapse rate of adult-onset IgA vasculitis ranges between 15% and 30%. In contrast, long-term complications and relapses are rare in pediatric IgA vasculitis [3].

In general, most patients with IgA vasculitis only require supportive treatment and adequate analgesia. Corticosteroids should be considered in cases of organ involvement associated with IgA vasculitis, apart from IgA vasculitis nephritis. Such involvement may include orchitis, cerebral vasculitis, pulmonary hemorrhage, and severe gastrointestinal manifestations. Recommended doses of oral corticosteroid are prednisolone 1-2 mg/kg/day (e.g., for 1-2 weeks with weaning over the following 2 weeks). For severe cases (e.g., severe cerebral, pulmonary or gastrointestinal involvement), pulsed IV methylprednisolone 10-30 mg/kg with a maximum of 1 g/day for 3 consecutive days may be considered.

Organ- or life-threatening involvement may also require the addition of cytotoxic immunosuppressants or even plasma exchange, as suggested by the SHARE (Single Hub and Access point for pediatric Rheumatology in Europe) group for rare systemic vasculitis [6]. The patient presented in our report received corticosteroid treatment with dexamethasone at a maximum dose of 20 mg/day (methylprednisolone equivalent dose 2 mg/kg/day), and then was slowly tapered based on clinical symptoms and signs. Methotrexate was given for severe nephritis, nephrotic range proteinuria, and renal failure; and hydroxychloroquine was also prescribed for immunomodulation. The skin lesion and renal function impairment finally recovered under the anti-TB drugs, corticosteroids, methotrexate and hydroxychloroquine.

Though rare, the coexistence of adult-onset IgA vasculitis and TB infection has been reported. In certain instances, IgA vasculitis has manifested prior to the initiation of anti-TB therapy in affected patients (Table 4). All patients improved either with anti-TB drugs alone or with anti-TB drugs associated with corticosteroid. It is suggested that TB infection may serve as a precipitating factor for IgA vasculitis, independent of the use of anti-TB medications.

The pathophysiology underlying TB and IgA vasculitis remains to be elucidated. Previous studies have shown that mycobacteria inhibit apoptosis of infected macrophages by regulating Mycobacterial heat shock proteins [13], and by prompting serine protease inhibitors [14-15]. There is also a lack of apoptotic cell clearance during mycobacterial infections [16]. Combining the 2 mechanisms above, *M. tuberculosis* infection promotes some pro-inflammatory cytokines (TNF-alpha, IL-6, IL-1b, IL-12, NO), human leukocyte antigens (HLAs), and co-stimulatory molecules (CD40, CD80, and CD86) expression, and this increases autoimmunity during mycobacterial infection, explaining the relationship between mycobacterial infection and autoimmunity.

Conclusion

Immunoglobulin A (IgA) vasculitis, formerly referred to as HSP, is a relatively rare condition in adults. Several case reports have

Table 4. Reported Adult-onset IgA Vasculitis Before anti-TB Drugs

Case report	Age/gender	Onset of IgA vasculitis	Clinical presentation of IgA vasculitis	Skin biopsy	TB infection	Treatment	Outcome
Masakazu Washio, *et al*. [9]	21, male	2 weeks after TB symptoms, before anti-TB drugs	Purpura, macroscopic hematuria and proteinuria	-	Pleuritis	INH + RMP + EMB + CS	Recovered
Pacheco A, *et al*. [10]	33, male	After TB, before anti-TB drugs	Palpable purpura in both legs, vasculitic lesions of the gut and skin	Deposition of IgA, IgM, C3, and C1Q in the walls of the small vessels	Pulmonary+ lymphadenitis	INH + RMP + EMB + CS	Recovered
Zen Isobe, *et al*. [11]	54, male	Concomitant with TB	Purpura in both legs, microscopic hematuria and proteinuria, renal function deterioration, and nephrosis appeared	Leukocytoclastic vasculitis	Pulmonary	INH + RMP + EMB + PZA + CS	Recovered
Jie Li, *et al*. [12]	24, male	3 weeks before TB was diagnosed	Palpable purpura on the extremities, especially on the lower extremities and buttocks, bloody stools and abdominal and bilateral knee pain	-	Pulmonary	INH+ RMP+ EMB	Recovered
(This case)	82, male	Concomitant with TB	Purpura in both legs, microscopic hematuria, nephrotic range proteinuria, and renal failure	Leukocytoclasia and fibrinoid necrosis of the vessel wall, with perivascular IgA	Miliary	INH + RMP + EMB + PZA + CS+ MTX + hydroxychloroquine	Recovered

ATD: anti-tuberculosis drugs, CS: corticosteroids, EMB: ethambutol, INH: isoniazid, PZA: pyrazinamide, RMP: rifampicin, SM: streptomycin, MTX: methotrexate, TB: tuberculosis.

documented the concurrent occurrence of IgA vasculitis and TB infection. Therefore, when an adult patient presents with symptoms consistent with IgA vasculitis, it is imperative to consider the possibility of TB to prevent misdiagnosis and ensure timely treatment. Meanwhile, IgA vasculitis may manifest as a presentation of TB. When purpura arises in a patient diagnosed with *M. tuberculosis*, early identification of IgA vasculitis is crucial for initiating appropriate management and preventing further involvement of vital organs.

Acknowledgements

I would like to express my sincere gratitude to my teachers, whose invaluable advice and support have been graciously provided amidst their demanding schedules. I am also deeply thankful to my colleagues for their assistance in

crafting this article and their collaborative efforts in our work. Additionally, I am immensely grateful to my wife for her unwavering support throughout all aspects of life.

References

1. Yıldırım R, Üsküdar Cansu D, Uludoğan BCE, *et al*. The coexistence of IgA vasculitis and tuberculosis: a case-based review. Rheumatol Int 2021 Sep; 41(9): 1683-1689.
2. Shaul GM, Richard JG. Massry and Glassock's textbook of nephrology. In: George BH ed. Henoch-Schonlein Purpura: Clinical Features, Etiology and Pathogenesis, Laboratory Findings, Pathology, Natural History, Management, and Transplantation, 4th ed. Philadelphia; Lippincott Williams & Wilkins, 2001: 804-808.
3. Kelly BG, Stratton DB, Mansour I, *et al*. Navigating the initial diagnosis and management of adult IgA vasculitis: a review. JAAD Int 2022 Jun 13; 8: 71-78.
4. Li J, Wang XZ, Wang RC, *et al*. Pulmonary tuberculosis presenting as Henoch-Schönlein purpura: case report and literature review. Medicine (Baltimore) 2020 Oct 2; 99(40): e22583.
5. Pandhi D, Kaur I, Singal A, *et al*. Atypical presentation of immunoglobulin A vasculitis in disseminated tuberculosis. Int J Dermatol 2019 Jan; 58: e1-e3.
6. Ozen S, Marks SD, Brogan P, *et al*. European consensus-based recommendations for diagnosis and treatment of immunoglobulin A vasculitis-the SHARE initiative. Rheumatology (Oxford) 2019 Sep 1; 58(9): 1607-1616.
7. Ozen S, Pistorio A, Iusan SM, *et al*. EULAR/PRINTO/PRES criteria for Henoch-Schönlein purpura, childhood polyarteritis nodosa, childhood Wegener granulomatosis and childhood Takayasu arteritis: Ankara 2008. Part II: Final classification criteria. Ann Rheum Dis 2010 May; 69(5): 798-806.
8. Nossent J, Raymond W, Keen HI, *et al*. Morbidity and mortality in adult-onset IgA vasculitis: a long-term population-based cohort study. Rheumatology (Oxford) 2021 Dec 24; 61(1): 291-298.
9. Washio M, Nanishi F, Onoyama K, *et a*l. Recurrence of Henoch Schoenlein purpura nephritis associated with tuberculous pleuritis. Nihon Jinzo Gakkai Shi 1988 Sep; 30(9): 1087-9.
10. Pacheco A. Henoch-Schönlein vasculitis and tuberculosis. Chest 1991 Jul; 100(1): 293-4
11. Isobe Z, Suga T, Aoki Y, *et al*. A case of anaphylactoid purpura associated with nephrosis followed by pulmonary tuberculosis. Nihon Kokyuki Gakkai Zasshi 2008 Aug; 46(8): 645-9. [In Japanese, English abstract]
12. Li J, Wang XZ, Wang RC, *et al*. Pulmonary tuberculosis presenting as Henoch-Schönlein purpura: case report and literature review. Medicine (Baltimore) 2020 Oct 2; 99(40): e22583.
13. Dubaniewicz A, Trzonkowski P, Dubaniewicz-Wybieralska M, *et al*. Comparative analysis of mycobacterial heat shock proteins-induced apoptosis of peripheral blood mononuclear cells in sarcoidosis and tuberculosis. J Clin Immunol 2006 May; 26(3): 243-50.
14. Gatto M, Iaccarino L, Ghirardello A, *et al*. Serpins, immunity and autoimmunity: old molecules, new functions. Clin Rev Allergy Immunol 2013 Oct; 45(2): 267-80.
15. Nagata S, Hanayama R, Kawane K. Autoimmunity and the clearance of dead cells. Cell 2010 Mar 5; 140(5): 619-30.
16. Osterloh A, Breloer M. Heat shock proteins: linking danger and pathogen recognition. Med Microbiol Immunol 2008 Mar; 197(1): 1-8.

Mixed Intrapulmonary Graft-Versus-Host Disease with Pulmonary Fibrosis after Blood Stem Cell Transplantation: A Case Report

Yu-Cheng Chang[1], Xu-Heng Chiang[1,2], Min-Shu Hsieh[3], Hsao-Hsun Hsu[1]

We presented the unique case of a 23-year-old woman with severe lung fibrosis associated with chronic graft-versus-host disease (GVHD) and bronchiolitis obliterans syndrome (BOS) following allogeneic hematopoietic stem cell transplantation for acute myeloid leukemia. This patient underwent bilateral sequential lung transplantation as salvage therapy. The histopathological analysis of the explanted lungs revealed constrictive bronchiolitis and interstitial fibrosis, which confirmed the diagnosis. This is a rare report of complex lung pathology after allogeneic hematopoietic stem cell transplantation involving GVHD and lung fibrosis that contributed to lung damage. These findings provide insights for pathologists, and aid in further exploration of the mechanisms underlying GVHD and BOS. ***(Thorac Med 2025; 40: 52-57)***

Key words: Blood stem cell transplantation, lung transplantation, graft-versus-host disease (GVHD), lung fibrosis, bronchiolitis obliterans syndrome (BOS)

Introduction

Graft-versus-host disease (GVHD) is a complication of bone marrow transplants. In some circumstances, immune cells in the donor organ (graft) attack the recipient's (host) tissues. GVHD primarily affects the skin, liver, and gastrointestinal tract, and in some cases, the lung tissue. GVHD can be acute or chronic, based on the symptoms of GVHD that show up. Symptoms include skin rash, jaundice, and diarrhea, and even pulmonary fibrosis. Preventive measures include matching the donor and recipient HLA types, and using immunosuppressive drugs. Treatment to manage symptoms and immune responses includes corticosteroids and

[1]Department of Surgery, National Taiwan University College of Medicine and National Taiwan University Hospital, Taipei, Taiwan. [2]Department of Medical Education, National Taiwan University Hospital, Taipei, Taiwan. [3]Department of Pathology, National Taiwan University College of Medicine and National Taiwan University Hospital, Taipei, Taiwan.
Address reprint requests to: Dr. Xu-Heng Chiang, No. 7, Chung Shan S. Rd. (Zhongshan S. Rd.), Zhongzheng Dist., Taipei City 100225, Taiwan (R.O.C.)

other immunosuppressants. Pulmonary involvement of GVHD does not often occur, but can be clinically challenging to treat. We present the case of a 23-year-old female who encountered GVHD after bone marrow transplant, and who received lung transplant as a treatment for GVHD.

Case Report

A 23-year-old non-smoking woman underwent haploidentical hematopoietic stem cell transplantation (HSCT) for acute myeloid leukemia (AML) with myelodysplasia-related changes. Bronchiolitis obliterans syndrome (BOS) then developed. Respiratory distress progressed to respiratory failure 5 years after HSCT. Bilateral sequential lung transplantation was performed 7 years after HSCT because she presented with initial symptoms of petechiae and ecchymosis on her trunk and extremities. Abnormal hemogram results were observed. A bone marrow examination confirmed the AML diagnosis. Complete remission was achieved after chemotherapy comprising idarubicin and cytarabine. However, relapse was detected by a bone marrow test and flow cytometry. Treatments including fludarabine and cytarabine were administered; however, a sequential bone marrow test showed regenerative bone marrow with residual leukemic cells (1.86%), indicating a relapse-refractory status.

Haploidentical HSCT was performed 1 month later. Although a bone marrow test revealed stable engraftment, skin rash, erythematous changes, and itchiness presented a few weeks after HSCT. During the following months, relapse occurred twice. She then underwent peripheral blood stem cell transplantation (PBSCT) at 2 and 4 months after HSCT.

Shortness of breath developed approximately 1 year after PBSCT. Surgical and invasive interventions were not performed for pneumomediastinum and pneumothorax. Chronic GVHD-related lung disease was suspected. GVHD symptoms occurred repeatedly, and were treated with ruxolitinib, but her clinical condition continued to deteriorate, and pulmonary function gradually declined. The pulmonary function test showed a restrictive pattern with a forced expiratory volume in 1 second (FEV_1) of 18.5%.

Bilateral sequential lung transplantation was then performed. Pathological examination of the native lungs revealed BOS and constrictive bronchiolitis with a florid foreign body giant cell reaction. Interstitial fibrosis of the lung parenchyma also was observed (Fig. 1-4). One nodule observed intraoperatively in the donor's right upper lung was adenocarcinoma with a free resection margin. Serial follow-up revealed no evidence of lung cancer. According to the pathological report, there was a solitary tumor, and the invasive part of the tumor was measured as 0.2 x 0.2 x 0.2 cm. The histological grade was well-differentiated, and subtypes were accounted for as acinar: 40%, papillary: 20%, and lepidic: 40%. The tumor was identified microscopically only, and was not grossly evident. There was no lymphovascular invasion, and the tumor did not invade the visceral pleura (PL0). Also, no evidence of spread through air spaces was recorded. The pathological staging of this tumor was pT1aN0M0.

Discussion

Signs of GVHD in the lungs and progressive worsening of lung function can confirm chronic GVHD with BOS. BOS was defined as a permanent decrease in FEV1. The 5- and 10-

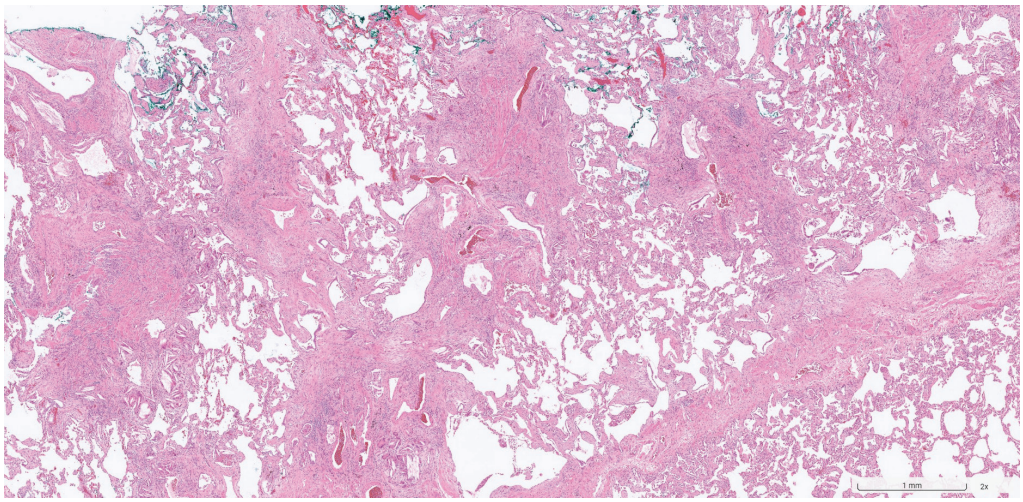

Fig. 1. A clustering of fibroblast cells aggregation, leading to a structural distortion.

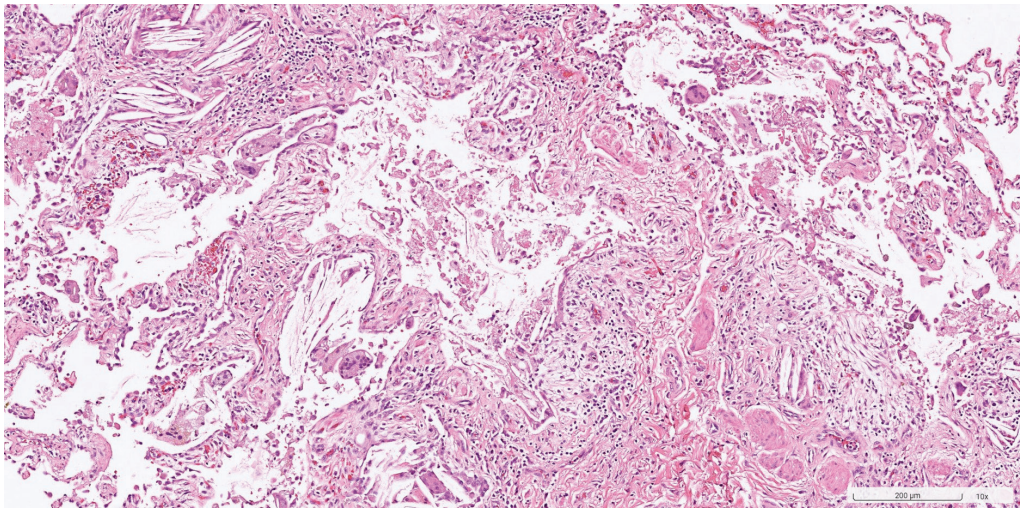

Fig. 2. Inflammation focused around the small airways; bridging fibrosis connecting adjacent areas was also observed.

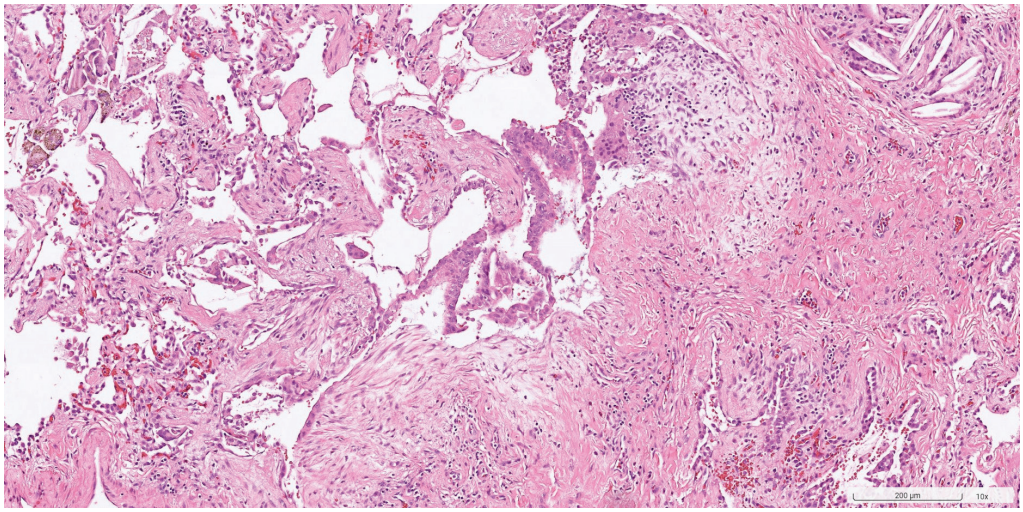

Fig. 3. A narrowing or obstruction of the bronchioles, and inflammation cells and fibrosis were found predominantly.

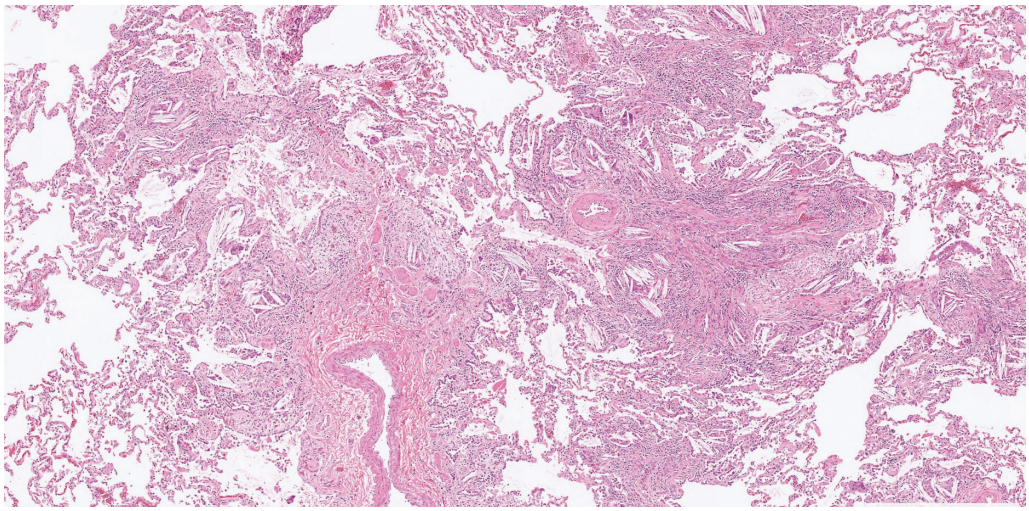

Fig. 4. There was a presence of cholesterol clefts within the area of fibrosis, and aggregation with inflammatory cells.

year survival rates of BOS are 53% and 30%, respectively [1, 2]. BOS has 3 main risk factors: alloimmune factors, non-alloimmune factors (such as primary graft dysfunction and infections), and medication non-adherence [3-4].

Diagnosis of GVHD of the lungs following a bone marrow transplant involves a combination of clinical evaluation, pulmonary function tests, imaging studies, and sometimes biopsy. Clinically, patients may present with symptoms such as a chronic cough, wheezing, dyspnea (shortness of breath), and decreased exercise tolerance. A thorough patient history and physical examination are essential to rule out other potential causes of respiratory symptoms.

Pulmonary function tests are crucial in the diagnosis. A hallmark of GVHD-related lung disease is a progressive decline in FEV1 without a corresponding decrease in forced vital capacity (FVC), indicating an obstructive pattern. A reduction in the FEV1/FVC ratio is often observed. Additionally, a decline in the diffusion capacity for carbon monoxide may be present.

Imaging studies, particularly high-resolution computed tomography (HRCT), are used to assess structural changes in the lungs. HRCT may show air trapping, bronchial wall thickening, and a mosaic attenuation pattern, which are indicative of small airway disease. In some cases, a lung biopsy may be performed to confirm the diagnosis. The biopsy can reveal features of bronchiolitis obliterans, such as fibrosis and inflammation in the bronchioles.

Bronchoscopy with bronchoalveolar lavage (BAL) can be useful to exclude infections and other conditions that mimic GVHD lung disease. BAL fluid analysis helps in identifying infections, which can complicate the diagnosis.

Overall, diagnosing GVHD lung disease requires a multidisciplinary approach, combining clinical, functional, and radiological data to arrive at a definitive diagnosis.

Pathological features of pulmonary GVHD include peribronchiolar T cells, apoptosis, and perivasculitis; these distinguish GVHD from infections [5]. Alloimmune responses that cause vascular rejection, lymphocytic bronchiolitis, antibody-mediated rejection, and infections can contribute to BOS.

HSCT and PBSCT are 2 methods of stem

cell transplantation, each with distinct implications for GVHD. In HSCT, stem cells are harvested from the bone marrow. This method is associated with a lower incidence of chronic GVHD, compared to PBSCT. However, it has a longer engraftment period, which can delay immune reconstitution.

PBSCT involves collecting stem cells from the peripheral blood after mobilization with growth factors. PBSCT is linked to a higher incidence and severity of both acute and chronic GVHD, due to the higher number of T-cells in the graft. Despite this, PBSCT generally leads to faster engraftment and quicker immune recovery. Our patient received both HSCT and PBSCT in sequence. Chronic GVHD developed after PBSCT, which may be compatible with the risk mentioned in previous studies. However, whether there would be a higher risk of developing GVHD after both HSCT and PBSCT is unclear[5].

The recipient's lungs had focal bronchiectasis in the medium and large bronchi, and constrictive bronchiolitis characterized by unclear fibrosis around the bronchiolar lumen. Some bronchioles had focal scars with bronchiolar smooth muscles near the small artery, but others were almost completely closed. More than half of the lungs had bronchioles on both sides.

Pathological features of BOS include epithelium damage, inflammation around the bronchi, and lung tissue scarring [6]. These were different from our observations of localized bronchiectasis affecting medium or large bronchi. We observed irregular fibrosis in the interstitium and subpleura, with varying degrees of severity in the affected areas. Some areas had distinct fibrotic nodules with trapped alveolar spaces. We did not observe clear signs of honeycombing in the lung. Some alveolar spaces contained glassy and eosinophilic materials; however, specific pathogens were not detected. Some areas had partial blockage by fibrosis of the inner lining of blood vessels, but there was no evidence of blood vessel inflammation.

According to the pathological analysis, the bronchiolitis was constrictive and accompanied by varying degrees of interstitial fibrosis. Pathology did not show any signs of lymphoma or lymphoproliferative disorders soon after transplantation. The patient presented with unusual pathological features, such as extensive damage to the medium and large bronchi, and focal areas of interstitial fibrosis. Therefore, progressive deterioration of lung function might have been caused by mixed GVHD affecting the bronchial epithelium, and by pulmonary fibrosis involving the alveolar septa. The patient also had a history of recurrent infections, particularly in the pulmonary system, which may have accelerated BOS. She experienced multiple episodes of extrapulmonary GVHD that affected the skin, and also had acute and chronic GVHD involving at least 2 organs. We hypothesized that GVHD in the lungs might have caused the initial decrease in pulmonary function, from 85% to 43%, after lung transplantation. Subsequent pulmonary fibrosis worsened the lung function. Repeated infections may have aggravated this process.

Conclusion

Patients with BOS after allogeneic HSCT may have both GVHD and pulmonary fibrosis. For these patients, bilateral lung transplantation may be a feasible treatment option.

References

1. Arai S, Arora M, Wang T, *et al*. Increasing incidence

of chronic graft-versus-host disease in allogeneic transplantation: a report from the Center for International Blood and Marrow Transplant Research. Biol Blood Marrow Transplant 2015; 21(2): 266-74. doi: 10.1016/j.bbmt.2014.10.021.

2. Hildebrandt GC, Fazekas T, Lawitschka A, *et al*. Diagnosis and treatment of pulmonary chronic GVHD: report from the consensus conference on clinical practice in chronic GVHD. Bone Marrow Transplant 2011; 46(10): 1283-95. doi: 10.1038/bmt.2011.35.
3. Chien JW, Duncan S, Williams KM, *et al*. Bronchiolitis obliterans syndrome after allogeneic hematopoietic stem cell transplantation--an increasingly recognized manifestation of chronic graft-versus-host disease. Biol Blood Marrow Transplant 2010; 16(1)(suppl): S106-14. doi: 10.1016/j.bbmt.2009.11.002.
4. Christie JD, Edwards LB, Kucheryavaya AY, *et al*. The Registry of the International Society for Heart and Lung Transplantation: 29th adult lung and heart-lung transplant report-2012. J Heart Lung Transplant 2012; 31(10): 1073-86. doi: 10.1016/j.healun.2012.08.004.
5. Maurer K, Kim HT, Garrity HM, *et al*. Lower incidence of chronic GVHD observed after transplantation with cryopreserved unrelated allogeneic stem cells. Blood Adv 2023 Jun 13; 7(11):2431-2435. doi: 10.1182/bloodadvances.2022009231. PMID: 36595453; PMCID: PMC10241844.
6. Estenne M, Maurer JR, Boehler A, *et al*. Bronchiolitis obliterans syndrome 2001: an update of the diagnostic criteria. J Heart Lung Transplant 2002; 21(3): 297-310. doi: 10.1016/s1053-2498(02)00398-4.

Reactivation of Tuberculosis Following Immunotherapy Combined with Chemotherapy and an Anti-angiogenic Agent in Non-small Cell Lung Cancer – A Case Report and Literature Review

Jiunn-Song Jiang[1], Yu-Wung Yeh[1,2]

Tuberculosis (TB) reactivation following immunotherapy is a rare adverse event, with only a few documented cases in the existing literature. The incorporation of immunotherapy into treatment strategies has expanded the range of options for patients with advanced non-small cell lung cancer. The reactivation of TB during lung cancer immunotherapy is becoming an increasingly recognized concern. The recognition and management of reactivated TB is not only crucial for the patient's cancer treatment outcome, but also for the health of treatment providers. Herein we present the case of a 56-year-old male with stage IV adenocarcinoma of the lung who received combination immunotherapy, chemotherapy, and an anti-vascular endothelial growth factor agent and experienced TB reactivation during treatment. This case highlights the importance of physicians remaining vigilant for potential opportunistic infections in patients undergoing immunotherapy. ***(Thorac Med 2025; 40: 58-64)***

Key words: atezolizumab, immune checkpoint inhibitor, immunotherapy, lung cancer, tuberculosis

Introduction

Lung cancer ranks as the most common cause of cancer deaths worldwide [1]. It was also the number one invasive cancer type in terms of both incidence and mortality rate in Taiwan in 2023 [2]. Immune checkpoint inhibitors (ICIs) have increasingly played a key role in lung cancer treatment in Taiwan since the reimbursement of certain regimens containing immunotherapy agents was instituted by Taiwan's National Health Insurance. It is well-known that cytotoxic cancer treatment poses a risk of tuberculosis (TB) reactivation in patients with latent tuberculosis infection (LTBI), due to immunosuppression [3]. ICI, on the other hand, by boosting the patient's immunity, does not promote immunocompromise in theory. Therefore, the precise mechanism of TB reactivation after ICI therapy is not well known. Oftentimes a reactivated TB lesion can be mistaken for cancer metastasis. This article will discuss the case

[1]Shin Kong Wu-Ho-Su Memorial Hospital, Taipei, Taiwan, [2]Fu Jen Catholic University, College of Medicine, New Taipei City, Taiwan.
Address reprint requests to: Dr. Yu-Wung Yeh, Division of Chest Medicine, Shin Kong Memorial Hospital, 95 Wenchang Rd, Shilin District, Taipei, Taiwan, 10111.

of a patient with non-small cell lung cancer (NSCLC) who developed TB reactivation following the use of combination immunotherapy, an anti-angiogenic agent, and chemotherapy, and includes a review of the relevant literature.

Case Report

A 56-year-old male initially presented with right-side chest pain radiating to his back for 3 months. He has a 30-pack-year smoking history. A computed tomography (CT) scan in April 2023 revealed a solitary mass in the right lower lobe (RLL), along with mediastinal lymphadenopathy, pan-lobular emphysema, and bilateral upper lung fibrotic changes. A biopsy of the lung tumor confirmed an adenocarcinoma. Epidermal growth factor receptor (EGFR) mutational analysis showed a wild-type EGFR allele. No anaplastic lymphoma kinase (ALK) rearrangement or c-ROS oncogene 1 (ROS-1) was found. Programmed death-ligand 1 (PD-L1) (SP263) assay indicated the presence of PD-L1 expression in tumor cells (TC) >= 50%. An ^{18}F-FDG positron emission tomography (PET) and delayed chest PET/CT study revealed increased FDG uptake in the RLL tumor, pleural retraction, and metastases in regional and distant lymph nodes (mediastinal, bilateral hilar, hepatic hilar, and para-aortocaval regions). The overall staging was cT2N3M1c, stage IVB. On June 12, 2023, the patient began a course of 6 sessions of pemetrexed (500 mg/m^2), cisplatin (70 mg/m^2), bevacizumab (7.5 mg/kg) and atezolizumab (1200 mg).

He was evaluated regularly every 3 months during therapy and follow-up. A CT scan revealed a partial response with regression in size of the RLL tumor, as well as the regional and distant lymph nodes (Figure 1A, 1B, axial view; Figure 1C, 1D, coronal view). However, progressive changes were noted in the previously

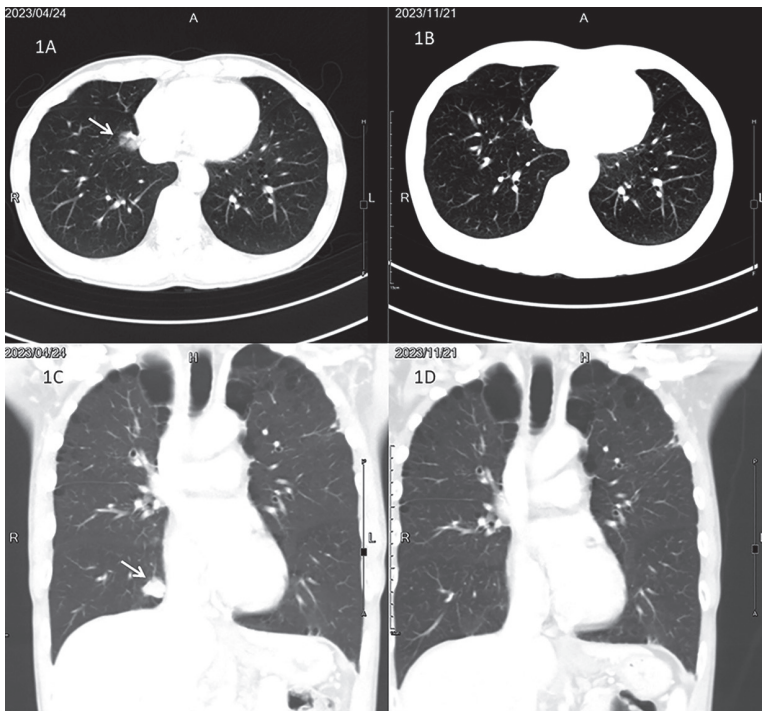

Fig. 1. Changes in lung tumor imaging before and after combination ICI therapy. Initial computed tomography at the time of diagnosis of lung cancer shows a 2.1 cm mass lesion (arrow) in the medial basal right lower lobe with focal pleural attachment (1A: axial view; 1C: coronal view). Tumor regression (arrowhead) is observed after combination ICI therapy (1B: axial view; 1D: coronal view).

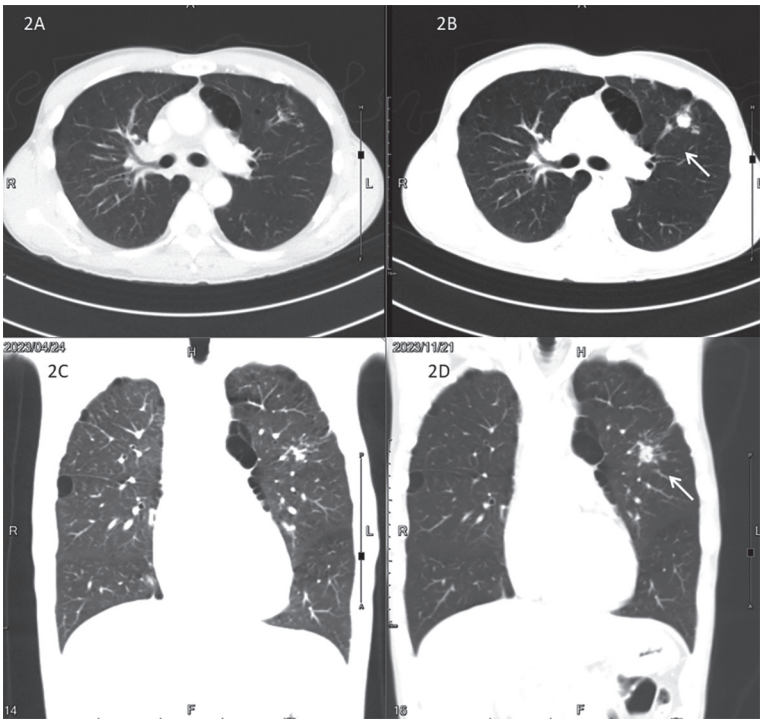

Fig. 2. Changes in granulomatous lesion imaging before and after combination ICI therapy. Initial computed tomography at the time of diagnosis of lung cancer reveals a small fibrocalcified granulomatous lesion (arrow) in the anterior segment of the left upper lobe (1A: axial view; 1C: coronal view). Progressive changes in the granulomatous lesions (arrowhead) are observed after combination ICI therapy (2B: axial view; 2D: coronal view).

small fibrocalcified granulomatous lesions in the left upper lobe (Figure 2A, 2B, axial view; Figure 2C, 2D, coronal view), accompanied by enlarged peribronchial nodules, suggesting possibly active granulomatous disease or new metastasis. A work-up was undertaken to search for infectious etiologies: the cryptococcus antigen test was negative while the QuantiFERON-TB (IGRA) test was positive. Bronchial brushing and broncho-alveolar lavage of the affected area were performed. Cytology examination from both procedures was negative for malignancy. No fungi were cultured from the lavage fluid after 21 days, but *Mycobacterium tuberculosis complex* (MTB) grew from both the lavage fluid and sputum on Lowenstein-Jensen medium after 24 days. He began a standard anti-TB regimen with isoniazid, rifampin, ethambutol, and pyrazinamide starting in January 2024.

Discussion

Cancer immunotherapy is designed to boost the immune system and restore the anti-tumor function of T cells [4]. However, the immune activation induced by ICIs can also result in immune-related adverse events (IRAEs). There is growing evidence that anti-PD-1/PD-L1 immunotherapy may lead to the reactivation of TB infection [5, 6, 7, 8].

In Taiwan, TB had an incidence rate of 28.2 cases per 100,000 population as of 2022 [9], falling from a high of 72.5 cases/100,000 in 2005 [10]. Globally, TB was still the second leading cause of death from a single infectious agent as of 2022, after COVID-19 [11]. MTB infection often persists for many years after initial infection, possibly for life. It is noteworthy that approximately 90-95% of individuals infected with MTB, who do not have a human

immunodeficiency virus (HIV) infection, do not progress to active TB disease [12]. Nevertheless, these individuals remain at risk of developing the disease in the future. The transition from latent to active TB infection is thought to indicate a weakened immune response. This is evident from the increased occurrence of TB in individuals with HIV infection [13] or following anti-tumor necrosis factor treatment for inflammatory conditions [14].

Since the 1970s, cancer has been identified as an independent risk factor for developing active MTB infection. Patients with solid cancers and hematological malignancies are immunocompromised from both the disease itself and the effects of chemotherapy. Dobler *et al*. [15] performed a systematic review and meta-analysis that included 13 studies with a total of 921,464 cancer patients. They reported a significantly higher risk of TB among cancer patients compared to the general population. Furthermore, the risk of TB significantly differs across various types of cancer, and is in turn influenced variably by the choice of anti-cancer treatments.

There is limited information regarding whether patients treated with ICIs have a higher incidence of TB reactivation than a reference group of patients with solid cancers and hematological malignancies. As immunotherapy in theory boosts the immune system and thus should not predispose the patient to reactivation of infection, the mechanism of TB reactivation following treatment with ICIs remains to be elucidated. Elkington *et al*. [16] performed an immunohistochemical analysis of TB lung lesions in patients with a presumed normal immune response and a patient who developed TB after anti–PD-1 immunotherapy. They found that the PD-1/PD-L1 pathway was active in TB granuloma with co-expression of both PD-L1 and CD8, whereas in the ICI-treated specimens, PD-1 reactivity was reduced.

The protective immunity against MTB in humans involves a complex interplay between the host and pathogenic factors. Although the immune system functions to defend against infections and maintain tissue equilibrium, overactive immune responses can lead to cytotoxicity and destruction of the extracellular matrix, thus leading to tissue damage, which may foster TB reactivation [17]. ICIs are now recognized as pivotal in this regulation by curbing excessive T-cell activation and thereby preventing immunopathology or autoimmunity [18]. The reactivation of effector functions observed with ICI in vitro can potentially worsen TB infection instead of enhancing control in vivo. Therefore, MTB may thrive in a hyper-inflammatory environment [19], such as that promoted by the use of ICIs through enhancement of T-helper type 1 (Th1) responses, breaking the equilibrium of host-pathogen interactions in the lung. Studies have shown that human T cell epitopes are highly conserved in MTB through evolution, indicating that adaptive T cell response may actually benefit the pathogen, perhaps by increasing tissue damage and aiding its spread [20].

How latent TB should be managed in cancer patients remains a topic of debate. While TB patients are more susceptible to the development of lung cancer [21-22], cancer patients are also at a higher risk for contracting TB regardless of whether they are receiving ICI treatment. The risk of developing active TB is 2 to 3 times higher in patients with solid cancer compared to the general population [3, 15, 23-24]. A retrospective cohort study conducted in Taiwan on patients with lung cancer revealed that the incidence of TB increased with advanc-

ing age [21].

In terms of the possibility of ICI treatment leading to TB development, however, data from a nationwide observational study in South Korea showed that ICI treatment was not significantly associated with a higher risk of TB [25]. They reported that while the rate of TB among cancer patients exposed to ICIs was 8 times greater than in the general population, the risk of cancer patients developing TB did not show a significant difference based on ICI exposure. Similarly, a retrospective study carried out at another Korean referral hospital reported a low (0.26%) incidence of TB in 1,144 solid-cancer patients who began treatment with ICIs from July 2014 to December 2018. However, it was unclear whether the TB incidence in these patients was similar to that in elderly cancer patients [26]. Since our patient received combination immunotherapy, chemotherapy, and an anti-angiogenic agent, it is impossible to definitively ascertain which agent played the central role in TB reactivation. Indeed, it might have been the aggregate of the above combination, in addition to his lung cancer.

Identifying TB following ICIs treatment in a cancer patient can be challenging, as its symptoms can overlap those of cancer progression. Although IGRA is widely used as a tool for identifying latent TB, it has a limited role in diagnosing active TB infection as it only detects the presence of an adaptive immune response directed towards a defined set of MTB antigens, which could have occurred in the past [27]. The gold-standard diagnosis of reactivated TB is still a positive TB culture in respiratory specimens. In the past, the approach to treating TB reactivation during the course of ICI treatment typically included discontinuing ICI therapy and starting anti-TB medications [28]. In certain situations, ICI treatment might be resumed once TB is under control. However, Shi *et al*. [29] demonstrated the safety of concurrent anti-TB and anti-PD-1 treatments for lung cancer complicated with MTB infection. In their retrospective study, 11 patients with old/latent MTB infections and 2 patients with active MTB infections were treated with ICI. Neither reactivation of old or latent TB nor progression of active TB infection was observed during immunotherapy. At present, there is no clear guidance on LTBI screening for cancer patients. The 2018 WHO guidelines discouraged LTBI screening for this group due to a lack of sufficient evidence [30].

In our case, the patient continues to receive ICI, chemotherapy, and an anti-VEGF agent, along with anti-TB medications. The patient's condition remained stable at the time of the drafting of this manuscript.

Conclusion

In summary, the reactivation of TB is increasingly recognized as a potential development during the use of ICI-containing regimens. The mechanism behind such reactivation is as yet unclear. Screening for latent TB and offering chemoprophylaxis to those with positive results concurrently with immunotherapy may be recommended.

References

1. World Health Organization. Lung Cancer: World Health Organization; 2023 [updated 6/26/2023; cited 2024 April 24]. Available from: https://www.who.int/news-room/fact-sheets/detail/lung-cancer
2. Taiwan Ministry of Health and Welfare. Cancer Registry Annual Report, 2021, Taiwan: Health Promotion Administration Ministry of Health and Welfare; 2021. Available from: https://www.hpa.gov.tw/File/

Attach/17639/File_23506.pdf
3. Simonsen DF, Farkas DK, Horsburgh CR, *et al*. Increased risk of active tuberculosis after cancer diagnosis. J Infect 2017; 74(6): 590-598.
4. Waldman AD, Fritz JM, Lenardo MJ. A guide to cancer immunotherapy: from T cell basic science to clinical practice. Nat Rev Immunol 2020 Nov; 20(11):651-668. doi: 10.1038/s41577-020-0306-5.
5. Van Eeden R, Rapoport BL, Smit T, *et al*. Tuberculosis infection in a patient treated with nivolumab for non-small cell lung cancer: case report and literature review. Front Oncol 2019; 9: 659.
6. Crawley D, Breen RA, Elkington PT, *et al*. Tuberculosis associated with triplet therapy for lung cancer. Thorax 2020; 75(7): 609-610.
7. Fujita K, Yamamoto Y, Kanai O, **et al**. Incidence of active tuberculosis in lung cancer patients receiving immune checkpoint inhibitors. Open Forum Infect Dis 2020 Apr; 7(5): ofaa126.
8. Jensen KH, Persson G, Bondgaard AL, *et al*. Development of pulmonary tuberculosis following treatment with anti-PD-1 for non-small cell lung cancer. Acta Oncol 2018 Aug; 57(8):1127-1128.
9. Taiwan CDC. Daily Tuberculosis Indicator Summary Taiwan CDC website: Taiwan CDC; 2022 [cited 2024 April 24]. Available from: https://daily.cdc.gov.tw/stoptb/Indicator.aspx.
10. Taiwan CDC. Taiwan Tuberculosis Annual Incidence Monitoring Chart Taiwan CDC website: Taiwan CDC; [cited 2024 April 24]. Available from: https://daily.cdc.gov.tw/stoptb/CareMagChart.aspx
11. World Health Organization. Global Tuberculosis Report 2023. https://www.who.int/teams/global-tuberculosis-programme/tb-reports/global-tuberculosis-report-20232023.
12. Vynnycky E, Fine PE. Lifetime risks, incubation period, and serial interval of tuberculosis. Am J Epidemiol 2000 Aug 1; 152(3):247-63. doi: 10.1093/aje/152.3.247. PubMed PMID: 10933272.
13. Getahun H, Gunneberg C, Granich R, *et al*. HIV infection—associated tuberculosis: the epidemiology and the response. Clin Infect Dis 2010; 50(Supplement_3): S201-S207.
14. Dobler CC. Biologic agents and tuberculosis. Microbiol Spectr. 2016 Dec; 4(6).
15. Dobler CC, Cheung K, Nguyen J, *et al*. Risk of tuberculosis in patients with solid cancers and haematological malignancies: a systematic review and meta-analysis. Eur Respir J 2017; 50(2).
16. Elkington PT, Bateman AC, Thomas GJ, *et al*. Implications of tuberculosis reactivation after immune checkpoint inhibition. Am J Respir Crit Care Med 2018; 198(11): 1451-1453.
17. Tiwari D, Martineau AR. Inflammation-mediated tissue damage in pulmonary tuberculosis and host-directed therapeutic strategies. Semin Immunol 2023 Jan; 65:101672. doi: 10.1016/j.smim.2022.101672. PubMed PMID: 36469987.
18. Pardoll DM. The blockade of immune checkpoints in cancer immunotherapy. Nat Rev Cancer 2012; 12(4): 252-264.
19. Wykes MN, Lewin SR. Immune checkpoint blockade in infectious diseases. Nat Rev Immunol 2018; 18(2): 91-104.
20. Comas I, Chakravartti J, Small PM, *et al*. Human T cell epitopes of Mycobacterium tuberculosis are evolutionarily hyperconserved. Nat Genet 2010; 42(6): 498-503.
21. Liao K-M, Shu C-C, Liang F-W, *et al*. Risk factors for pulmonary tuberculosis in patients with lung cancer: a retrospective cohort study. J Cancer 2023; 14(4): 657.
22. Wu CY, Hu HY, Pu CY, *et al*. Pulmonary tuberculosis increases the risk of lung cancer: a population-based cohort study. Cancer 2011; 117(3): 618-624.
23. Seo GH, Kim MJ, Seo S, *et al*. Cancer-specific incidence rates of tuberculosis: a 5-year nationwide population-based study in a country with an intermediate tuberculosis burden. Medicine 2016; 95(38): e4919.
24. Cheng MP, Chakra CNA, Yansouni CP, *et al*. Risk of active tuberculosis in patients with cancer: a systematic review and metaanalysis. Clin Infect Dis 2017; 64(5): 635-644.
25. Bae S, Kim Y-J, Kim M-j, *et al*. Risk of tuberculosis in patients with cancer treated with immune checkpoint inhibitors: a nationwide observational study. J Immunother Cancer 2021; 9(9).
26. Im Y, Lee J, Kim SJ, *et al*. Development of tuberculosis in cancer patients receiving immune checkpoint inhibitors. Respir Med 2020; 161: 105853.
27. European Centre for Disease Prevention and Control.

Use of interferon-gamma release assays in support of TB diagnosis. Stockholm: ECDC, 2011. Available from: https://www.ecdc.europa.eu/sites/default/files/media/en/publications/Publications/1103_GUI_IGRA.pdf

28. Lin C, Feng T, Li S. Tuberculosis infection following immune checkpoint inhibitor treatment for advanced cancer: a case report and literature review. Front Immunol 2023; 14: 1162190.
29. Shi J, Li J, Wang Q, *et al*. The safety and efficacy of immunotherapy with anti-programmed cell death 1 monoclonal antibody for lung cancer complicated with Mycobacterium tuberculosis infection. Transl Lung Cancer Res 2021; 10(10): 3929.
30. World Health Organization. Latent tuberculosis infection: updated and consolidated guidelines for programmatic management. World Health Organization; 2018. (WHO/CDS/TB/2018.4).

Abbreviations

TB, tuberculosis; LTBI, latent tuberculosis infection; NSCLC, non-small cell lung cancer; CT, computed tomography; EGFR, epidermal growth factor receptor; PD-1/PD-L1, programmed death 1/programmed death-ligand 1; MTB, *Mycobacterium tuberculosis complex*; ICI, immune checkpoint inhibitor; CTLA-4, cytotoxic T-lymphocyte-associated protein 4; IRAE, immune-related adverse event; WHO, World Health Organization.

Pirfenidone for the Treatment of Post-Amniotic Fluid Embolism-related Acute Respiratory Distress Syndrome in a 34-year-old Female

Ping-Chen Kuo[1], Yu-Wen Chang[2], Chien-Hao Lai[3], Yi-Hsuan Tsai[3,4]

Acute respiratory distress syndrome (ARDS) is common in patients with amniotic fluid embolism (AFE). This critical condition usually leads to a high mortality rate and can have serious sequelae even in the acute phase. Currently, there are limited effective drugs for this condition. We reported a 34-year-old pregnant woman with no underlying medical conditions who was admitted to the hospital for regular abdominal delivery. During the procedure, the bilateral lung consolidation suddenly collapsed. AFE was diagnosed, and emergency use of extracorporeal membrane oxygenation (ECMO) was begun. After suffering from ARDS, she had difficulty weaning from mechanical ventilation and was supported by ECMO for nearly 2 months. We started pirfenidone while in the intensive care unit, and she was successfully extubated and discharged from the hospital after treatment. After discharge, her activities of daily living were completely independent and oxygen was not required at home. Our case suggests that antifibrotic agents such as pirfenidone may be an effective treatment option for patients with ARDS. ***(Thorac Med 2025; 40: 65-72)***

Key words: amniotic fluid embolism, acute respiratory distress syndrome, antifibrotic, pirfenidone, extracorporeal membrane oxygenation

Introduction

Amniotic fluid embolism (AFE) is a rare but fatal condition with a high mortality rate. The diagnosis is based on clinical observations such as hypoxia, hypotension, and coagulopathy, with an onset during labor. The pathophysiology of AFE has been incompletely studied, but seems to involve abnormal activation of pro-inflammatory mediators related to systemic inflammatory response syndrome. Lung injury or acute respiratory distress syndrome (ARDS) is seen in 93% of patients [1].

Among ARDS patients, observational studies report greater than 30% hospital mortality [2]. Even after surviving the acute inflammatory phase, patients often find evidence of fibrotic changes in the lungs. Survivors of ARDS may

[1]Department of Internal Medicine, Kaohsiung Chang Gung Memorial Hospital, [2]Division of Pharmacy, Kaohsiung Chang Gung Memorial Hospital, [3]Division of Pulmonary & Critical Care Medicine, Department of Internal Medicine, Kaohsiung Chang Gung Memorial, [4]Lee's Clinic.
Address reprint requests to: Dr. Yi-Hsuan Tsai, Lee's Clinic, Wenshan branch. No. 157, Sec. 3, Jianguo Rd., Fengshan Dist., Kaohsiung City, 830734, Taiwan.

experience motor limitation and physical and psychological sequelae [3].

The main pathogenesis of ARDS was described as dysregulated inflammation and increased lung endothelial and epithelial permeability. The high levels of pro-inflammatory cytokines cause further alveolar injury [4].

In contrast to lung protective ventilation, pharmacotherapies for ARDS have been limited, and many of the clinical trials have failed to find effective medications [2]. Pirfenidone is an oral antifibrotic drug that is used as a treatment for idiopathic pulmonary fibrosis (IPF), and that has antifibrotic, anti-inflammatory, and antioxidant properties [5]. A series of case reports have shown the benefit of antifibrotic agents used in ARDS patients, but the results are still inconclusive, and therefore do not play a role in early ARDS treatment guidelines.

Because of this situation, we considered the potential benefits of using antifibrotic drugs in patients with ARDS. Here, we report the case of an ARDS patient treated with pirfenidone who had a good prognosis.

Case Descriptiont

A 34-year-old female with an obstetrics history of gravida: 3, para: 1, and artificial abortion: 1 was admitted at 38 weeks of gestation, and was prepared to receive abdominal delivery. She denied any medical history or family history of respiratory disease. Cesarean section under spinal anesthesia was performed on the 2nd day of admission. Then, a sudden onset of bradycardia with chest pain and pulseless ventricular tachycardia occurred. During cardiopulmonary cerebral resuscitation (CPCR), intubation was completed. After 12 minutes of CPCR and 5 defibrillations, the patient was not resuscitated, and venous-arterial extracorporeal membrane oxygenation (VA-ECMO) was urgently begun. Initial laboratory data were: d-dimer: > 35 mg/dL, CRP: 1.52 mg/L, and NT-proBNP: 3808 pg/mL. Arterial blood gas analysis (ABG) showed pH: 7.59, pCO_2: 26 mmHg, pO_2: 343 mmHg, and HCO_2: 24.4 mmol/L under ECMO support. Chest radiograph (CXR) (Fig. 1A) and chest computed tomography (CT) (Fig. 2) showed consolidation over the bilateral lung without evidence of intraluminal thromboembolism in the main pulmonary artery, or aortic dissection. Echocardiography revealed borderline left ventricle (LV) performance, and an LV ejection fraction (EF) ratio of 51%. Pulmonary edema related to post-CPCR acute decompensated heart failure was suspected. Disseminated intravascular coagulation was found with a platelet count: 80,000/uL, fibrinogen: 166 mg/dL with INR: 1.23, and PT: 12.4s, with the patient febrile at that time. Due to all these findings, she was diagnosed with AFE.

She was sent to the intensive care unit for further care. Due to her stable hemodynamic status, VA-ECMO was changed to veno-venous ECMO (VV-ECMO) on the 6th day. Since the consolidation in both lungs did not improve, she underwent bronchoscopy and bronchoscopic lavage. The results were: galactomannan test: 0.1, cryptococcus antigen: negative, acid-fast stain: negative, and culture colony count <100 CFU/mL, below the normal limit. VV-ECMO was removed on the 10th day. CXR follow-up showed improved consolidation at the bilateral lungs (Fig. 1B).

However, low tidal volume (100-200 ml) with a high fraction of inspiration O_2 (FiO_2: 100%) was found on the 20th day. ABG showed hypoxia (PaO_2: 44.4 mmHg) and hypercapnia ($PaCO_2$: 51 mmHg). With the diagnosis of se-

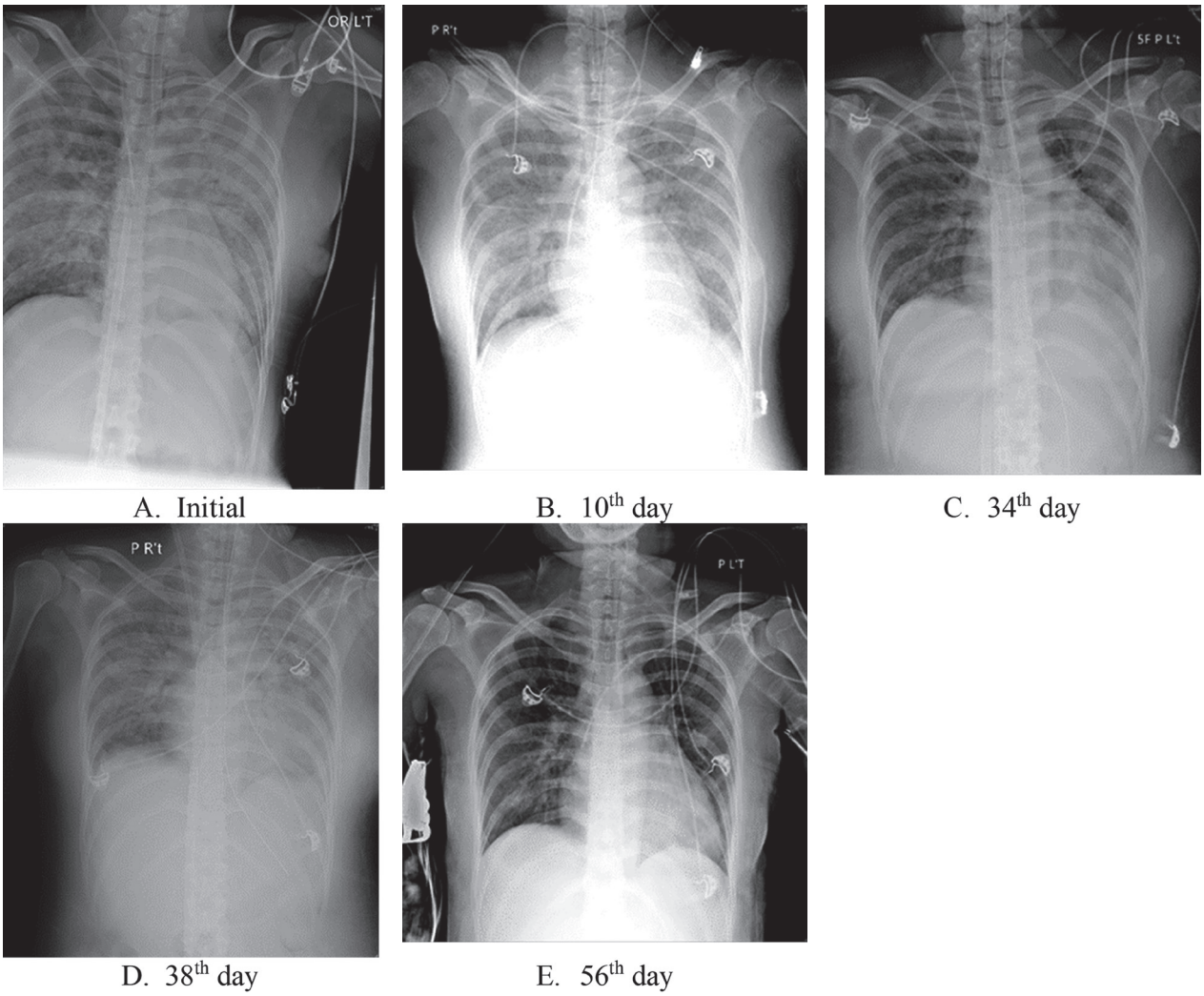

Fig. 1. Chest radiograph.

vere ARDS, a lung protective ventilation setting with total sedation under midazolam and cisatracurium was started. Unfortunately, the patient's hypoxia was persistent, so VV-ECMO was started again. Lab data revealed NTproBNP: 6122 pg/mL. Echocardiography revealed an EF ratio of 61%, adequate left and right ventricular pressure, and that pulmonary edema related to heart failure was less likely. Follow-up chest CT (Fig. 2) showed progressive diffuse patchy consolidation and ground-glass opacities (GGO), as well as interlobular septal thickening over the bilateral lungs. With the patient's ARDS in the exudative phase, methylprednisolone 40 mg intravenous infusion twice daily was added on the 21st day. Then, using diuretics to maintain a negative fluid state (negative intake/excretion of approximately -1000 ml per day), the patient's symptoms and CXR (Fig. 1C) improved, and ECMO was removed on the 34th day.

However, agitation and dyspnea under ven-

tilator with 100% FiO_2 support occurred again on the 38th day. ABG showed severe respiratory acidosis (pH: 6.9, pCO_2: 167 mmHg, pO_2: 77 mmHg, HCO3: 37 mmol/L). CXR (Fig. 1D) revealed worsened consolidation; thus, VV ECMO was started for the third time.

Chest CT follow-up on the 42nd day showed bilateral patchy consolidation with multiple GGO patterns. (Fig. 2) We started pirfenidone (200 mg) 1# TID on the 43rd day. After treatment, her CXR improved on the 56th day. Then, VV-ECMO was removed. ABG showed pH: 7.46, pO_2: 128.5 mmHg with pCO_2: 45 mmHg under a ventilator setting of FiO_2: 35%, and PEEP: 8. Pirfenidone (200 mg) was titrated to 2# TID on the same day. The ventilator weaning protocol started on the 57th day, and the patient was successfully extubated on the 58th day.

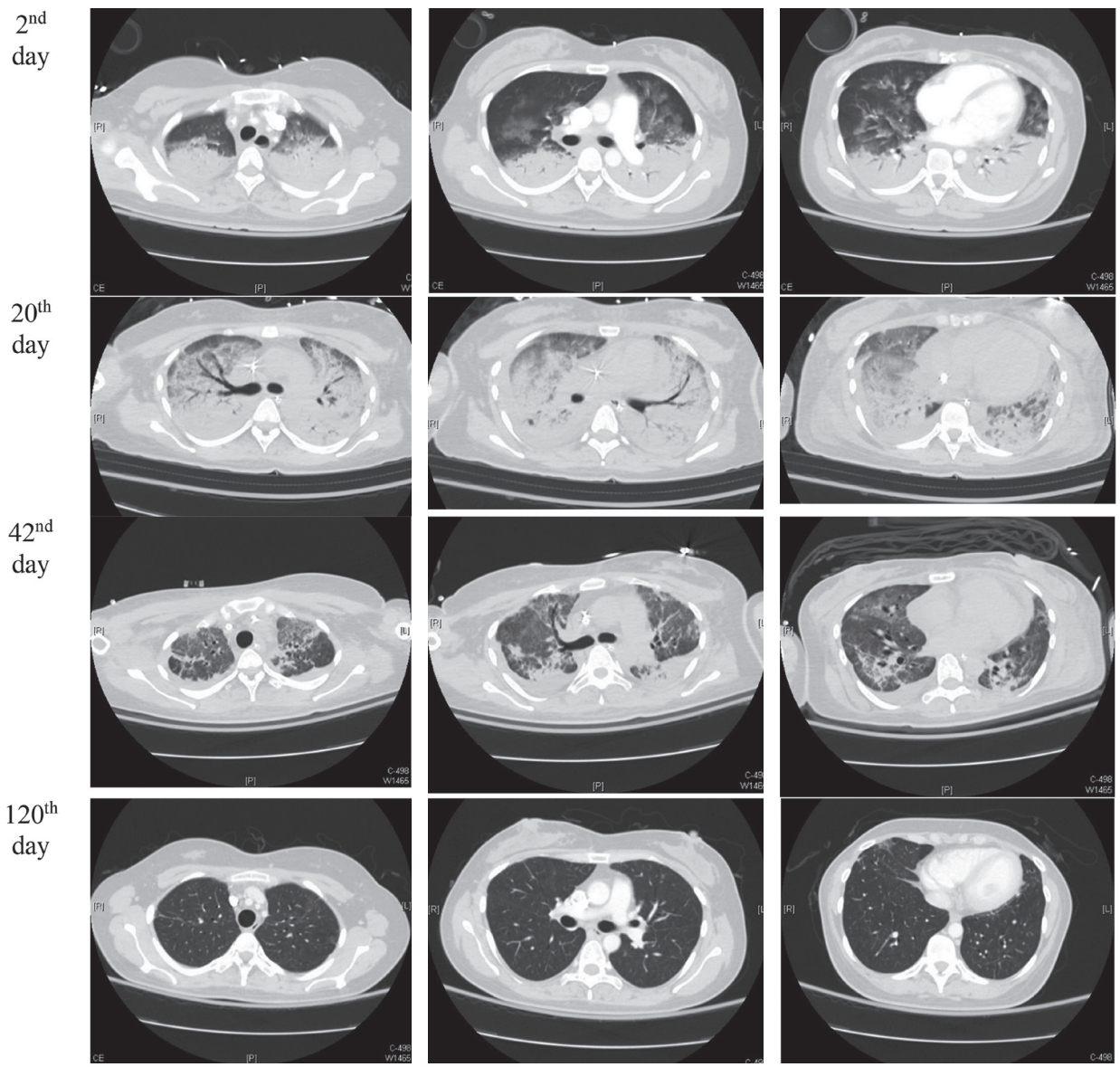

Fig. 2. Chest computed tomography.

Under stable condition, she was discharged on the 71st day. Chest CT follow-up on the 120th day (Fig. 2) revealed resolution of consolidation and fibrotic changes in the bilateral apical and right lower lobes. A pulmonary function test showed FVC: 2.32 L, FVC: 66%, and FEV1/FVC: 88%, resulting in moderate restrictive ventilatory impairment. The patient's current activities of daily living (ADL) are independent and do not require an oxygen prescription. Pirfenidone (200 mg) 1# TID was used for a total of 140 days.

Discussion

After nearly 60 days of ventilation and ECMO use, our patient, with severe ARDS, was successfully weaned and discharged without oxygen support. Imaging followed by chest CT tracking also showed minimal fibrotic changes. We think that this good outcome may be related to the use of antifibrotic drugs.

We reviewed past case reports and systematically listed 43 patients worldwide who were diagnosed with ARDS and treated with antifibrotic drugs, including pirfenidone and nintedanib, and found that the majority initially experienced respiratory failure with ventilator support (Table 1). Medication was started between the 1st day of mechanical ventilation and the 65th day, and the majority of patients then experienced regression in fibrotic changes on chest images and improved quality of life [6-12].

Regarding the pathogenesis, we found that the high levels of pro-inflammatory cytokines such as interleukin (IL)-1β, IL-8, tumor necrosis factor-α (TNFα), and transforming growth factor-β1 (TGF-β1) increased as the pulmonary edema of the ARDS patients progressed. When excessive levels of cytokines were present, alveolar injury occurred and alveolar fluid clearance was reduced. During lung injury, the increased thrombin, TNF-α, and leukocytes in the lungs also destabilized the vascular endothelial-cadherin bonds, resulting in increased endothelial permeability and the accumulation of alveolar fluid [2]. After the acute stage, ARDS will progress to proliferative changes and end-stage fibrosis. Fibrosis was noted in 4% of patients with disease for less than 7 days, and progressed to 61% after 21 days [13].

Pirfenidone, used to block all the dysregulation of inflammation and fibrotic change, is a synthetic pyridine compound that is initially used to inhibit the progression of lung fibrosis. We thought that the anti-inflammatory properties of pirfenidone might also be helpful in ARDS patients. The anti-inflammatory properties were attributed to inhibiting the release of proinflammatory cytokines such as IL-1β, IL-6, TNF-α, and platelet-derived growth factor (PDGF). It also reduced the production of TGF-β1 to attenuate fibroblast proliferation [3, 14-15].

In further animal studies, pirfenidone had a profound effect on endoplasmic reticulum (ER) stress and mitochondrial dysfunction via upregulation of BAP31, which is an ER transmembrane protein associated with acute lung injury [16]. Reduced NLRP3 inflammasome activation and subsequent IL-1β secretion were also seen [17].

During the global COVID-19 pandemic, pirfenidone might also have played an important role in treatment. COVID-19 infection induced a cytokine storm, which caused lung injury and led to lung fibrosis. Ongoing studies and hypotheses have suggested that antifibrotic therapy used at the early stage of SARS-CoV-2 infection could be effective in reducing fibrotic

Table 1. ARDS Patients Treated with Antifibrotic Agents

Journal/year	Case number	Age/ Gender	Country	Cause of ARDS	Intubation/ Length	Treatment	Outcome
Sacoidosis Vasculitis and Diffuse Lung Disease/2018 [10]	3	40y/ M 45y/ M 59y/ M	India	H1N1 influenza	Yes >2 weeks	Pirfenidone (600/2400 mg QD for 3 months) *1	-HRCT scan showed regression of fibrotic and bronchiectatic changes.
Frontiers in Medicine/2022 [12]	1	66y / F	China	COVID-19	Yes 58 days	Pirfenidone (600 mg/1800 per day for 2 years) *2	- CT screened on day 758 showed reduced reticular abnormalities. - mMRC scores from 4 to 2.
Diffuse Lung Disease/2019 [7]	1	66y / M	Taiwan	Influenza	Yes 41 days	Pirfenidone (200 mg TID for 12 days) (since 27th day of ventilation)	-Weaned from ventilator 7 days after discontinuing pirfenidone.
Advances in Respiratory Medicine/2021 [8]	4	62y / F 36y/ M 72y/ M 52y/M	India	COVID-19	NIV NIV NRBM NIV	Nintedanib (150 mg BID for 3-4 weeks)	-Weaned off oxygen. - CXR with significant clearing of fibrotic opacities.
International Journal of Infectious Diseases/2021 [11]	30	66-80y/ 23y M 7y F	Japan	COVID-19t	Yes 20/30/60 days	Nintedanib (150 mg BID during ventilation days since 1st day, max 28 days)	-Lengths of ventilation were significantly shorter.
Frontiers in Medicine/2021 [6]	3	42y/ F 48y/ M 52y/ F	Italy	COVID-19	Yes 20/40/60 days	Nintedanib (150 mg BID for 67/71/79 days since the 10th/20th/30th days after ventilation)	-CT showed further improvement of lung parenchyma and reduction of residual lung damage
Respirology Case Reports/2021 [9]	1	78y / F	Japan	COVID-19	Yes 28 days	Nintedanib (300/200 mg per day for 90 days since the 65th day after ventilation) *3	- CT showed ground-glass opacities of the lung mildly attenuated without further progression.

Non-invasive ventilation (NIV), Non-rebreather mask (NRBM)

*1. Azithromycin (500 mg TIW) and prednisolone (600 mg daily → 2400 mg daily) escalated in 1 month with tolerance.

*2. 600 mg kept for 1 week then titrated to 1800 mg.

*3. lower dose (300>200 mg) due to elevated liver function.

damage [18-19]. The mechanism could be related to the inhibition of apoptosis, downregulation of ACE receptor expression, a decrease in inflammation by several mechanisms, and an amelioration of oxidative stress [20].

Another anti-fibrotic agent, nintedanib, also might be helpful in the treatment of post-ARDS lung fibrosis. This tyrosine kinase inhibitor targets the inhibition of fibroblast growth factor receptor (FGFR), platelet-derived growth factor receptor (PDGFR), and vascular endothelial growth factor receptor (VEGFR), which lead to lung fibrosis [21]. This may explain the benefits of nintedanib use in patients in our summary table list.

In our case, the patient's oxygenation improved after we started pirfenidone on the 43rd day of mechanical ventilation. Subsequently, the ECMO was removed and extubation was successful shortly after. The patient finally recovered well and was discharged. Chest CT showed significant resolution of fibrotic changes and continued improvement during outpatient follow-up. She had independent ADL and did not require oxygen therapy at home. The pirfenidone was effective, and the side effects, such as gastrointestinal and skin-related events (no reports of grade 4 adverse events), were minimal [5]. We will be looking forward to further clinical trials on pirfenidone use in the treatment of post-ARDS pulmonary fibrosis.

Conclusion

Based on our experience, antifibrotic agents such as pirfenidone may be an effective treatment option in ARDS patients, especially during a global COVID-19 pandemic. Further clinical randomized-controlled trials are required for validation.

References

1. Shamshirsaz AA, Clark SL. Amniotic fluid embolism. Obstet Gynecol Clin North Am 2016; 43(4): 779-790.
2. Meyer NJ, Gattinoni L, Calfee CS. Acute respiratory distress syndrome. Lancet 2021; 398(10300): 622-637.
3. Herridge MS, Tansey CM, Matté A, *et al*. Functional disability 5 years after acute respiratory distress syndrome. N Engl J Med 2011; 364(14): 1293-1304.
4. Huppert LA, Matthay MA, Ware LB. Pathogenesis of acute respiratory distress syndrome. Paper presented at: Seminars in respiratory and critical care medicine 2019.
5. Kim ES, Keating GM. Pirfenidone: a review of its use in idiopathic pulmonary fibrosis. Drugs 2015; 75(2): 219-230.
6. Bussolari C, Palumbo D, Fominsky E, *et al*. Case report: nintedaninb may accelerate lung recovery in critical coronavirus disease 2019. Front Med 2021; 8: 766486.
7. Chen H. Pirfenidone can enhance the patient's recovery from fibrotic phase of ARDS: a case report. Chest 2019; 155(4): 138A.
8. Marwah V, Choudhary R, Malik V, *et al*. Early experience of nintedanib in COVID-19 ARDS-related pulmonary fibrosis: a case series. Adv Respir Med 2021; 89(6): 589-596.
9. Ogata H, Nakagawa T, Sakoda S, *et al*. Nintedanib treatment for pulmonary fibrosis after coronavirus disease 2019. Respirol Case Rep 2021; 9(5): e00744.
10. Saha A, Vaidya PJ, Chavhan VB, *et al*. Combined pirfenidone, azithromycin and prednisolone in post-H1N1 ARDS pulmonary fibrosis. Sarcoidosis Vasc Diffuse Lung Dis 2018; 35(1): 85.
11. Umemura Y, Mitsuyama Y, Minami K, *et al*. Efficacy and safety of nintedanib for pulmonary fibrosis in severe pneumonia induced by COVID-19: an interventional study. Int J Infect Dis 2021;108: 454-460.
12. Zhou X, Yang D, Kong X, *et al*. Case report: pirfenidone in the treatment of post-COVID-19 pulmonary fibrosis. Front Med 2022; 9: 925703.
13. Thille AW, Esteban A, Fernández-Segoviano P, *et al*. Chronology of histological lesions in acute respiratory distress syndrome with diffuse alveolar damage: a prospective cohort study of clinical autopsies. Lancet Respir Med 2013; 1(5): 395-401.
14. Spond J, Case N, Chapman R, *et al*. Inhibition of

experimental acute pulmonary inflammation by pirfenidone. Pulmon Pharmacol Ther 2003; 16(4): 207-214.

15. Ruwanpura SM, Thomas BJ, Bardin PG. Pirfenidone: molecular mechanisms and potential clinical applications in lung disease. Am J Respir Cell Mol Biol 2020; 62(4): 413-422.
16. Du Y, Zhu P, Wang X, *et al*. Pirfenidone alleviates lipopolysaccharide-induced lung injury by accentuating BAP31 regulation of ER stress and mitochondrial injury. J Autoimmun 2020; 112: 102464.
17. Li Y, Li H, Liu S, *et al*. Pirfenidone ameliorates lipopolysaccharide-induced pulmonary inflammation and fibrosis by blocking NLRP3 inflammasome activation. Mol Immunol 2018; 99: 134-144.
18. Ferrara F, Granata G, Pelliccia C, *et al*. The added value of pirfenidone to fight inflammation and fibrotic state induced by SARS-CoV-2. Eur J Clin Pharmacol 2020; 76(11):1615-1618.
19. George PM, Wells AU, Jenkins RG. Pulmonary fibrosis and COVID-19: the potential role for antifibrotic therapy. Lancet Respir Med 2020; 8(8): 807-815.
20. Seifirad S. Pirfenidone: a novel hypothetical treatment for COVID-19. Med Hypotheses 2020; 144: 110005.
21. Wollin L, Maillet I, Quesniaux V, *et al*. Antifibrotic and anti-inflammatory activity of the tyrosine kinase inhibitor nintedanib in experimental models of lung fibrosis. J Pharmacol Exp Ther 2014; 349(2): 209-220.

Two Cases of Pulmonary Ciliated Muconodular Papillary Tumor: Case Report and Literature Review

Kheng-An Ho[1], Wen-Chieh Huang[1], Mei-Lin Chan[1]

Ciliated muconodular papillary tumors (CMPTs) are rare. Owing to the continuous basal cell layer, lack of mitosis, necrotic changes, and immunohistochemical features, CMPT is considered a benign tumor with the potential to be an early precursor of mucinous adenocarcinoma. We reported the clinical and pathological findings of 2 cases of CMPT without recurrence 16 and 30 months, respectively, after surgery. With this case report, we hope to improve the management of CMPTs. ***(Thorac Med 2025; 40: 73-79)***

Key words: Ciliated muconodular papillary tumor, pulmonary, bronchiolar adenoma

Introduction

Ciliated muconodular papillary tumors (CMPT) were first described by Ishikawa in 2002. This introduction led to the concept of bronchiolar adenoma (BA), a nodular lesion in the lungs consisting of a bi-layered bronchiolar-type epithelium and a continuous layer of basal cells, first described by Chang *et al*. in 2018 [1]. BA can be divided into a proximal type, which is reminiscent of CMPT and possesses features of proximal bronchioles, including mucinous and ciliated cells, and a distal type, which is similar to respiratory bronchioles, but lacks mucinous and ciliated cells [1]. To date, only about 80 cases of CMPT have been reported in the English literature. The condition has a slight female predominance (M:F=1:1.1), and mostly occurs in patients aged 50-80 years [2-3]. The majority of reported cases are from East Asia [3-5], and approximately 45% of patients present with a smoking history [2-3].

Patients with CMPT are usually asymptomatic or present with nonspecific respiratory symptoms. Many of these are detected during health examinations or the evaluation of other diseases [3, 5]. The main diagnostic tools used to identify this condition are computed tomography (CT) and pathological examination. On CT images, CMPT appears as solid, partially solid, or ground-glass opacities (GGO) in the peripheral lungs [2-3]. The tumor is most likely located in the lower lobes of the lungs, where central cavitation may be observed [6]. Patho-

[1]Division of Chest Surgery, Department of Surgery, Mackay Memorial Hospital.
Address reprint requests to: Dr. Wen-Chieh Huang, Division of Thoracic Surgery, Department of Surgery, Mackay Memorial Hospital, No. 92, Chung-Shan North Road, Taipei 104, Taiwan.

logically, CMPT is characterized by ciliated columnar, mucinous, and a single layer of basal cells aligned in a predominantly papillary pattern. Mucin pools within the tumor and adjacent alveoli are often observed. Atypia has been reported in only a few cases, and no mitosis or necrosis has been reported to date [2, 7-9].

Given that the clinical and imaging findings of CMPT often mimic those of lung cancer, CMPT is commonly treated with surgical resection, and is pathologically diagnosed after surgery. To date, no reports have documented the recurrence or metastasis of CMPT. Here, we report 2 cases of CMPT that were surgically managed in our hospital and followed up for 16 and 30 months, respectively, without recurrence.

Case 1

A 68-year-old female presented with hypertension, gastroesophageal reflux, and moderate tricuspid regurgitation. She had a cough with pinkish sputum for months, and the CT scan revealed a 4x3 cm peribronchial GGO in the posterior segment of the left lower lobe, with traction bronchiectasis. Bronchoscopy demonstrated no remarkable mucosal lesions, and endobronchial ultrasonography revealed a concentric lesion with an air bronchogram in the left bronchus 10 (LB10). A biopsy was performed and the pathological report revealed chronic inflammation and fibroelastosis. We performed a CT scan 3 months later, and the GGO remained unchanged. Thoracoscopic surgery was performed under the suspicion of lung cancer. Wedge resection of the GGO was initially performed, and frozen pathology indicated an adenocarcinoma. Therefore, a left lower lobe lobectomy with lymph node dissection was performed.

Grossly, the tumor was a firm mass measuring 2.5 x 2 x 1.5 cm with grayish-white content, and the pleura overlying the tumor was smooth.

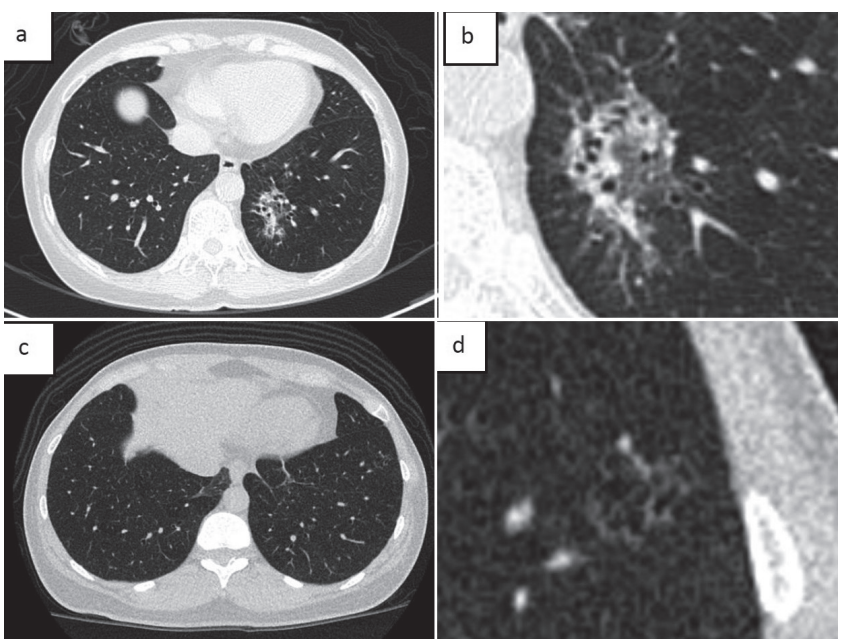

Fig. 1. (a) and (b) Computed tomography (CT) scans of case 1, displaying 4 × 3 cm ground-glass opacities with traction bronchiectasis. (c) and (d) Low-dose CT demonstrating a 1.4 cm sub-solid nodule with air-cyst formation at the peripheral left lower lobe of the lung.

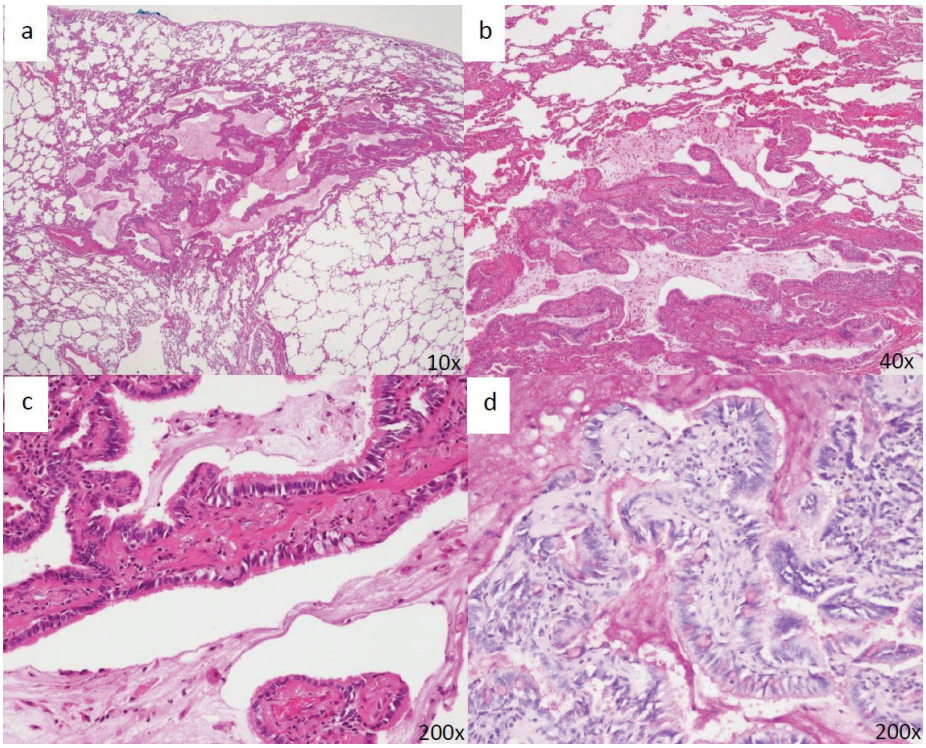

Fig. 2. (a) A well-defined tumor with mucin-containing cysts. (b) The epithelial cells lining the cysts are arranged in papillary and lepidic patterns. (c) The cysts are lined with ciliated columnar epithelial cells, with scattered goblet cells, and a continuous layer of basal cells underneath. (d) Mucicarmine stain highlighted the mucin secretions and goblet cells.

The largest lymph node measured 1.5 cm. In the microscopic exam, the tumor was relatively well-defined with mucin secretion. Additionally, the tumor was predominantly composed of ciliated cells, scattered mucinous columnar epithelial cells, and a continuous layer of basal cells underneath, arranged in papillary and lepidic patterns (Fig. 2).

The immunohistochemical profile confirmed the positivity of epithelial cells for cytokeratin (CK) 7 and thyroid transcription factor 1 (TTF-1). The epithelial cells were negative for hepatocyte nuclear factor-4 alpha (HNF-4α), and the basal cells were positive for CK5/6 and p40. The epithelial cells displayed a low Ki-67 labeling index (Fig. 3). The morphology and immunohistochemical profile were consistent with those of CMPT. The lymph nodes were not

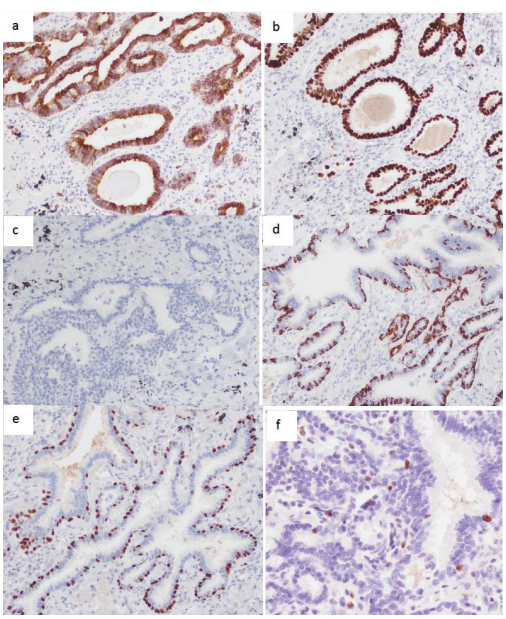

Fig. 3. Immunohistochemical profile of case 1. The epithelial cells are positive for (a) cytokeratin (CK) 7, and (b) thyroid transcription factor 1 (focal), and negative for (c) hepatocyte nuclear factor-4 alpha. The basal cells are positive for (d) CK5/6 and (e) p40. The (f) Ki-67 index is low.

affected by the tumor cells. The patient's admission course was uneventful, and follow-up CT scans performed until 16 months after surgery displayed no local recurrence.

Case 2

The patient was a 42-year-old female with thalassemia and a history of viral pneumonia with respiratory failure, requiring hospital admission 8 years before this presentation. A low-dose CT scan during a health examination revealed she had a 1.4 cm sub-solid nodule with air-cyst formation in the peripheral left lower lobe of the lung. She did not present any other symptoms. We performed thoracoscopic wedge resection of the left lower lobe nodule and lymph node sampling at stations 5 and 7. The tumor was soft, and the pleura overlying the tumor was smooth. The largest lymph node measured 1.2 cm. In the microscopic exam, the tumor was well-defined and showed abundant mucin secretion. The tumor was predominantly composed of ciliated columnar epithelial cells and scattered goblet cells, with a continuous layer of basal cells underneath, arranged in papillary and lepidic patterns.

The immunohistochemical profile revealed that the epithelial cells were positive for CK7 and TTF-1 (focal) and the basal cells were positive for CK5/6 and p40 (Fig. 4). Mucicarmine stain revealed mucin secretion and the presence of goblet cells. The morphology and immunohistochemical profile were consistent with those of CMPT. The lymph node findings were unremarkable. The patient recovered well after surgery and was free from local recurrence or metastasis during the 30-month follow-up period.

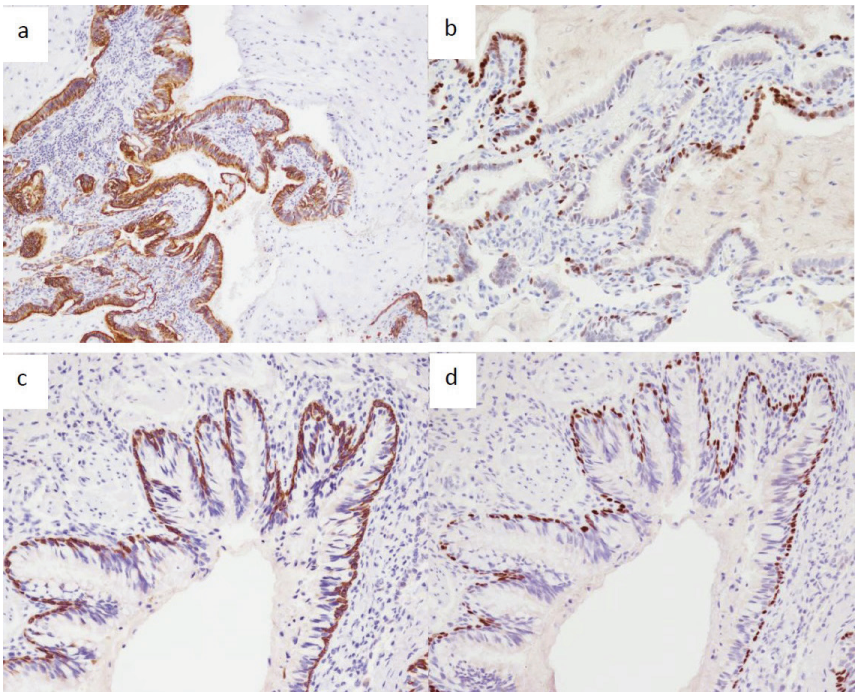

Fig. 4. Immunohistochemical profile of case 2. The epithelial cells are positive for (a) cytokeratin (CK) 7 and (b) thyroid transcription factor 1 (focal), and the basal cells are positive for (c) CK5/6 and (d) p40.

Discussion

CMPTs are rare neoplasms that often present as asymptomatic nodules or masses in the peripheral lungs [6, 10-11]. The tumor may be solid, partially solid, or GGO. Moreover, central cavitation is often observed [2-3, 6]. The largest tumor reported so far was 4.5 cm, while the average size of the CMPT was 1.1 cm [12]. The image findings were similar to those of early lung cancer or metastasis. Positron emission tomography-CT could help differentiate benign from malignant lesions, but it is not a routine exam before surgery for lung cancer owing to the high cost [5, 11]. Transthoracic needle biopsy is difficult due to the small tumor size, and carries the risk of hemothorax, pneumothorax, air embolism, tumor seeding, or hemoptysis [5, 13]. The rarity and nonspecific clinical and imaging findings make the differential diagnosis of CMPT before surgical intervention challenging. The tumor is usually diagnosed based on pathological findings.

Macroscopically, a CMPT is a pale or grayish, well-circumscribed nodule without a capsule or envelope. The center may be gelatinous, cavitated, or filled with mucus. No pleural retraction was observed in the tumors close to the pleural surface [2, 14]. Microscopically, CMPT consists of ciliated columnar and mucinous cells aligned in glandular, papillary, or lepidic patterns, surrounded by a continuous single layer of basal cells without intervention [2, 14]. Mucin accumulation is often observed in the center of tumors and the adjacent alveoli [2, 9]. Atypia has been reported in only a few cases; however, no cases of mitosis or necrosis have been reported to date [2-3, 5, 8]. Frozen sections of CMPT are often misdiagnosed as adenocarcinomas [14-15].

CMPT differs from malignant tumors due to its lack of mitotic and necrotic changes [4, 6]. Malignant tumors either lack basal cells or the basal cell layer is interrupted by tumor infiltration. Ciliated cells are rare in malignant lung tumors [2]. Mucinous adenocarcinoma and mucoepidermoid carcinoma, which are both common differential diagnoses for CMPT, do not consist of ciliated cells [2].

Immunohistochemistry helps diagnose CMPT. Positive CK7, carcinoembryonic antigen (CEA), HNF-4α, and mucin (MUC)5B (MUC5B), and negative CK20, CD56, caudal type homeobox 2 (CDX2), and programmed death ligand 1(PD-L1) have been reported in the literature, whilst p53, MUC1 and MUC5AC (in ciliated cells only) varied in their presence. CMPT was initially reported to be positive for TTF-1 [3]. After the broader family of BAs was examined, those lacking mucinous or ciliated cells and exhibiting positive TTF-1 expression were classified as distal-type BA, resembling respiratory bronchioles. Typical CMPTs are considered negative for TTF-1 and resemble proximal bronchioles [1]. Furthermore, CK5/6, p40, and p63 have been expressed in basal cells. The proliferation index (Ki-67) is usually less than 10%, suggesting a less aggressive nature [2, 5, 8-9].

Several features of CMPT, including ciliated cells, continuous basal cells, lack of necrosis and mitosis, and a low Ki-67 index, suggest that the tumor is benign, whereas destroyed alveolar walls, skip lesions, lack of encapsulation, a papillary pattern, positive CEA staining, and central fibrosis suggest malignancy. The proliferation of CMPT along the alveolar walls also resembles that of adenocarcinoma in situ. The positive CK7 and negative CK20 expressions of CMPT are similar to those of pulmonary adeno-

carcinoma [16].

Although BA is classified as a benign tumor, immunohistochemical and genetic findings suggest that the tumor may be an early precursor to mucinous adenocarcinoma [8]. The final diagnosis of CMPT requires a pathological section, and surgical resection is usually performed. Local resection with adequate free margins is considered sufficient. CMPT recurrence after surgery or lymphatic metastasis has not yet been reported. However, the CMPT image cannot be differentiated from adenocarcinoma, and the intraoperative frozen section sometimes appears similar to that of adenocarcinoma. Lobectomy and lymph node dissection may be performed based on images and frozen sections. Lung segmental resection/sub-lobectomy can achieve radical tumor resection for both CMPT and adenocarcinomas, and avoid unnecessary lung volume loss in cases of CMPT. Lymph node dissection is not necessary for CMPT, but may be performed if adenocarcinoma cannot be ruled out in the initial diagnosis.

Conclusion

In conclusion, this report presents 2 cases of CMPT, along with their imaging and pathological findings, treatment, and outcomes. Our treatment plan for CMPT is simple resection owing to the benign to early malignant nature of the tumor. Our findings are consistent with those reported in English-language studies. We believe that the findings of this case report will serve as a cornerstone for future studies on CMPT.

Acknowledgments

We are extremely grateful to Dr. Wei-Chin Chang, who provided us with his knowledge and experience in the pathology of CMPT. This case would not have been possible without his support.

References

1. Chang JC, Montecalvo J, Borsu L, *et al*. Bronchiolar adenoma: expansion of the concept of ciliated muconodular papillary tumors with proposal for revised terminology based on morphologic, immunophenotypic, and genomic analysis of 25 cases. Am J Surg Pathol 2018; 42: 1010-26.
2. Lu YW, Yeh YC. Ciliated muconodular papillary tumors of the lung. Arch Pathol Lab Med 2019; 143: 135-9.
3. Shao K, Wang Y, Xue Q, *et al*. Clinicopathological features and prognosis of ciliated muconodular papillary tumor. J Cardiothorac Surg 2019; 14: 143.
4. Liu L, Aesif SW, Kipp BR, *et al*. Ciliated muconodular papillary tumors of the lung can occur in Western patients and show mutations in BRAF and AKT1. Am J Surg Pathol 2016; 40: 1631-6.
5. Yao X, Gong Y, Zhou J, *et al*. A surgical case of ciliated muconodular papillary tumor. Thorac Cancer 2019; 10: 1019-22.
6. Kamata T, Yoshida A, Kosuge T, *et al*. Ciliated muconodular papillary tumors of the lung: a clinicopathologic analysis of 10 cases. Am J Surg Pathol 2015; 39: 753-60.
7. Chuang HW, Liao JB, Chang HC, *et al*. Ciliated muconodular papillary tumor of the lung: a newly defined peripheral pulmonary tumor with conspicuous mucin pool mimicking colloid adenocarcinoma: a case report and review of literature. Pathol Int 2014; 64: 352-7.
8. Udo E, Furusato B, Sakai K, *et al*. Ciliated muconodular papillary tumors of the lung with KRAS/BRAF/AKT1 mutation. Diagn Pathol 2017; 12: 62.
9. Yang X, Hou Y, Geng J, *et al*. Ciliated muconodular papillary tumors of the lung: distinct molecular features of an insidious tumor. Front Genet 2020; 11: 579737.
10. Kon T, Baba Y, Fukai I, *et al*. Ciliated muconodular papillary tumor of the lung: a report of five cases. Pathol Int 2016; 66: 633-9.
11. Onishi Y, Ito K, Motoi N, *et al*. Ciliated muconodular

papillary tumor of the lung: 18F-FDG PET/CT findings of 15 cases. Ann Nucl Med 2020; 34: 448-52.

12. Ishikawa M, Sumitomo S, Imamura N, *et al*. Ciliated muconodular papillary tumor of the lung: report of five cases. J Surg Case Rep 2016; 2016: rjw144.
13. Wiener RS, Wiener DC, Gould MK. Risks of transthoracic needle biopsy: how high? Clin Pulm Med 2013; 20: 29-35.
14. Chu HH, Park SY, Cha EJ. Ciliated muconodular papillary tumor of the lung: the risk of false-positive diagnosis in frozen section. Human Pathol: Case Rep 2017; 7: 8-10.
15. Shirsat H, Zhou F, Chang JC, *et al*. Bronchiolar adenoma/pulmonary ciliated muconodular papillary tumor. Am J Clin Pathol 2021; 155:832-44.
16. Su YC, Hsu YC, Chai CY. Role of TTF-1, CK20, and CK7 immunohistochemistry for diagnosis of primary and secondary lung adenocarcinoma. Kaohsiung J Med Sci 2006; 22: 14-9.

Refractory Pleural Effusion Attributed to Metastatic Adenocarcinoma Originating from the Prostate Gland

Chi-Yi Yen[1], Jung-Yueh Chen[1,2], Yi-Ru Chen[3]

A 70-year-old man presented with exertional dyspnea and orthopnea for more than 2 weeks, accompanied by a dry cough. Despite regular medications, his symptoms persisted. Initial autoimmune profile testing reported normal results. Imaging revealed bilateral pleural effusion and a semi-consolidated lung lesion. Pleural fluid analysis indicated an exudative lymphocyte-predominant effusion with normal carcinoembryonic antigen levels. Cardiac echo revealed normal left ventricular contractility and mild valvular heart disease. Video-assisted thoracoscopic surgery confirmed metastatic adenocarcinoma from the prostate gland. Elevated serum prostate-specific antigen (PSA) levels and positive immunohistochemical staining corroborated the diagnosis. Bone scan showed diffuse bone metastases. The patient was diagnosed with stage IVB prostate cancer and received androgen deprivation therapy, resulting in symptom improvement and decreased PSA levels. Pleural effusion regression was observed post-treatment. Prostate cancer-induced pleural effusion is rare, but can present diagnostic challenges. Immunohistochemistry and PSA assessment play crucial roles in the diagnosis. The prognosis for patients with malignant pleural effusion secondary to metastatic prostate adenocarcinoma is typically poor, with an average survival period of approximately 18 months under treatment. Further research is warranted to improve diagnostic and therapeutic strategies for this rare presentation of prostate cancer. ***(Thorac Med 2025; 40: 80-87)***

Key words: malignant pleural effusion, prostate adenocarcinoma, metastatic prostate cancer

Introduction

Pleural effusion, the accumulation of fluid in the pleural cavity, can result from malignancies, infections, and cardiovascular conditions. While lung and breast cancers are the most common causes of malignant pleural effusion, it is rare in metastatic prostate cancer, accounting for less than 1% of cases.

[1]Department of Internal Medicine, E-Da Hospital, I-Shou University, Kaohsiung, Taiwan, [2]School of Medicine, College of Medicine, I-Shou University, Kaohsiung, Taiwan, [3]Department of Pathology, E-Da Hospital, I-Shou University, Kaohsiung, Taiwan.
Address reprint requests to: Dr. Jung-Yueh Chen, School of Medicine, College of Medicine, I-Shou University, Kaohsiung, Taiwan. Department of Internal Medicine, E-DA Hospital, I-Shou University, Kaohsiung, Taiwan. No.1, Yida Road, Jiao-su Village, Yan-chao District, Kaohsiung City 824, Taiwan.

Case Presentation

We reported a 70-year-old man who presented with exertional dyspnea and orthopnea that had lasted for more than 2 weeks. Dry cough without fever was also noted. He had a medical history of hypertension, coronary artery disease, congestive heart failure and dyslipidemia under regular medications, including amlodipine, valsartan, spironolactone, diltiazem, aspirin, and atorvastatin. He had been previously admitted twice for progressive dyspnea, orthopnea and dizziness, 2 years and 6 months ago, at another medical center. Progressive pleural effusion and leg edema were noted, despite aggressive diuretics usage and thoracentesis. Exudative pleural effusion was diagnosed. Since he had experienced repeated episodes of similar symptoms without improvement, he visited our pulmonology outpatient clinic for further management.

The chest radiograph at our clinic showed a bilateral blunting costophrenic angle and lower lung patchy infiltrates (Fig. 1). Due to the refractory nature of the pleural effusion, a chest CT scan was taken and revealed bilateral pleural effusion and a semi-consolidated lesion in the right upper lobe of the lung, measuring up to 2.6 cm (Fig. 2, Fig. 3). Pleural fluid analysis showed turbid yellowish fluid with glucose levels of 124 mg/dL, protein levels of 4.6 g/dL, lactate dehydrogenase levels of 159 U/L, and adenosine deaminase levels of 4 IU/L. The pleural effusion carcinoembryonic antigen level was within normal range. The differential cell counts of the pleural fluid showed 54% lymphocytes, 1% neutrophils, 36% mesothelial cells, and 9% monocyte cells. Lymphocyte-predominant exudative pleural effusion was noted. Repeated cytology plus cell block ex-

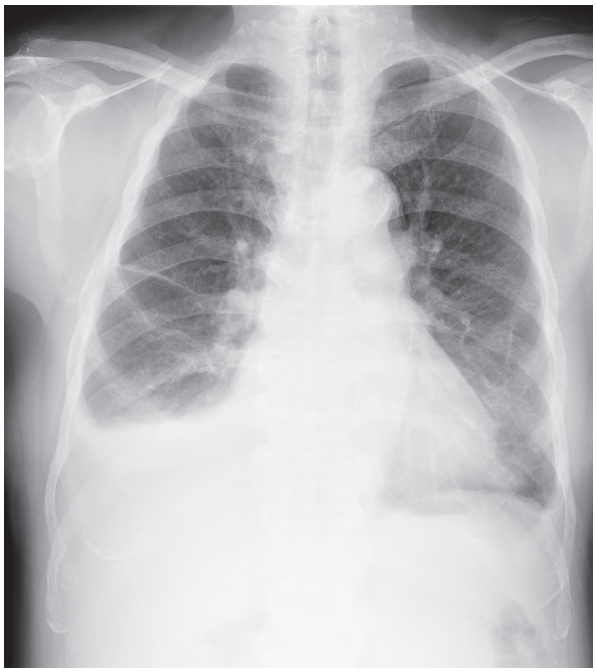

Fig. 1. Chest radiograph showed bilateral blunting of the costophrenic angle and lower lung patchy infiltrates.

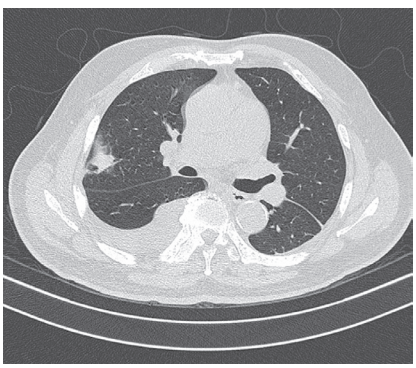

Fig. 2. Chest CT scan revealed bilateral pleural effusion and a semi-consolidated lesion in the right upper lobe of the lung, measuring up to 2.6 cm.

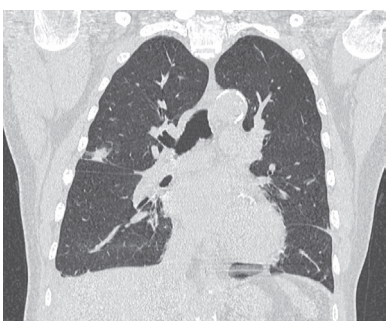

Fig. 3. Chest CT scan revealed bilateral pleural effusion and a semi-consolidated lesion in the right upper lobe of the lung, measuring up to 2.6 cm.

aminations were negative for malignant cells. A cardiac echo was performed due to a suspicion of congestive heart failure-related progressive leg edema and pleural effusion, and revealed normal left ventricular contractility and mild valvular heart disease. The tricuspid regurgitation pressure gradient was 37.37 mmHg.

Due to the inconclusive thoracentesis results, video-assisted thoracoscopic surgery (VATS) was performed, involving wedge resection of the right upper lobe, partial pleurectomy, and pleurodesis with mechanical abrasion. Pathological examination revealed metastatic adenocarcinoma, with positive immunohistochemical staining for AE1/AE3 and NKX3.1, and negative staining for CK7, CK20, TTF-1, PAX-8, and calretinin (Fig. 4-5). Based on the histopathology and immunohistochemical stain profiles, metastasis from the prostate was first considered.

Subsequent investigation revealed an elevated serum prostate-specific antigen (PSA) level of 8280.632 ng/mL (normal range < 4 ng/mL). Transrectal ultrasound of the prostate with echo-guided biopsy confirmed adenocarcinoma, with a right-side Gleason score of 8, and a left-side Gleason score of 9. Bone scan reported diffusely increased radioactivity in the skull,

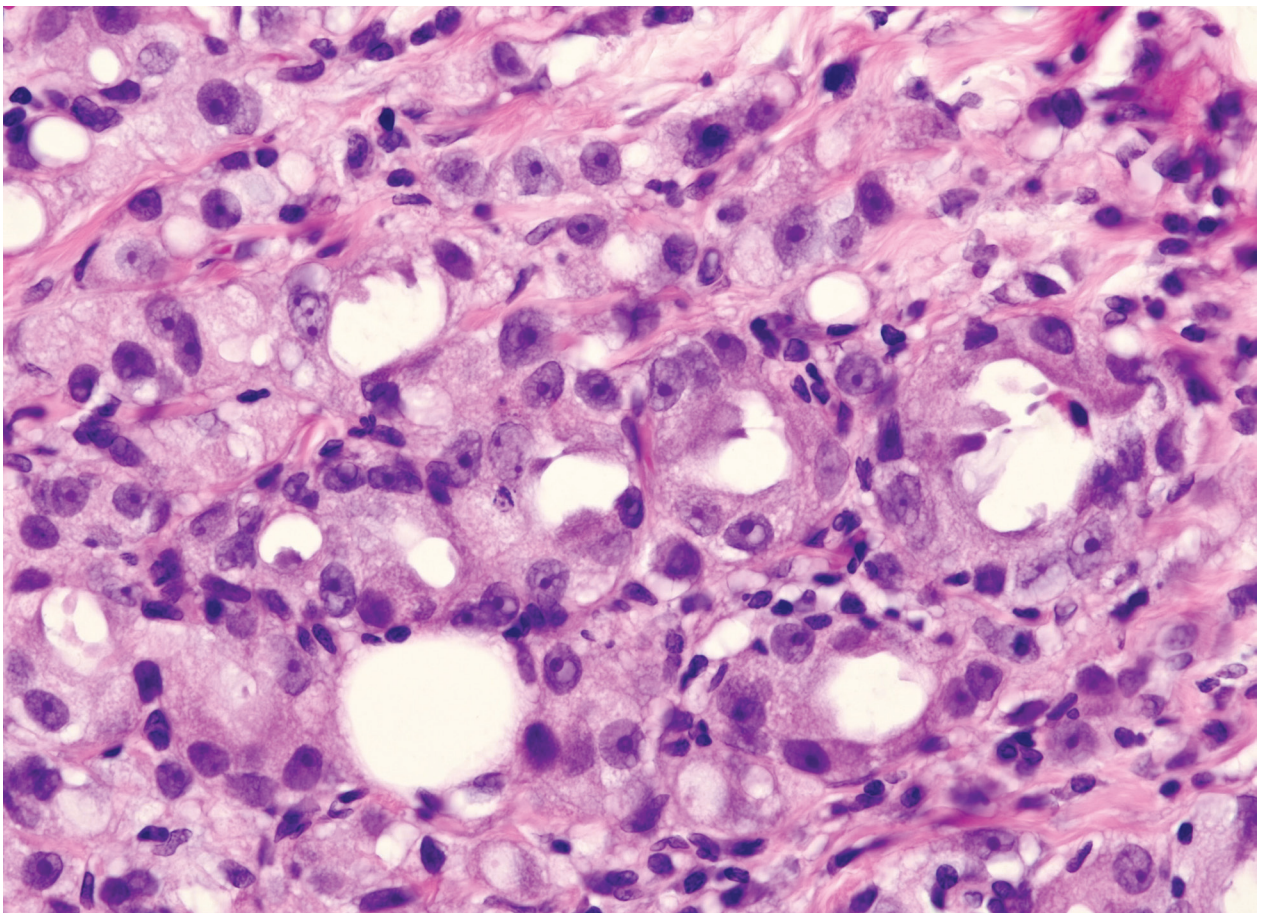

Fig. 4. Higher magnification images. The image reveals well-formed or fused glands, with nuclear enlargement, clear or pale granular cytoplasm, and prominent nuclei.

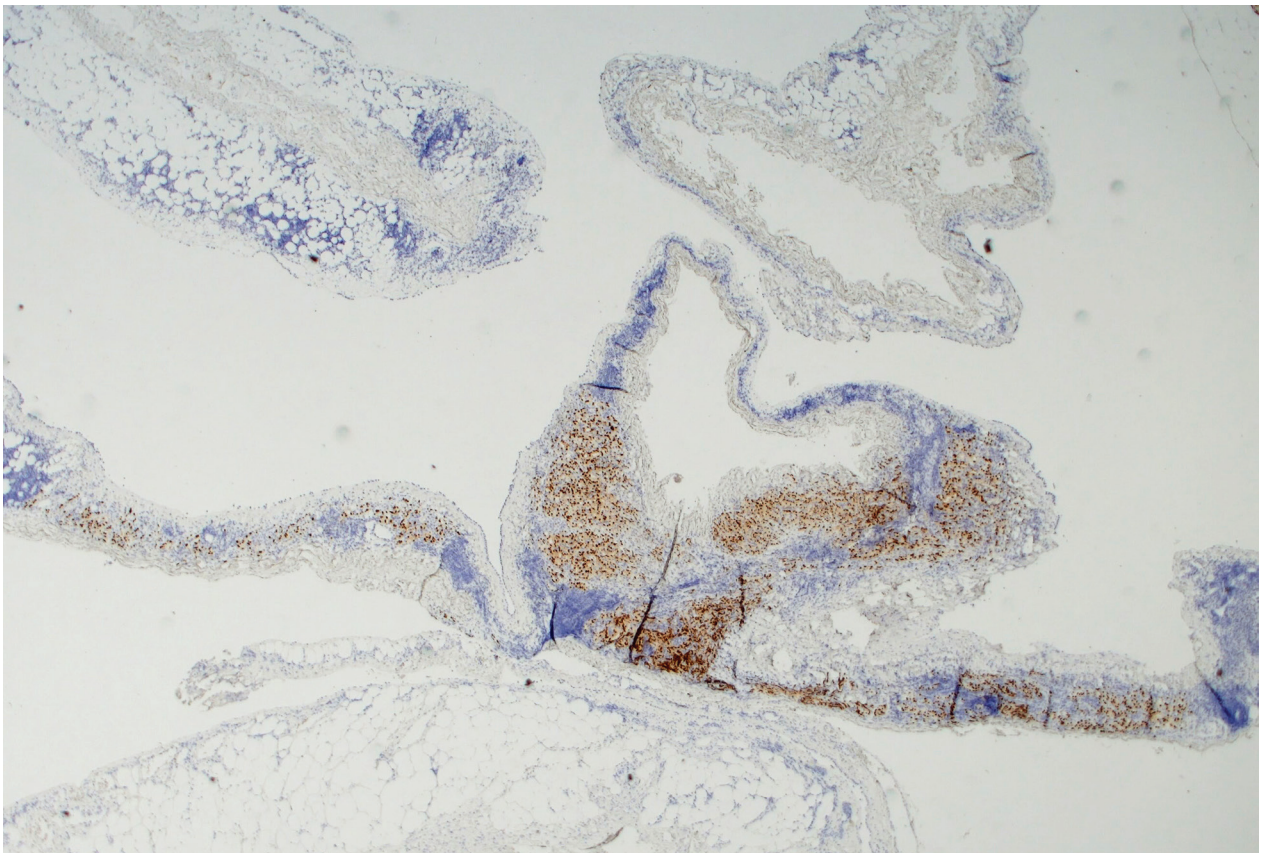

Fig. 5. The immunohistochemical staining of ANKX3.1(+).

cervical, thoracic, and lumbar spines, sacrum, sternum, rib cages, bilateral clavicles, bilateral scapulae, bilateral humeri, bilateral SI joint, bilateral pelvic bones, and bilateral femora, suggesting bone metastases. Prostate cancer cT2N1M1b stage IVB with pleural and diffuse bone metastasis was diagnosed. Androgen deprivation therapy (ADT), using enzalutamide, triptorelin pamoate (gonadotropin-releasing hormone agonist), and denosumab, was prescribed for prostate cancer with bone metastasis. After treatment, the patient's dyspnea gradually improved. The follow-up chest X-ray showed the pleural effusion in regression (Fig. 6). The serum PSA level decreased to 2.301 ng/ml.

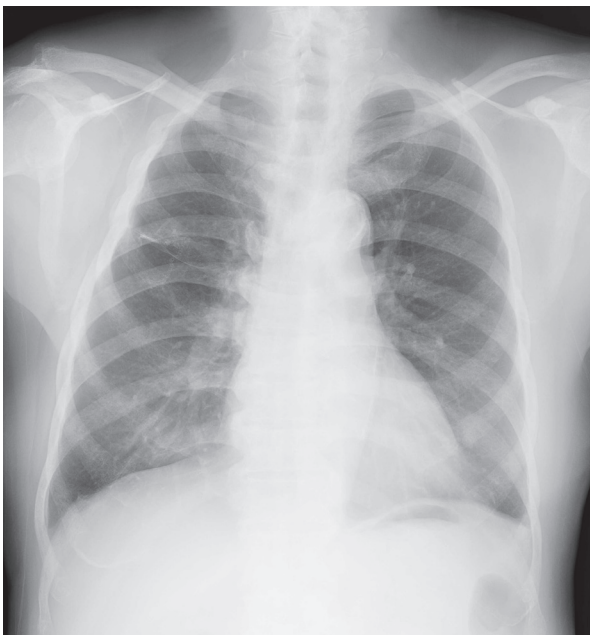

Fig. 6. Chest X-ray showed the pleural effusion in regression after treatment.

Discussion

Pleural effusion, while commonly associated with malignancy, presents diagnostic challenges, particularly when conventional diagnostic modalities such as cytology and imaging fail to pinpoint the primary tumor site. Notably, while malignant pleural effusions are frequently attributed to lung and breast cancer (accounting for 50-65%) [1], prostate cancer-induced pleural effusion is exceedingly rare, comprising less than 1% of cases [2].

Prostate cancer typically metastasizes to the bone and lymph nodes (pelvic and retroperitoneal area); however, atypical metastatic sites such as the lungs, pleura, liver, supradiaphragmatic lymph nodes, and adrenal glands can also be involved [1]. There are variations in metastatic patterns reported in different populations, as evidenced by disparities between retrospective and autopsy studies. Autopsy studies have shown higher prevalence rates of bone metastasis (90%), pulmonary metastasis (46%), and pleural metastasis (21%) [2-3].

Immunohistochemical staining plays a pivotal role in characterizing the tumor, demonstrating positivity for AE1/AE3 and NKX3.1, consistent with prostatic origin. Negative staining for CK7, CK20, TTF-1, PAX-8, and calretinin helps to exclude other cancer origins, such as lung, gastric, pancreatic, and colon cancer, or mesothelioma. PSA serves as the primary biomarker for prostate cancer screening and monitoring treatment efficacy. Assessing PSA levels in pleural fluid can supplement diagnostic efforts in identifying metastatic prostate cancer [4]. Nevertheless, immunocytochemical analysis of PSA may exhibit negative, weak, or focal staining in cases of poorly differentiated carcinoma or among individuals with a history of hormone and/or radiation therapy [1]. Besides, in evaluating malignant pleural effusion, the value of the effusion PSA level for metastatic prostate cancer diagnosis is inconclusive.

We reviewed data and formed a simple table outlining the case reports of prostate cancer with pleural metastasis (Table 1) [1-2, 5-9]. Two studies did not provide further data of pleural effusion and PSA levels [10-11]. Another study focused on how to differentiate malignant effusion from prostate cancer or other solid organ cancer [12]. Most of the prostate cancer patients with malignant pleural effusion revealed an elevated PSA level. However, only 2 case reports disclosed the pleural effusion PSA level. Despite insufficient evidence, the elevated pleural effusion PSA level may be an auxiliary way for prostate cancer pleural metastasis diagnosis. However, we still need more evidence and standardized reference values if clinical practice is indicated. The VATS procedure and histopathological examination of the pleural tissue were crucial in establishing the diagnosis of metastatic adenocarcinoma.

The 5-year survival of patients with prostate cancer with metastasis is only 30% [20]. However, the 5-year survival of localized prostate cancer patients can reach 98%. A case report also mentioned that a patient with malignant pleural effusion also had concurrent osseous metastases [7]. The prognosis for patients with malignant pleural effusion secondary to metastatic adenocarcinoma originating from the prostate gland is typically poor, with an average survival period of approximately 18 months under treatment [3].

According to the Prostate Cancer, Version 4.2023, NCCN Clinical Practice Guidelines in Oncology [13], a patient with identified prostate cancer with a Gleason score of more than 8,

Table 1. Reported Cases of Malignant Pleural Effusion from Prostate Cancer

Author	Year Published	Age (yr)	Effusion side	Intrathoracic involvement/bone metastasis	Pleural fluid cytology	PSA ng/mL		Pleural LDH U/L	Pleural differential count (%)				
						fluid	serum		LYM	Seg	MCs	His	Mono
Glassman L, *et al*. (2)	2021	92	Left	Pleural nodularity with PE/ B(+)	Adenocarcinoma	-	-	-	-	-	-	-	-
Sachpekidis C, *et al*. (8)	2019	76	Right	Isolated PE/ B(+)	Adenocarcinoma	-	24.7	-	-	-	-	-	-
Jeon J, *et al*. (1)	2018	55	Bilateral	Isolated PE/ B(+)	Adenocarcinoma	21.5	44.71	1,113	7	41	5	47	0
Knight, *et al*. (7)	2014	73	Bilateral	Pleura with lung entrapment/ -	Atypical cells	1,619	2,540	-	-	-	-	-	-
Bajpai, *et al*. (6)	2014	84	Right	Isolated PE/ B(x)	Adenocarcinoma	-	>148	-	80	20	0	0	0
Shimizu, *et al*. (5)	1993	65	Bilateral	Lung, lymphangitis carcinomatosis/ B(+)	Adenocarcinoma	-	292	-	-	-	-	-	-

PSA, prostate-specific antigen; PE, pleural effusion; LDH, lactate dehydrogenase; Seg, neutrophil; MCs, mesothelial cells; His, histocyte; Mono, monocyte; -, not recorded; B(+), bone metastasis; B(x), no bone metastasis

bone metastasis, and proven malignant pleural effusion falls into the category of high-risk metastatic castration-sensitive prostate cancer (mCSPC). High-risk mCSPC has features of high-volume disease with visceral metastases and/or ≥ 4 bone lesions, a high Gleason score (≥ 8), and a rapid PSA doubling time.

However, high-risk mCSPC patients have demonstrated improvements in overall survival (OS) in several studies published between 2018 and 2023 [14-18]. According to the guidelines [13], there are 6 options for first-line treatment for high-risk mCSPC. These treatment options include: 1. abiraterone, 2. apalutamide, 3. enzalutamide, 4. ADT with docetaxel, 5. ADT with docetaxel and abiraterone, and 6. ADT with docetaxel and darolutamide. OS can extend to 49.2 months, although some studies are not yet in a state in which statistics can be reliably counted (50% of patients have died). The value of prostate cancer malignant pleural effusion detection is that we can use ADT with other drug combinations for this high-risk group of patients to achieve better survival outcomes.

ADT has many side effects, including an increased risk of bone fractures. Denosumab is a monoclonal antibody that targets and inhibits RANKL (receptor activator of nuclear factor kappa-B ligand), a protein involved in the formation, function, and survival of osteoclasts, which are responsible for bone resorption. Denosumab helps to prevent skeletal-related events such as fractures and spinal cord compression, and it reduces the progression of bone lesions and the destruction induced by metastatic prostate cancer cells in the bone microenvironment. Denosumab is a critical agent in the supportive care of patients with prostate cancer with bone metastases, contributing to the prevention of complications and the enhancement of patient outcomes [19].

Conclusion

In conclusion, this case underscores the importance of maintaining a broad differential diagnosis for recurrent pleural effusion, particularly in cases where conventional diagnostic methods yield inconclusive results. It highlights the value of thorough histopathological and immunohistochemical analyses in elucidating the underlying etiology, especially in rare presentations such as prostate cancer-induced malignant pleural effusion. In addition, the pleural effusion PSA level may be an auxiliary way for prostate cancer pleural metastasis diagnosis.

References

1. Jeon J, Kim TJ, Park HS, *et al*. Malignant pleural effusion from mmetastatic prostate cancer: a case report with unusual cytologic findings. J Pathol Transl Med 2018; 52(4): 257-61.
2. Glassman L, Wilkinson J, Jaffe G, *et al*. A rare case of malignant pleural effusion due to prostate cancer. Chest 2021; 160(4): A2117-A8.
3. Masue T, Hattori S, Takagi K, *et al*. [Prostate cancer detected from pleural effusion: two case reports]. Hinyokika Kiyo 2008; 54(8): 565-8.
4. Wu YB, Xu LL, Wang XJ, *et al*. Diagnostic value of medical thoracoscopy in malignant pleural effusion. BMC Pulm Med 2017; 17(1): 109.
5. Shimizu T, Shibata Y, Uchida T, *et al*. Severe flare-up in a prostate cancer patient treated with luteinizing hormone-releasing hormone analogue depot. Hinyokika Kiyo 1993; 39(10): 953-5.
6. Bajpai PA, Joshi P, Joseph D, *et al*. A case of recurrent massive right sided pleural effusion-an unusual presentation of carcinoma prostate. Lung India 2014; 31(4): 423-4.
7. Knight JC, Ray MA, Benzaquen S. Malignant pleural effusion from prostate adenocarcinoma. Respir Med Case Rep 2014; 13: 24-5.

8. Sachpekidis C, Alberts I, Rominger A, *et al*. 68Ga-prostate-specific membrane antigen uptake in a malignant pleural effusion from metastatic prostate cancer after pleurodesis. Clin Nucl Med 2019; 44(10): 838-9.
9. Lat T, Paul M. Malignant effusion 2022 [updated October 22, 2022.] Available from: https://www.ncbi.nlm.nih.gov/books/NBK519522/.
10. Mai KT, Roustan Delatour NL, Assiri A, *et al*. Secondary prostatic adenocarcinoma: a cytopathological study of 50 cases. Diagn Cytopathol 2007; 35(2): 91-5.
11. Carrascosa M, Perez-Castrillon JL, Mendez MA, *et al*. Malignant pleural effusion from prostatic adenocarcinoma resolved with hormonal therapy. Chest 1994; 105(5): 1577-8.
12. Renshaw AA, Nappi D, Cibas ES. Cytology of metastatic adenocarcinoma of the prostate in pleural effusions. Diagn Cytopathol 1996; 15(2): 103-7.
13. Schaeffer EM, Srinivas S, Adra N, *et al*. Prostate Cancer, Version 4.2023, NCCN Clinical Practice Guidelines in Oncology. J Nat Compr Canc Netw 2023; 21(10): 1067-96.
14. Kyriakopoulos CE, Chen Y-H, Carducci MA, *et al*. Chemohormonal therapy in metastatic hormone-sensitive prostate cancer: long-term survival analysis of the randomized phase III E3805 CHAARTED trial. J Clin Oncol 2018; 36(11): 1080-7.
15. Armstrong AJ, Szmulewitz RZ, Petrylak DP, *et al*. ARCHES: a randomized, phase III study of androgen deprivation therapy with enzalutamide or placebo in men with metastatic hormone-sensitive prostate cancer. J Clin Oncol 2019; 37(32): 2974-86.
16. Kumar G. LATITUDE: A landmark trial for high-risk metastatic castration-sensitive prostate cancer: final overall survival analysis. Indian J Urol 2020; 6(1): 71-2.
17. Merseburger AS, Suttmann H. [TITAN study: evaluation of apalutamide in patients with metastatic hormone-sensitive prostate cancer - treatment of metastatic hormone-sensitive prostate cancer (mHSPC)]. Aktuelle Urol 2021; 52(2): 155-60.
18. Aragon-Ching JB. ARASENS: making sense out of first-line metastatic hormone-sensitive prostate cancer treatment. Asian J Androl 2023; 25(1): 1-4.
19. Boopathi E, Birbe R, Shoyele SA, *et al*. Bone health management in the continuum of prostate cancer disease. Cancers (Basel) 2022; 14(17).
20. UpToDate: Overview of approach to prostate cancer survivors in 2024/05.

Case Report: A 61-Year-Old Man with Chronic Obstructive Pulmonary Disease Presenting a Worsening Cough and Breathlessness for 3 Months

Chang-Ru Lin[1], Shih-Chi Ku[1]

We reported the case of a 61-year-old man with a history of chronic obstructive pulmonary disease (COPD) who suffered frequent exacerbations and developed a new nodule in the left upper lung. He was ultimately diagnosed with phaeohyphomycosis based on pathological findings, which revealed necrotizing granulomatous inflammation with pigmented fungal hyphae. His primary symptoms were exertional dyspnea and a productive cough persisting for several months. A series of chest X-rays revealed a subpleural lung nodule. Later, a wedge resection disclosed a necrotic lung nodule with pigmented fungal hyphae, confirming phaeohyphomycosis. After surgery, the patient experienced improved dyspnea and better FEV1, leading to de-escalation in his COPD treatment. This case underscores the need to investigate potential underlying chronic fungal infections when managing unstable COPD. ***(Thorac Med 2025; 40: 88-94)***

Key words: COPD exacerbation, phaeohyphomycosis

Introduction

Chronic obstructive pulmonary disease (COPD) and COPD acute exacerbations (AE) are prevalent worldwide, particularly among smokers [1]. Pulmonary infections, primarily bacterial and viral, are common causes of AE [1]. However, recent studies suggest that COPD may increase the risk of fungal infections, which in turn can intensify the frequency of COPD AE [2-3]. This case report describes a patient with recurrent AE, which were later confirmed to be caused by a rare fungal infection, leading to COPD AE.

Case Presentation

A 61-year-old man, a heavy smoker with a history of hypertension and COPD, was previously treated with amlodipine, olmesartan, and vilanterol/umeclidinium at another hospital. Due to frequent AE, characterized by produc-

[1]Division of Chest Medicine, Department of Internal Medicine, National Taiwan University Hospital, Taipei, Taiwan. Address reprint requests to: Dr. Shih-Chi Ku, Division of Chest Medicine, Department of Internal Medicine, National Taiwan University Hospital #7, Chung Shan S. Rd., Zhongzheng District, Taipei City 100225, Taiwan.

tive cough and dyspnea, he came to our emergency department for help on May 29, 2018. After his symptoms improved, he was referred to our chest clinic for further management. A treatable trait screening was conducted there. The lung function test showed a post-bronchodilator FEV1/FVC ratio of 48.2%, confirming COPD. The FEV1 was at 50.3% of predicted value, indicating a moderate obstructive ventilatory defect. Chest computed tomography (CT) revealed bilateral pulmonary emphysema. The patient had elevated eosinophil (380/uL) and IgE (281 IU/mL) levels, suggesting eosinophilic COPD or asthma and COPD overlap. No definitive allergen was found.

The treatment plan was then adjusted to include fluticasone/vilanterol, umeclidinium, and aminophylline. Under treatment, his elevated eosinophil level improved (from 380 to 149/uL) and IgE levels normalized (from 281 to 69 IU/mL). Following this, he experienced only 1 AE episode in 2019. By 2023, his airflow obstruction had worsened, with FEV1 decreasing from 47.2% to 32.1% of predicted value. Despite this decline, his COPD was manageable in an outpatient setting. His treatment regimen was adjusted from fluticasone/umeclidinium/vilanterol to salmeterol/fluticasone plus tiotropium.

The patient remained stable until May 2023, when he developed exertional dyspnea accompanied by mild chest tightness and a productive cough with yellow sputum. He also experienced intermittent fever and wheezing on exertion. A chest X-ray (CXR) revealed increased pulmonary infiltration with ill-defined opacities in both lungs, without pneumonia patches. His symptoms varied despite being on triple therapy and oral corticosteroids. In July 2023, further CXR revealed a small nodular opacity in the left upper lung zone (Fig. 1). Chest CT dis-

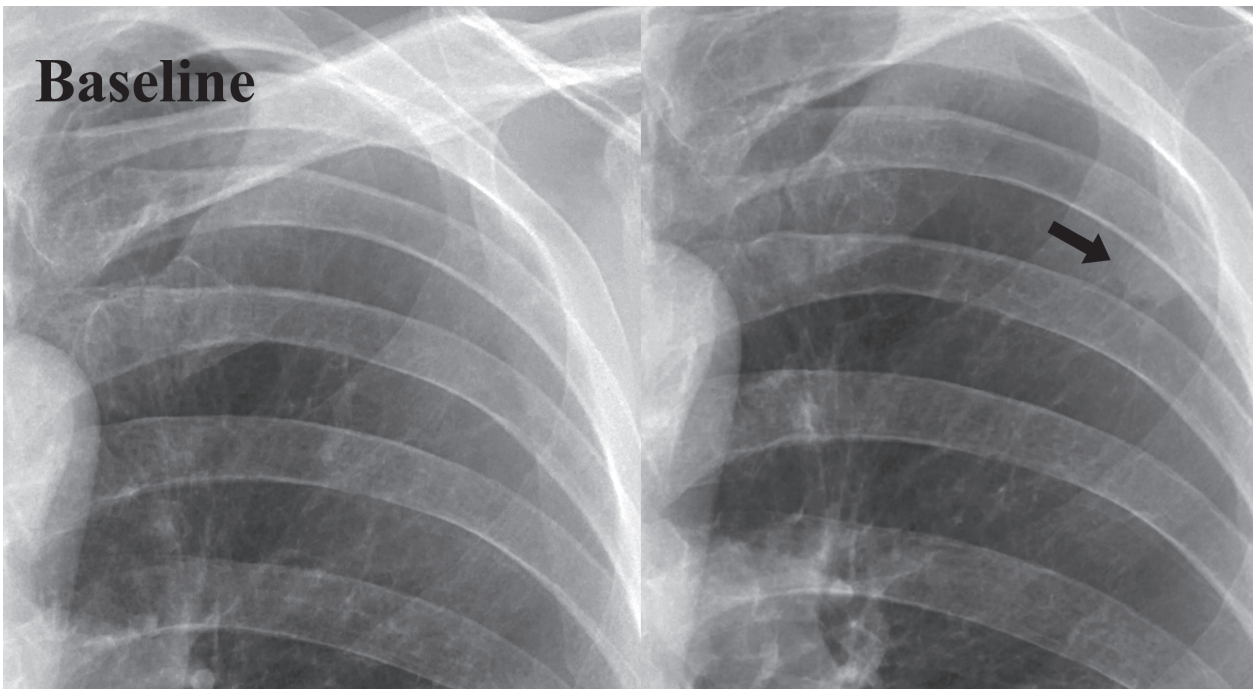

Fig. 1. Chest X-ray revealed a small nodular opacity in the left upper lung zone.

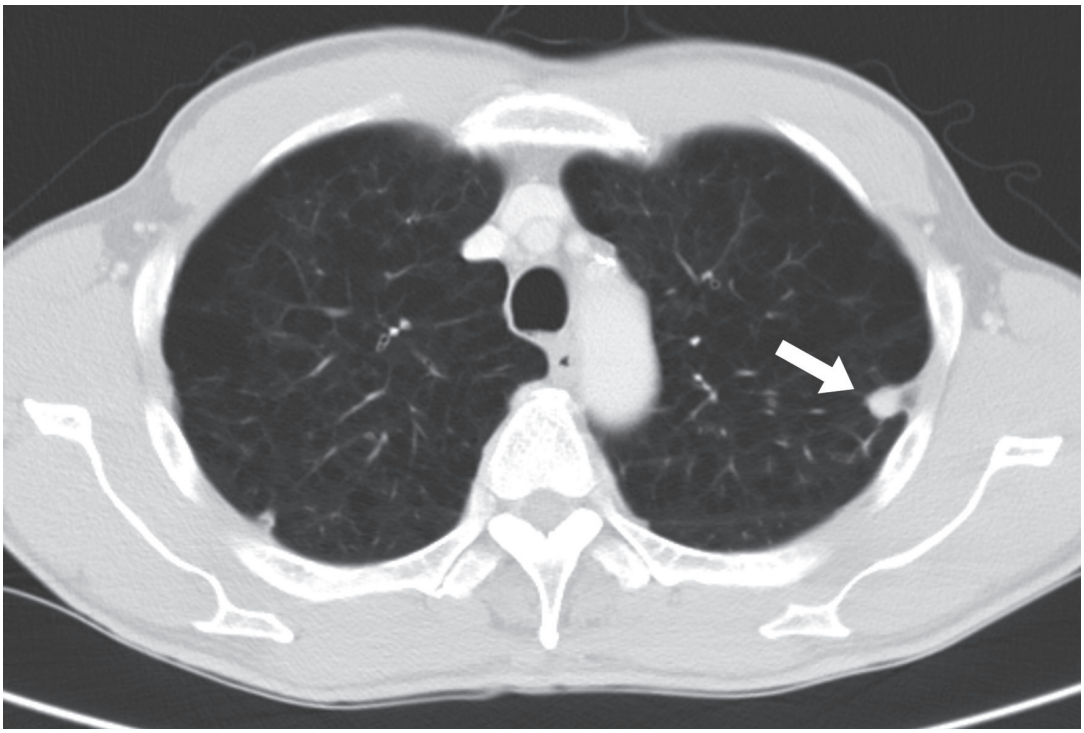

Fig. 2. Chest computed tomography showed a subpleural solid nodule in the left upper lung.

closed a new subpleural solid nodule, approximately 1 cm in size, with pleural retraction (Fig. 2).

A uniportal video-assisted thoracoscopic surgery (VATS) was performed for left upper lobe wedge resection, to clarify the lesion. The surgery revealed a well-defined, yellowish, soft, and necrotic lung nodule measuring 1.0 x 0.8 x 0.6 cm (Fig. 3). Pathological analysis showed necrotizing granulomatous inflammation with pigmented and separated fungal hyphae, resulting in a diagnosis of phaeohyphomycosis (Fig. 4).

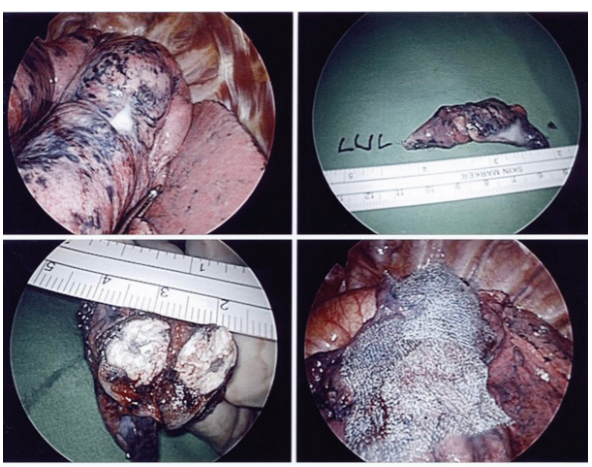

Fig. 3. Surgical findings and specimens.

Post-surgery, the patient experienced less dyspnea and was able to tolerate tapering off oral corticosteroid. His COPD Assessment Test score dropped from 16 to 7, and his FEV1 improved from 32.1% to 45.5% of predicted value. COPD treatment was adjusted to olodaterol/tiotropium. In the meantime, the phaeohyphomycosis was treated with voriconazole, following the advice of an infectious disease specialist. However, due to leg edema attributed to voriconazole, the antifungal treatment

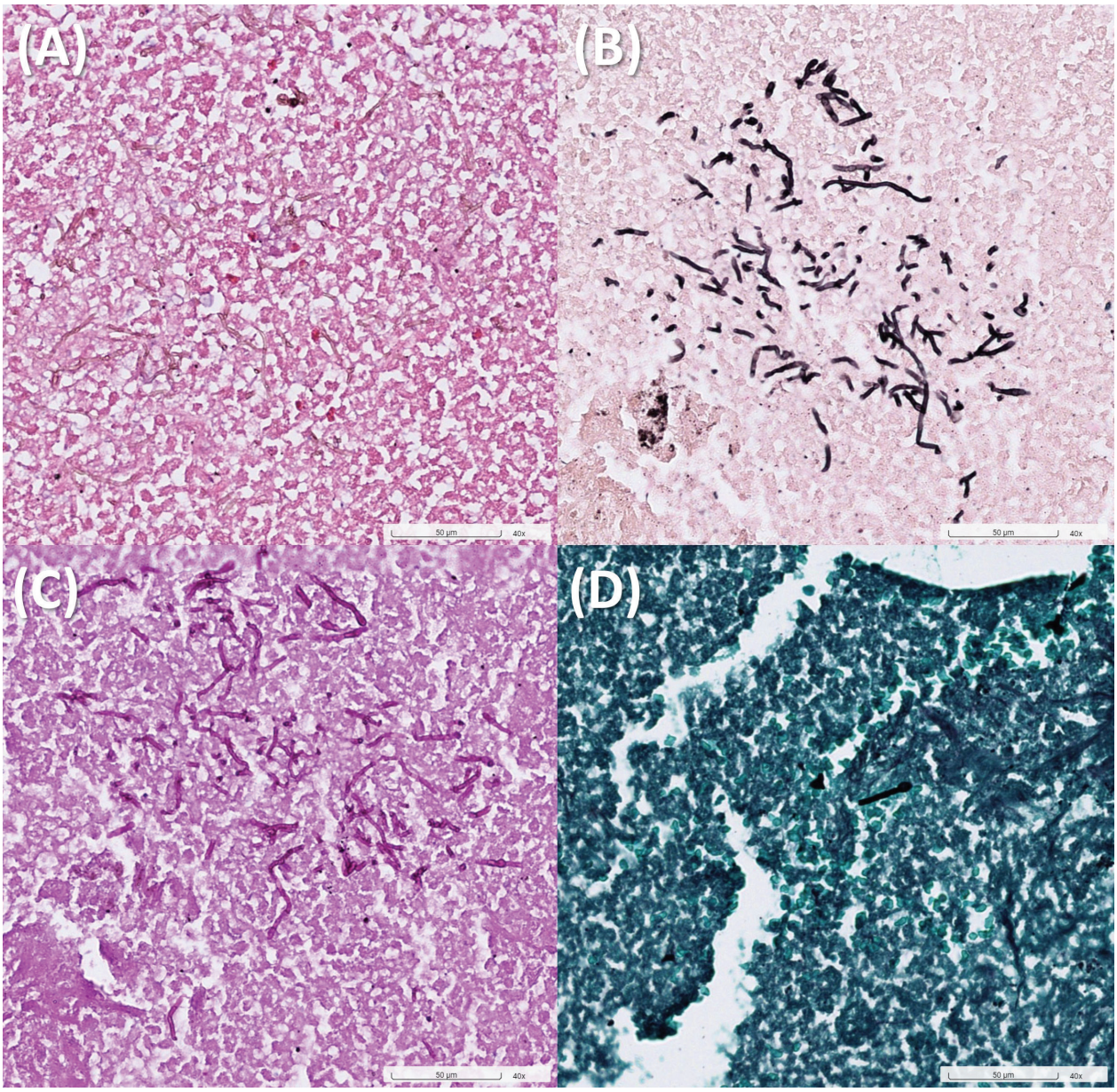

Fig. 4. High-power field (400x) view of hematoxylin and eosin staining (A) disclosed dematiaceous hyphae with special stains for fungus, including, (B) Fontana-Masson stain, (C) Periodic acid-Schiff stain, and (D) Grocott-Gomori methenamine silver stain.

was switched to isavuconazole, which was later discontinued due to a skin rash. After thorough discussions and shared decision-making, the antifungal treatment was suspended. One month later, the patient remained stable without recurrent symptoms at the follow-up clinic.

Discussion

We reported the case of a 61-year-old man with COPD who contracted phaeohyphomycosis, and presented with worsening exertional dyspnea and a productive cough. Imaging

identified a subpleural lung nodule. A wedge resection was performed, and pathological findings confirmed necrotizing granulomatous inflammation with pigmented fungal hyphae. Post-surgery, the patient exhibited improved symptoms and FEV1, prompting an adjustment in COPD treatment.

Phaeohyphomycosis, a fungal infection caused by darkly pigmented fungi that are known as dematiaceous or melanized molds, involves over 150 species and 70 genera [4]. These fungi possess melanin, which acts as a free radical scavenger and provides protection against immune system oxidants, aiding their survival and pathogenicity within human tissues [5].

Phaeohyphomycosis is an opportunistic infection with sporadic cases reported in many regions, particularly in tropical and subtropical areas. There has been an increasing trend in the number of cases recently in China [5]. Between 1987 and 2021, 39 cases with phaeohyphomycosis were documented in Taiwan. This rise may be attributed to heightened awareness, enhanced diagnostic methods, or environmental conditions favorable to fungal growth. The average age at diagnosis is 48 years, ranging from 2 to 89 years [6]. Major risk factors include traumas, diabetes, and corticosteroid use, as noted in 37%, 11%, and 11% of cases, respectively [6]. This infection primarily targets immunocompromised individuals, but evidence also shows that hosts without obvious immune deficiencies can contract the infection [6]. Furthermore, acute exacerbations of COPD have been found to be associated with fungal infections [7].

Phaeohyphomycosis can involve a variety of anatomical sites, including superficial cutaneous and subcutaneous sites, paranasal sinusitis, and even lead to disseminated infections. This fungal infection is frequently seen affecting vital organs such as the lungs, where it can manifest as pneumonia, asymptomatic pulmonary nodules, or endobronchial lesions [8,9]. Specimens for diagnosis are typically derived from lung tissues, sputum, or bronchoalveolar lavage fluid, with findings frequently showing nonspecific inflammation, necrosis, or granulomatous inflammation [10-11].

Some phaeohyphomycosis patients have exhibited elevated galactomannan index values, likely due to cross-reactivity [1]. However, research has shown that strains testing positive for galactomannan antigenemia are often non-reactive, indicating that the presence of galactomannan might suggest simultaneous invasive aspergillosis [12]. Monitoring serum aspergillus IgG can help differentiate the diagnoses and guide treatment [13].

Although traditional tests have limited effectiveness in diagnosing phaeohyphomycosis, molecular methods like polymerase chain reaction and matrix-assisted laser desorption/ionization-time of flight mass spectrometry are proving useful for their timely and accurate detection [14-15]. Further studies are necessary to determine their clinical application.

Phaeohyphomycosis can trigger immune hyper-responsiveness, resulting in the clinical features of allergic bronchopulmonary mycosis (ABPM), which presents as poorly controlled obstructive lung disease with symptoms like coughing, shortness of breath, and mucus plug expectoration [5, 9, 16]. Diagnostic approaches for ABPM include serology and imaging, with elevated IgE levels (> 200 IU/ml) indicating atopy, and levels sometimes surpassing 1000 IU/ml in severe cases. Serum total IgE is a key biomarker for monitoring disease activity and

treatment response [18]. While standardized antigen kits test for specific allergens, they don't cover all fungi. Eosinophilia is also associated with ABPM, but must be distinguished from other causes of high eosinophil counts. Steroid use can mask eosinophilia in ABPM patients. Radiologically, ABPM may show non-specific opacities, migratory consolidations, lung fibrosis, bronchiectasis, and pleural thickening. Treatment focuses on managing fungal infections, minimizing exposure to environmental fungi, using immunosuppressants, and improving airway hygiene [17].

Treatment typically involves surgical excision of isolated pulmonary nodules in immunocompetent patients and antifungal therapy using agents such as intravenous liposomal amphotericin B or mold-active azoles like itraconazole, voriconazole, or posaconazole, depending on the severity and specific host factors [19-20]. The prognosis varies, with mortality rates as high as 55% in cerebral cases, 36% for disseminated infections, and 25% for pulmonary cases [6]. Prompt and accurate diagnosis is crucial for effectively managing phaeohyphomycosis, given its generally poor response to treatment [21].

In summary, this case highlights the importance of recognizing chronic fungal infection as a potential trigger in COPD patients experiencing deteriorating disease control while under adequate medical treatment. Timely diagnosis and proper treatment, including surgery and specific antifungal medication, result in prompt improvement in the patient's condition.

Conclusion

In cases of COPD AE where the initial investigation fails to identify a cause, it is essential to actively exclude various possibilities, including fungal infections. Our case demonstrates that the patient's COPD AE was associated with phaeohyphomycosis, a rare fungal infection. Following surgical intervention and antifungal treatment, the patient's COPD showed marked improvement.

References

1. Mannino DM, Buist AS. Global burden of COPD: risk factors, prevalence, and future trends. Lancet 2007; 370(9589):765-773. https://doi.org/10.1016/s0140-6736(07)61380-4.
2. Venkatesan P. GOLD COPD report: 2024 update. Lancet Respir Med 2024; 12(1): 15-16. https://doi.org/10.1016/s2213-2600(23)00461-7.
3. Tiew P Y, Mac Aogáin M, Ter SK, *et al*. Respiratory mycoses in COPD and bronchiectasis. Mycopathologia 2021; 186(5): 623-638. https://doi.org/10.1007/s11046-021-00539-z.
4. Guo L, Wu X, Wu X. Aspergillus infection in chronic obstructive pulmonary diseases. Clin Respir J 2023; 17(3): 129-138. https://doi.org/10.1111/crj.13585.
5. Arcobello JT, Revankar SG. Phaeohyphomycosis. Semin Respir Crit Care Med 2020; 41(1): 131-140. https://doi.org/10.1055/s-0039-3400957.
6. He Y, Zheng HL, Mei H, *et al*. Phaeohyphomycosis in China. Front Cell Infect Microbiol 2022; 12:895329. https://doi.org/10.3389/fcimb.2022.895329.
7. Chen SC, Blyth CC, Sorrell TC, *et al*. Pneumonia and lung infections due to emerging and unusual fungal pathogens. Semin Respir Crit Care Med 2011; 32(6): 703-716. https://doi.org/10.1055/s-0031-1295718.
8. Han S, Meng X. Prediction of risk for secondary lower respiratory tract fungal infection during the acute exacerbation phase of COPD. J Infect Dev Ctries 2023; 17(2): 268-275. https://doi.org/10.3855/jidc.16088.
9. Revankar SG, Patterson JE, Sutton DA, *et al*. Disseminated phaeohyphomycosis: review of an emerging mycosis. Clin Infect Dis 2002; 34(4): 467-476. https://doi.org/10.1086/338636.
10. Revankar SG, Sutton DA. Melanized fungi in human disease. Clin Microbiol Rev 2010; 23(4): 884-928.

https://doi.org/10.1128/cmr.00019-10.

11. Ben-Ami R, Lewis RE, Raad II, *et al*. Phaeohyphomycosis in a tertiary care cancer center. Clin Infect Dis 2009; 48(8):1033-1041. https://doi.org/10.1086/597400.
12. Guarner J, Brandt ME. Histopathologic diagnosis of fungal infections in the 21st century. Clin Microbiol Rev 2011; 24(2): 247-280. https://doi.org/10.1128/cmr.00053-10.
13. Ben-Ami R, Lasala PR, Lewis RE, *et al*. Lack of galactomannan reactivity in dematiaceous molds recovered from cancer patients with phaeohyphomycosis. Diagn Microbiol Infect Dis 2010; 66(2): 200-203. https://doi.org/10.1016/j.diagmicrobio.2009.09.015.
14. Otu A, Kosmidis C, Mathioudakis AG, *et al*. The clinical spectrum of aspergillosis in chronic obstructive pulmonary disease. Infection 2023: 51(4): 813-829. https://doi.org/10.1007/s15010-022-01960-2.
15. Schoch CL, Seifert KA, Huhndorf S, *et al*. Nuclear ribosomal internal transcribed spacer (ITS) region as a universal DNA barcode marker for Fungi. Proc Natl Acad Sci U S A 2012; 109(16): 6241-6246. https://doi.org/10.1073/pnas.1117018109.
16. Stein M, Tran V, Nichol KA, *et al*. Evaluation of three MALDI-TOF mass spectrometry libraries for the identification of filamentous fungi in three clinical microbiology laboratories in Manitoba, Canada. Mycoses 2018; 61(10): 743-753. https://doi.org/10.1111/myc.12800.
17. Chowdhary A, Agarwal K, Kathuria S, *et al*. Allergic bronchopulmonary mycosis due to fungi other than Aspergillus: a global overview. Crit Rev Microbiol 2014; 40(1): 30-48. https://doi.org/10.3109/1040841x.2012.754401.
18. Fink JN. Therapy of allergic bronchopulmonary aspergillosis. Indian J Chest Dis Allied Sci 2000; 42(4): 221-224.
    (this reference (the original #19) was repeated from reference #17 above and was deleted).
19. Greig JR, Khan MA, Hopkinson NS, *et al*. Pulmonary infection with Scedosporium prolificans in an immunocompetent individual. J Infect 2001; 43(1): 15-17. https://doi.org/10.1053/jinf.2001.0808.
20. Chowdhary A, Meis JF, Guarro J, *et al*. ESCMID and ECMM joint clinical guidelines for the diagnosis and management of systemic phaeohyphomycosis: diseases caused by black fungi. Clin Microbiol Infect 2014; 20(3): 47-75. https://doi.org/10.1111/1469-0691.12515.
21. Naggie S, Perfect JR. Molds: hyalohyphomycosis, phaeohyphomycosis, and zygomycosis. Clin Chest Med 2009; 30(2): 337-353, vii-viii. https://doi.org/10.1016/j.ccm.2009.02.009.

A Rare Case of Foreign Body Ingestion

Hsiu-Ping Chou[1], Kuan-Hsun Lin[1]

Both younger and older age, as well as mental retardation, are frequent causative factors in the ingestion of foreign bodies. Such cases are usually sent to the emergency department, regardless of whether the patients have symptoms or not. We reported the case of a 60-year-old male patient with dysphagia and nausea who ingested an unusually-shaped object and was brought to the emergency department. The diagnosis was confirmed by kidney, ureter, and bladder X-ray exam, the patient's clinical history, and imaging findings. The location of the foreign bodies was identified by computed tomography. Surgical treatment was performed immediately, and successfully removed the foreign bodies. In most cases, ingested foreign bodies are typically found in the gastrointestinal tract due to spontaneous passage. It is possible that a foreign body can be removed by endoscopy (success rate >95%). However, in our case, the foreign bodies had an unusual shape or were in a challenging position; hence, the endoscopic approach was difficult to perform. Surgical treatment was required to remove them. ***(Thorac Med 2025; 40: 95-98)***

Key words: foreign body ingestion; removal; surgical treatment

Introduction

Foreign body ingestion is commonly seen in emergency departments, especially among the pediatric and elderly populations. In the United States, the incidence of foreign body ingestion is approximately 4%, with 1500 patients dying as a result of this condition annually [1]. Medical interventions are performed in 10% to 20% of patients with foreign body ingestion. Mental retardation is the common causative factor among young adults [2].

For the diagnosis of foreign body ingestion located in the gastrointestinal tract, a thorough clinical history-taking is important. A simple X-ray may establish the final diagnosis. However, if a definitive diagnosis cannot be determined based on the plain films, computed tomography (CT) is indicated. In addition, endoscopy can provide a definitive diagnosis. Here, we present a rare case of foreign body ingestion.

[1]Division of Thoracic Surgery, Department of Surgery, Tri-Service General Hospital, National Defense Medical Center.
Address reprint requests to: Dr. Kuan-Hsun Lin, Division of Thoracic Surgery, Department of Surgery, Tri-Service General Hospital, 325, Section 2, Cheng-Kung Road, Taipei 114, Taiwan, R.O.C.

Case Report

A 60-year-old unmarried man with a history of schizophrenia and gastral esophageal reflux disease, which was being treated, reported a foreign body sensation in his esophagus and abdomen after food intake. The patient initially had the symptoms of dysphagia, both liquids and solids, but the symptoms were relieved after a while. No respiratory symptoms were mentioned. He was sent to the emergency department after a medical evaluation in an otorhinolaryngology clinic, where no evidence of a foreign body was revealed during laryngoscopy.

According to the patient's family, he swallowed a metal object because he felt hungry. The patient denied that he attempted suicide. However, no specific finding was noted on the chest and neck film. The kidney, ureter and bladder (KUB) exam showed 2 radiopaque materials in the abdomen (Fig. 1). Non-contrast enhanced CT of the abdomen was performed, which revealed 2 extremely high-density materials. The foreign bodies were found in the stomach and in the first portion of the duodenum. Therefore, a chest surgeon was consulted.

Multiple attempts at endoscopy were performed with an Endoloop (Olympus) and forceps, but the foreign bodies still could not be removed. Due to the failure of endoscopic treatment, surgical extraction was planned after consultation with a general surgeon. Exploration laparotomy was then performed. A C-arm-guided foreign body localization was conducted during the operation. Two pieces of a heavy statue of Buddha (4 x 2 cm in size) were found in the stomach and a piece of a nut was noted in the first portion of the duodenum. All of the foreign bodies were extracted via gastrotomy (Fig. 2). Subsequently, the gastrotomy was closed.

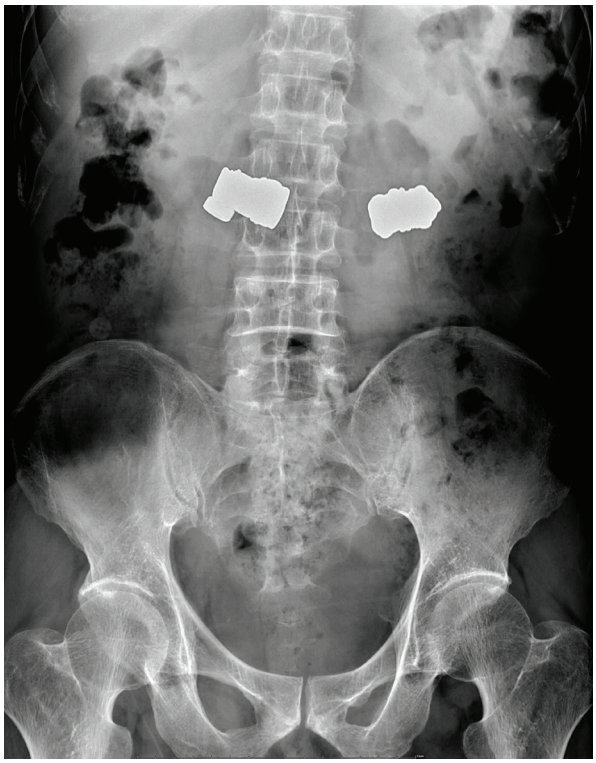

Fig. 1. A kidney, ureter, and bladder X-ray film. Two metallic foreign bodies are found in the abdomen.

Fig. 2. Operative images. Two pieces of a heavy statue of Buddha (4 x 2 cm in size) were found in the stomach and a piece of a nut was noted in the first portion of the duodenum.

One Sil-Med drain was placed into a Morrison pouch. The whole procedure was conducted smoothly.

Postoperatively, the patient was transferred to the general ward for monitoring. The postoperative care plan was to perform conservative management, which included enteral nutrition using a nasojejunal tube, and shifting to oral feeding as well as daily wound care with antibiotic therapy. The patient was discharged 10 days after hospitalization. No nosocomial infections or other complications were noted.

Discussion

Consultations in the emergency room for ingestion of a foreign body frequently occur. However, most cases can be resolved with an endoscopic procedure [1]. Compared to the foreign bodies frequently encountered, including coins, fish or chicken bone, and food bolus, the type of foreign body in our case is rarely seen worldwide.

According to the European Society of Gastrointestinal Endoscopy, the diagnosis of foreign body ingestion is established clinically, and then supplemented with simple radiography. When achieving a definitive diagnosis is difficult, CT (especially in cases with a suspicion of some complications) and endoscopy [3] are both suitable choices. In the present case, the plain X-ray film easily revealed the foreign body due to its metallic composition. CT was also used to localize the foreign bodies.

There have been several cases of foreign bodies stuck in the upper gastrointestinal tract due to accidental swallowing. Commonly ingested materials include coins, bones, etc. Retention of food boluses is seen in patients with pre-existing esophageal lesions [4]. Our case was rare, since the ingested objects had bizarre shapes or locations.

The indications for use of endoscopy are as follows: emergent, urgent, and non-urgent. Emergent endoscopy should be performed within the first 2 hours when an individual has a battery or sharp material stuck in the esophagus. Urgent endoscopy should be performed within the first 6 hours when a battery or sharp material is in the stomach. However, for cases of ingestion of blunt foreign bodies, there is no indication to perform emergent endoscopy to remove them, rather, endoscopy is performed in the first 24 hours. Endoscopy, with its high success rate of up to 95.6%, owing to technological improvement and advances in staff training over time, makes it the treatment of choice. This approach has resulted in a decrease in both healthcare costs and the rate of associated complications [5]. In our case, endoscopy was performed, but it was unsuccessful. Imaging findings alone were utilized to establish the diagnosis and locate the foreign body . Retention of ingested foreign objects in the duodenum bulb is rare [4]. Thus, surgical treatment, rather than the endoscopic approach, was arranged for the removal of the foreign bodies in this patient to avoid treatment failure.

Surgical treatment plays an important role in cases that are unresolvable by endoscopy, as in our case. Approximately 1.6% of patients require surgery when esophageal perforation or failure of endoscopic treatment occurs [4, 6].

Our patient had a satisfactory recovery after the operation, and had no complications. Since an appropriate diagnostic strategy and therapeutic plan was used for this case of foreign body ingestion, the object was removed smoothly.

Conclusion

An appropriate diagnostic strategy is important to accurately identify and localize an ingested foreign body. Then, an optimal therapeutic plan can be developed, leading to the smooth removal of the foreign body.

References

1. Birk M, Bauerfeind P, Deprez PH, *et al*. Removal of foreign bodies in the upper gastrointestinal tract in adults: European Society of Gastrointestinal Endoscopy (ESGE) clinical guideline. Endoscopy 2016; 48(5): 489-96.
2. Kamal I, Thompson J, Paquette DM. The hazards of vinyl glove ingestion in the mentally retarded patient with pica: new implications for surgical management. Can J Surg 1999; 42(3): 201-4.
3. Shahi S, Bhandari TR, Thapa PB, *et al*. Foreign body esophagus: six years of silence. SAGE Open Med Case Rep 2020; 8: 2050313X20944322.
4. Emara MH, Darwiesh EM, Refaey MM, *et al*. Endoscopic removal of foreign bodies from the upper gastrointestinal tract: 5-year experience. Clin Exp Gastroenterol 2014; 7: 249-53.
5. Yuan J, Ma M, Guo Y, *et al*. Delayed endoscopic removal of sharp foreign body in the esophagus increased clinical complications: an experience from multiple centers in China. Medicine (Baltimore) 2019; 98(26): e16146.
6. Yu S, Wang X, Chen X. Removal of giant spherical foreign body in the esophagus by double-forceps endoscope and double balloon. J Int Med Res 2020; 48(8): 300060520941332.